



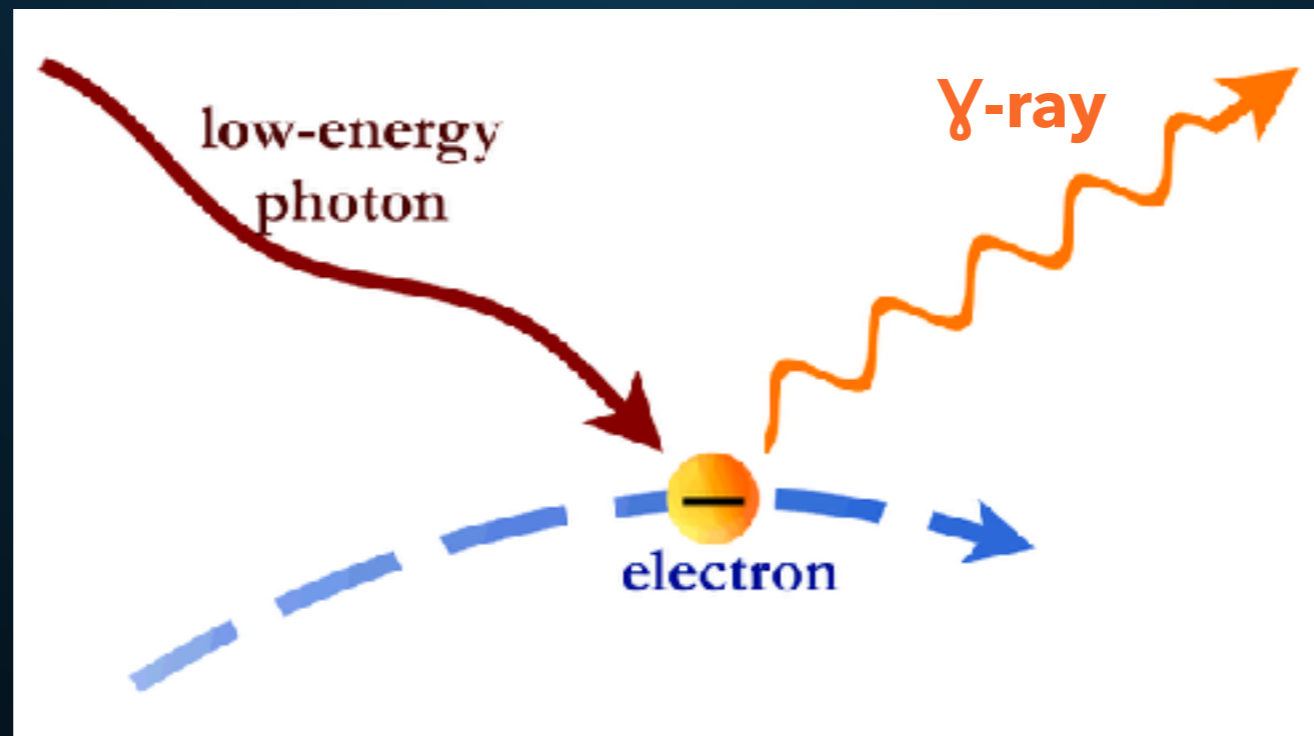
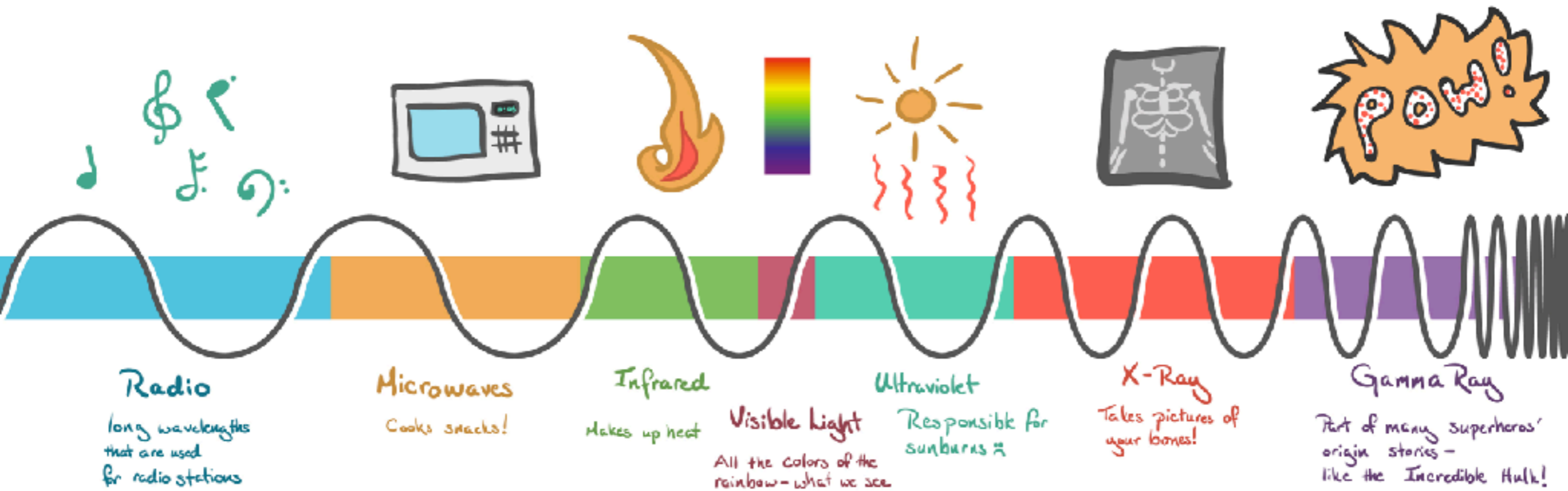
TIM LINDEN

● **THE RISE OF THE LEPTONS**
PULSAR EMISSION DOMINATES THE TEV GAMMA-RAY SKY

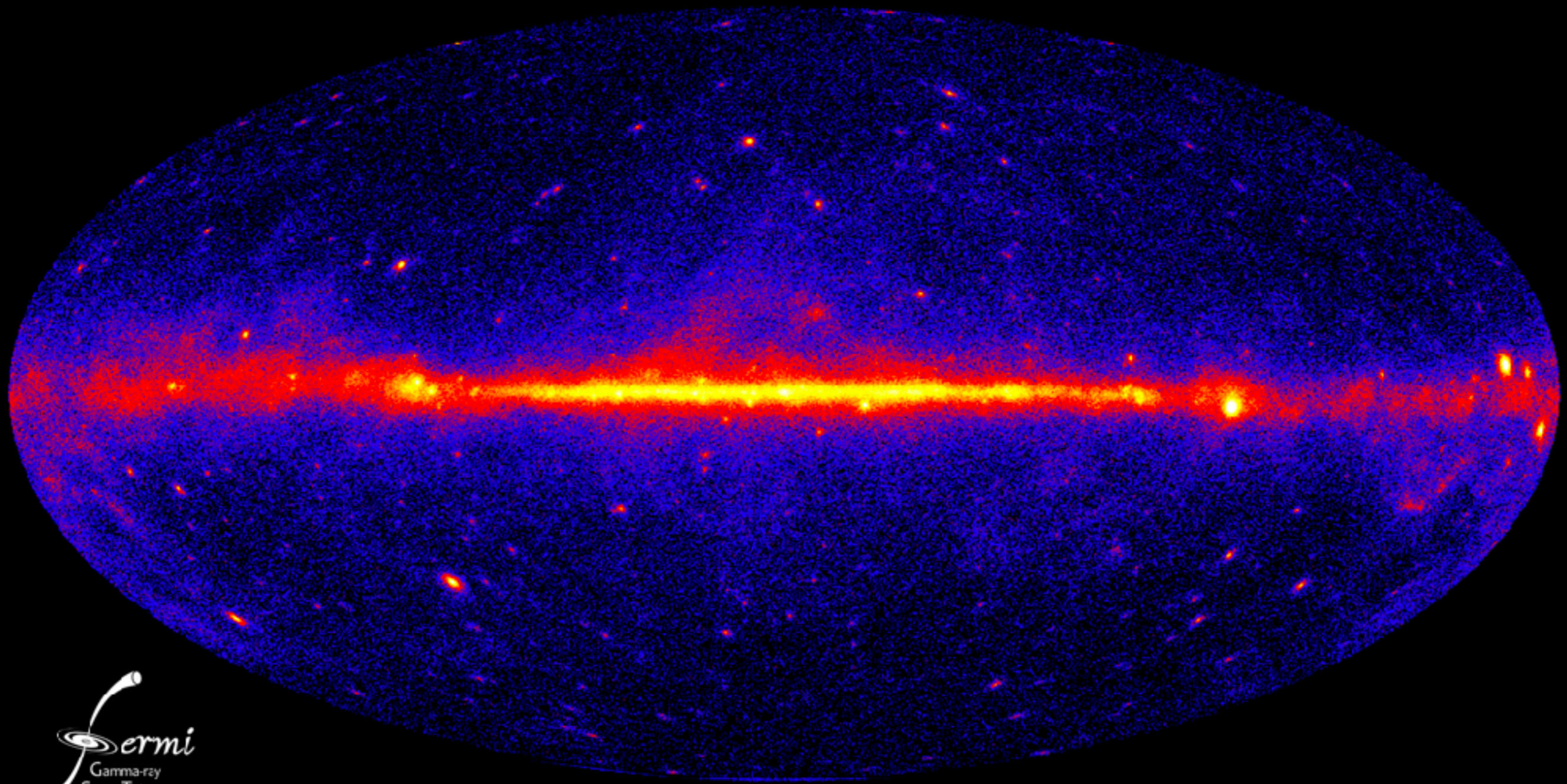
Gran Sasso Science Institute Colloquium Room
Floating Through the Interweb-sphere
1 April 2020



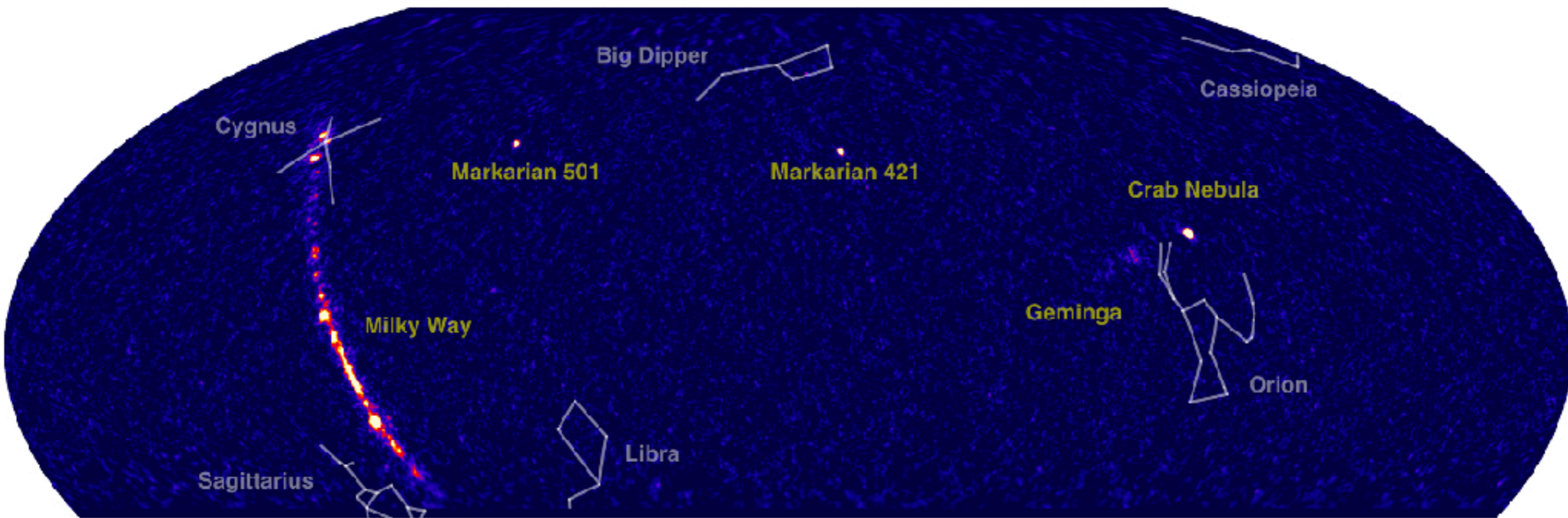
The Electromagnetic Spectrum



THE GEV SKY



THE TEV SKY



- **Diffuse Emission decreases in intensity, while sources remain bright**

- n.b., Comparing a flux map vs. a TS map

TEV HALOS



Moon (To Scale)

• Angular Resolution

———— 10 pc (Geminga distance)

Geminga

PSR B0656+14
(Monogem)







TEV HALOS



Moon (To Scale)

• Angular Resolution

———— 10 pc (Geminga distance)

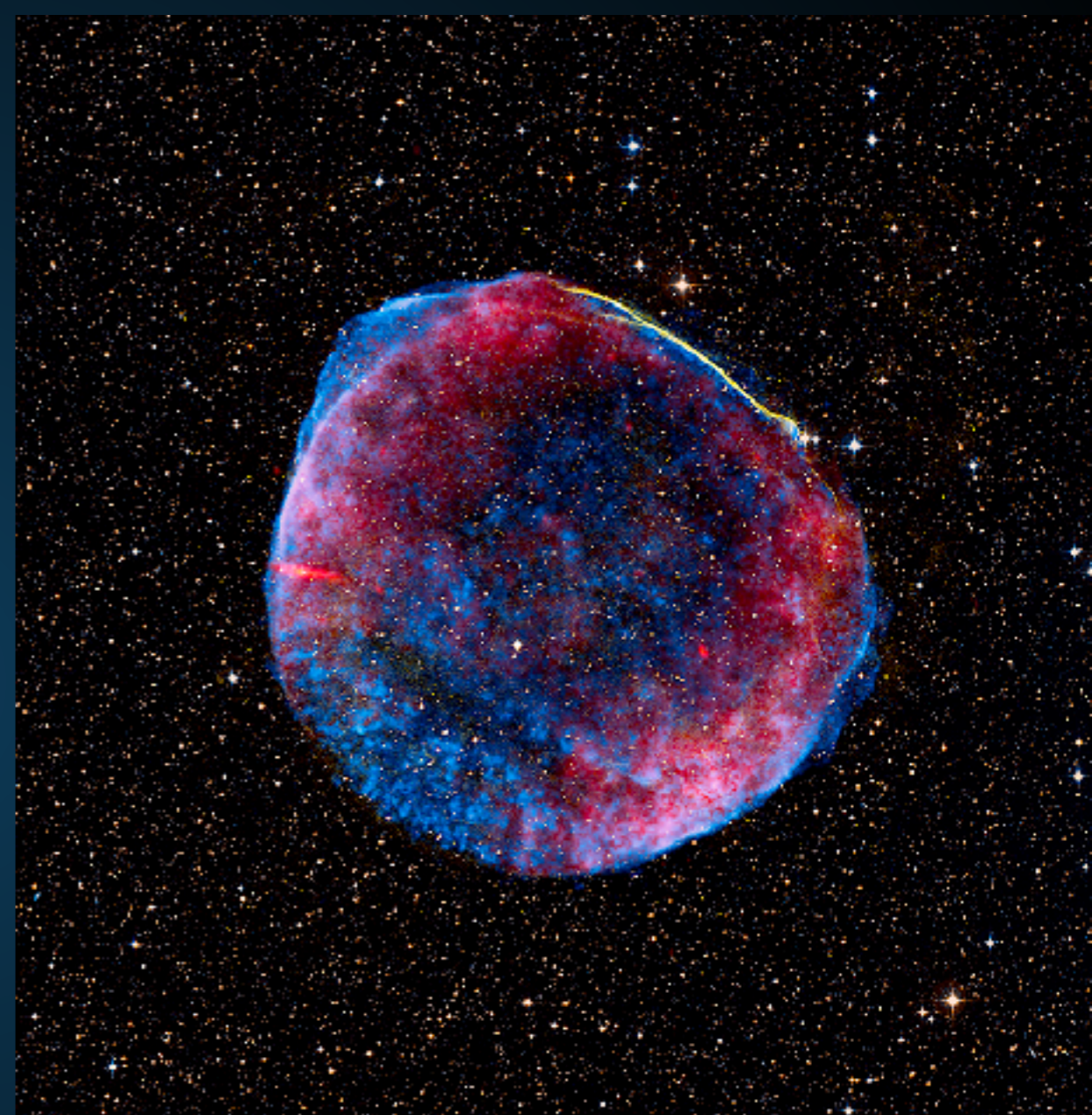
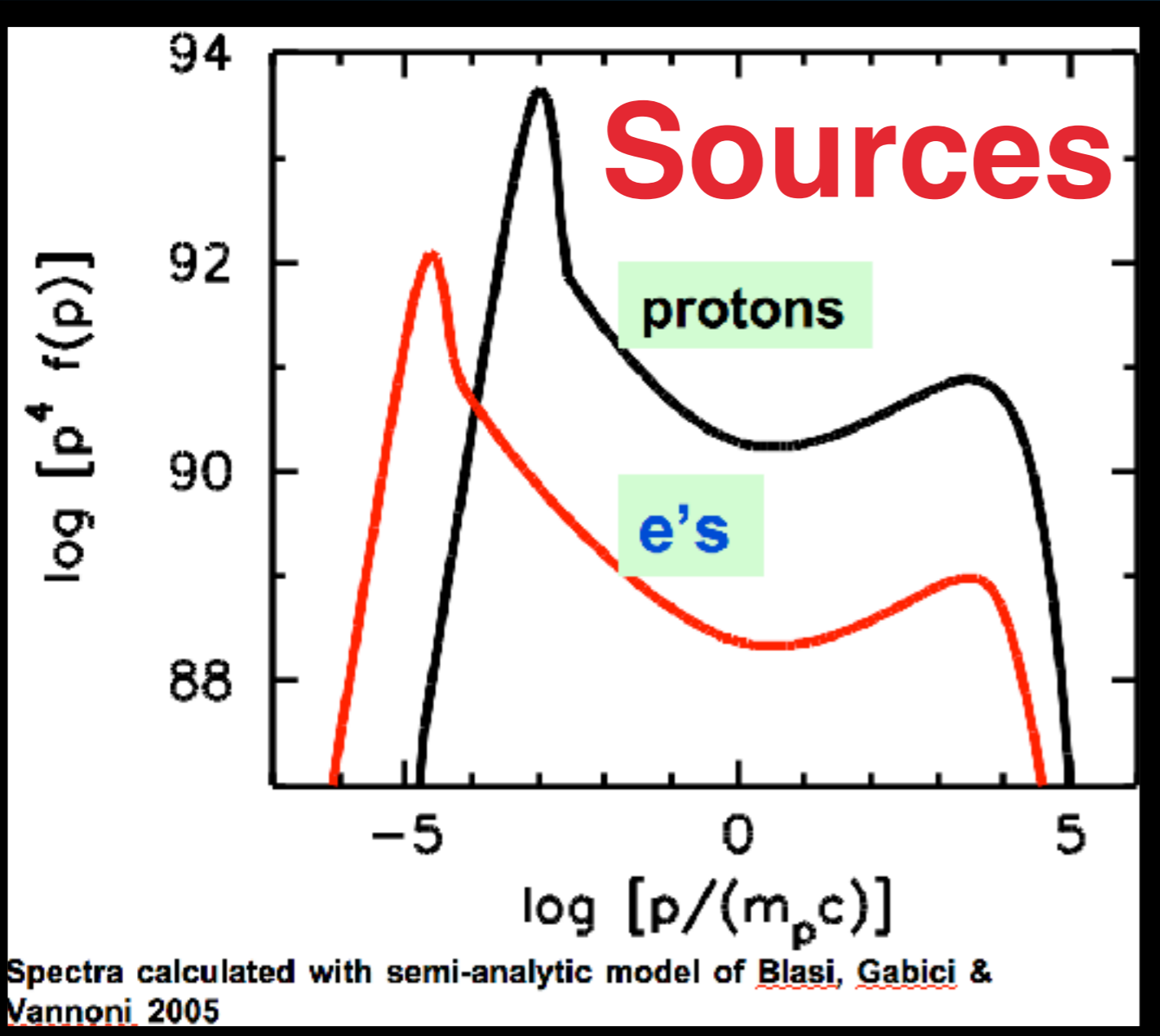
Geminga

PSR B0656+14
(Monogem)

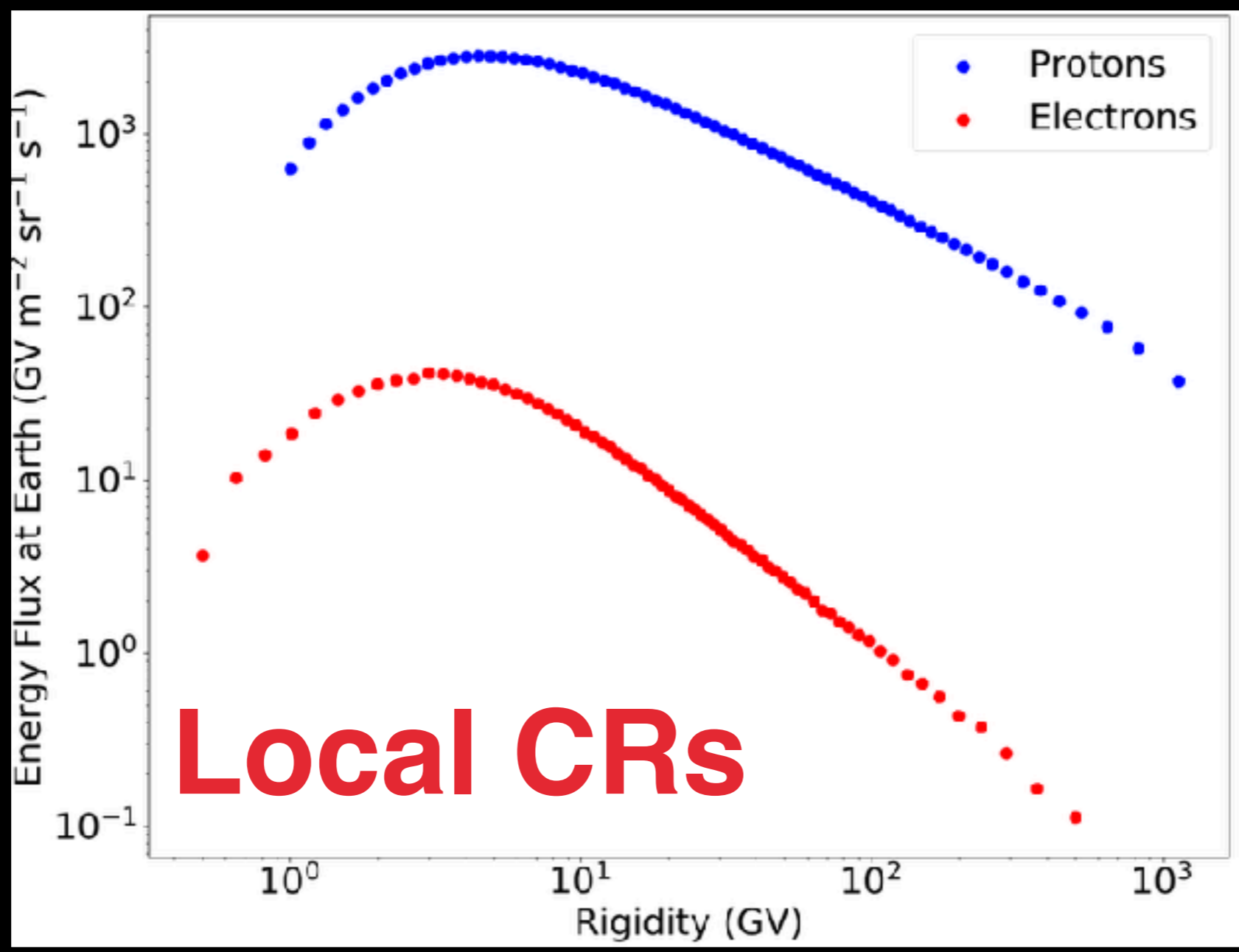


The Hadronic Fairy Tale

A UNIVERSE DOMINATED BY PROTONS



A UNIVERSE DOMINATED BY PROTONS



94
92
90
88

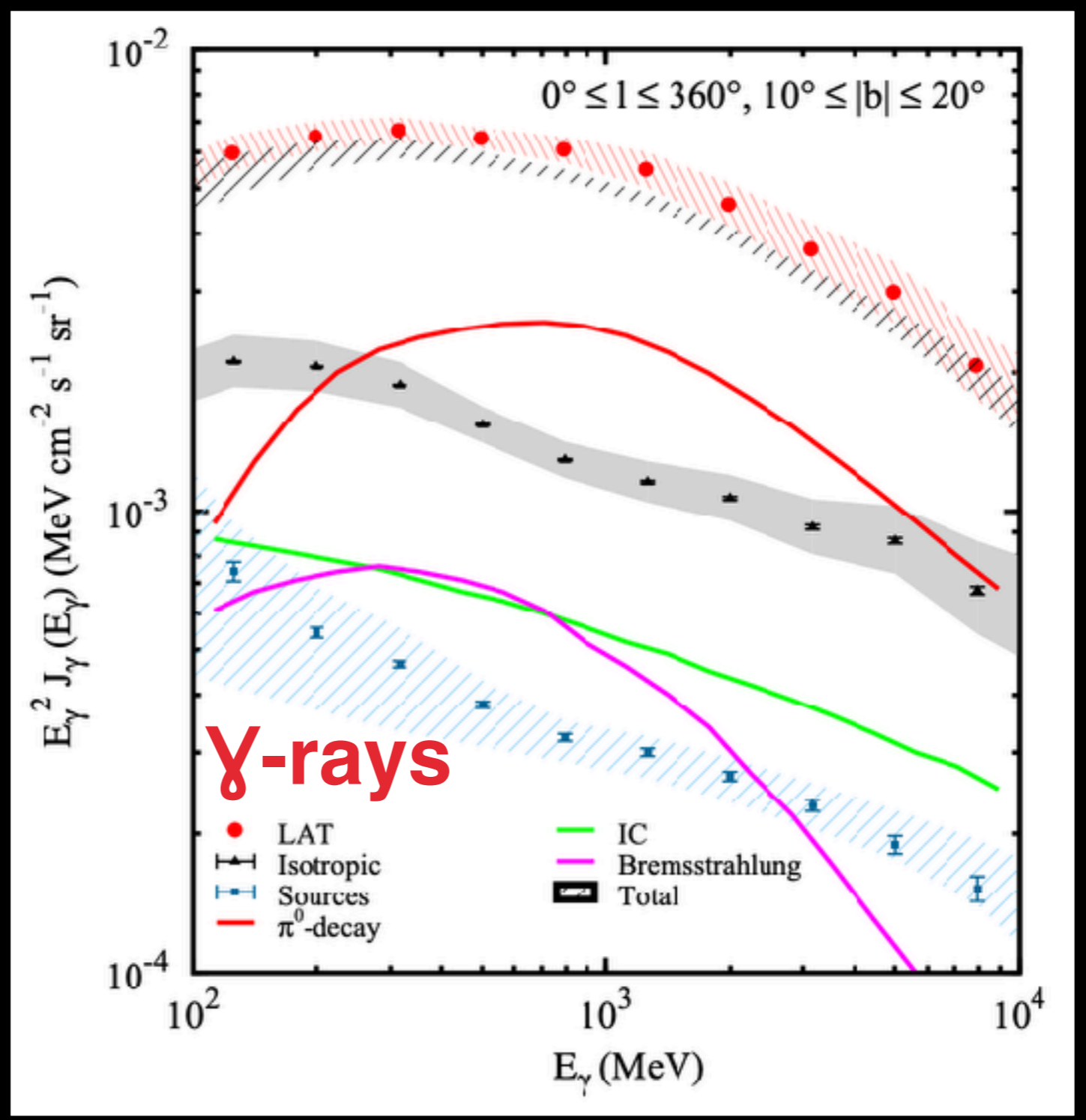
$\log [p^4 f(p)]$

Spectra calculated
Vannoni 2005



A UNIVERSE DOMINATED BY PROTONS

Sources



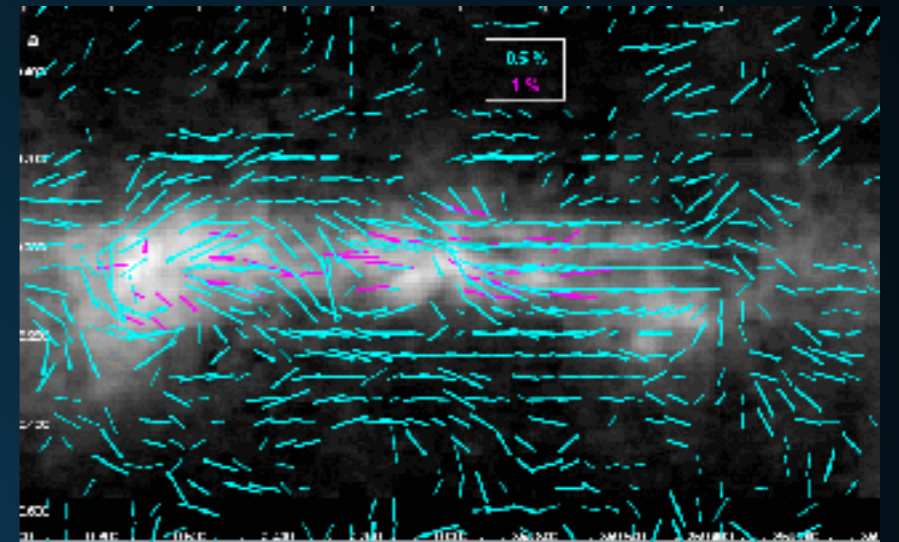
Spectra calculated with semi-analytic model
Vannoni 2005

COSMIC-RAY ACCELERATION AND PROPAGATION

Start with a source of relativistic cosmic-rays



cosmic rays propagate



$$\frac{\partial \psi}{\partial t} = q(\vec{r}, p) + \vec{\nabla} \cdot (D_{xx} \vec{\nabla} \psi - \vec{V} \psi) + \frac{\partial}{\partial p} p^2 D_{pp} \frac{\partial}{\partial p} \frac{1}{p^2} \psi - \frac{\partial}{\partial p} \left[\dot{p} \psi - \frac{p}{3} (\vec{\nabla} \cdot \vec{V}) \psi \right] - \frac{1}{\tau_f} \psi - \frac{1}{\tau_r} \psi$$

Solved Numerically:
e.g. Galprop

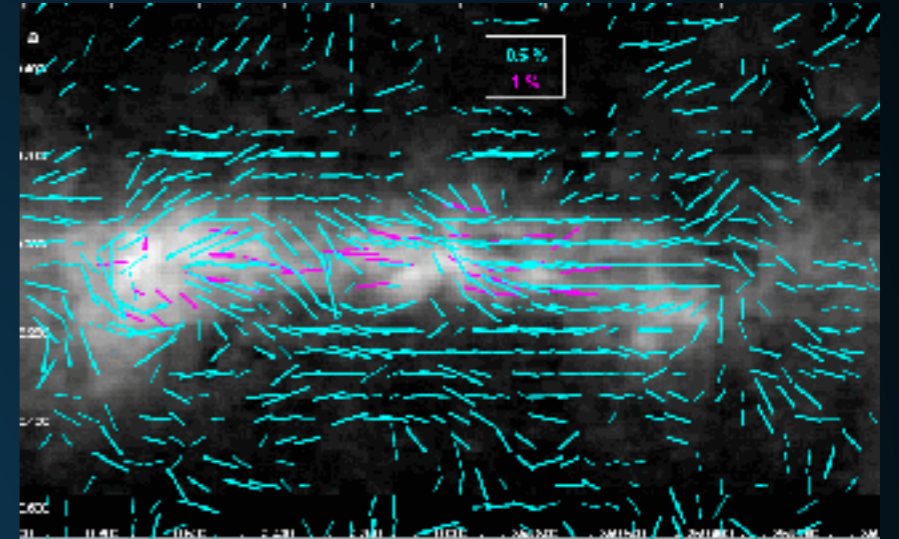
- If they propagate to Earth, can be detected:
 - AMS-02/PAMELA
 - CREAM/HEAT/CAPRICE

COSMIC-RAY ACCELERATION AND PROPAGATION

Start with a source of relativistic cosmic-rays



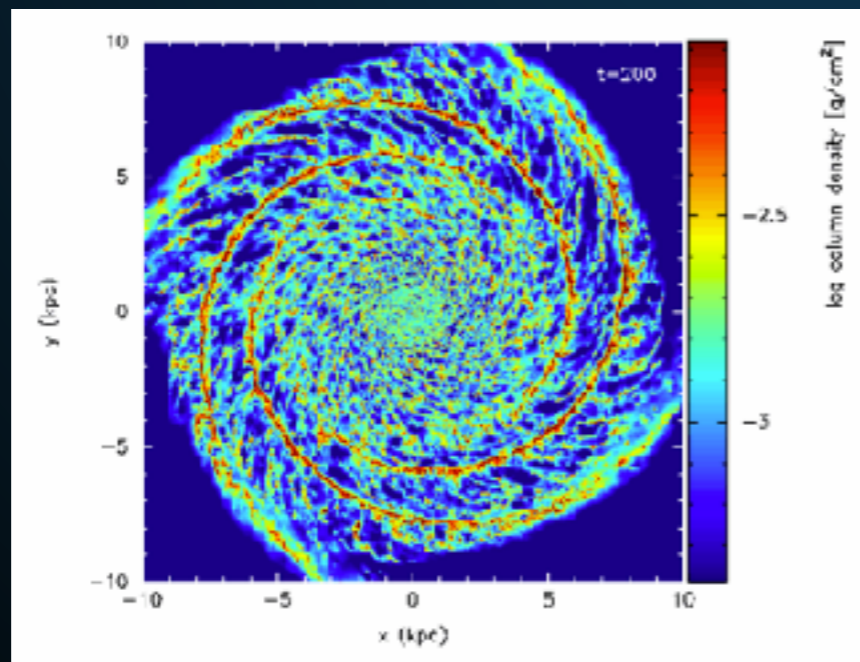
cosmic rays propagate



$$\frac{\partial \psi}{\partial t} = q(\vec{r}, p) + \vec{\nabla} \cdot (D_{xx} \vec{\nabla} \psi - \vec{V} \psi) + \frac{\partial}{\partial p} p^2 D_{pp} \frac{\partial}{\partial p} \frac{1}{p^2} \psi - \frac{\partial}{\partial p} \left[p \psi - \frac{p}{3} (\vec{\nabla} \cdot \vec{V}) \psi \right] - \frac{1}{\tau_f} \psi - \frac{1}{\tau_r} \psi$$

Solved Numerically:
e.g. Galprop

Gas/ISRF



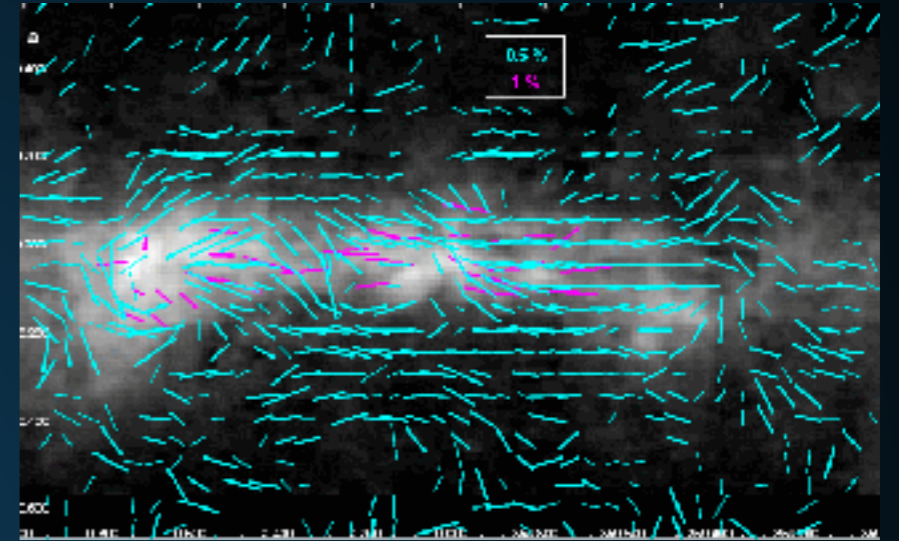
- Alternatively can collide with Galactic gas or the interstellar radiation field.

COSMIC-RAY ACCELERATION AND PROPAGATION

Start with a source of relativistic cosmic-rays



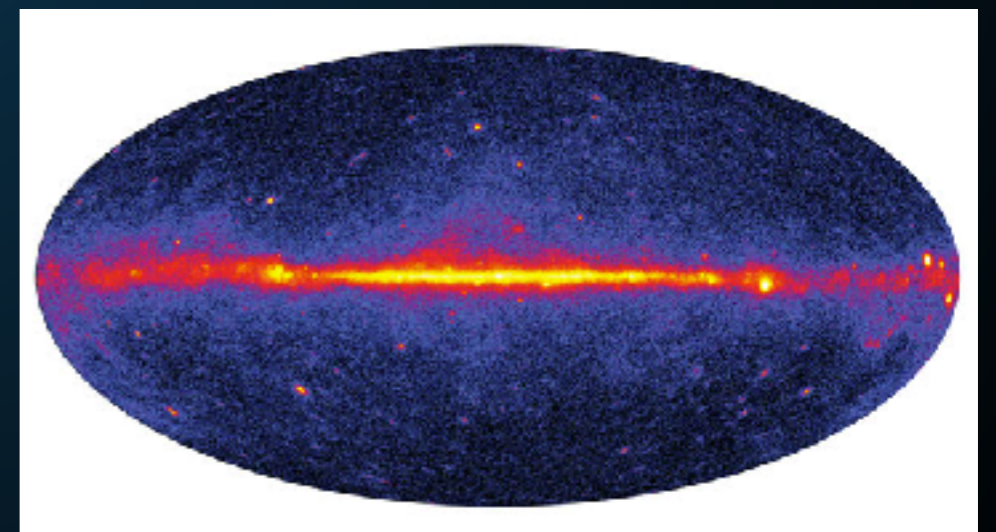
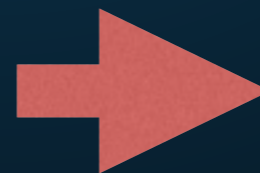
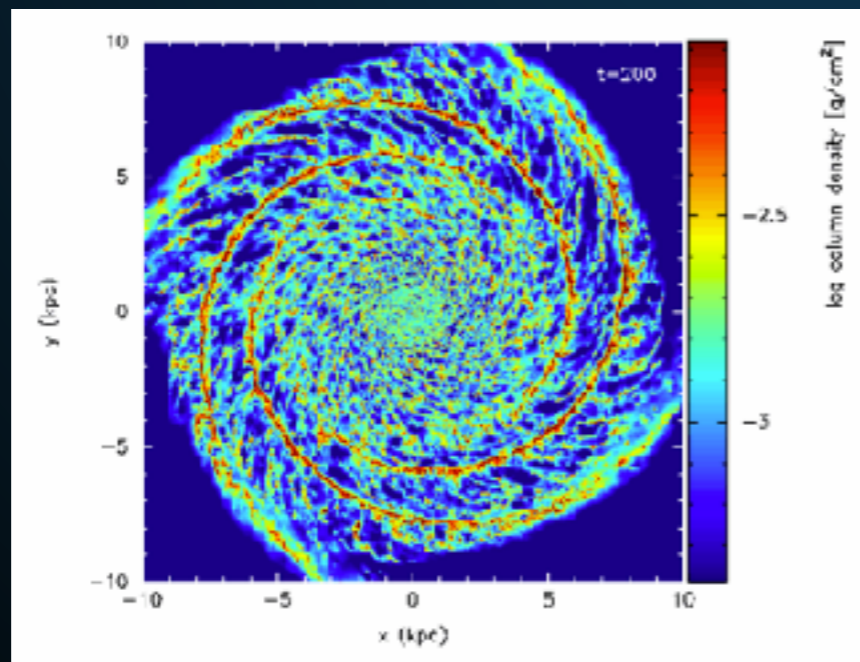
cosmic rays propagate



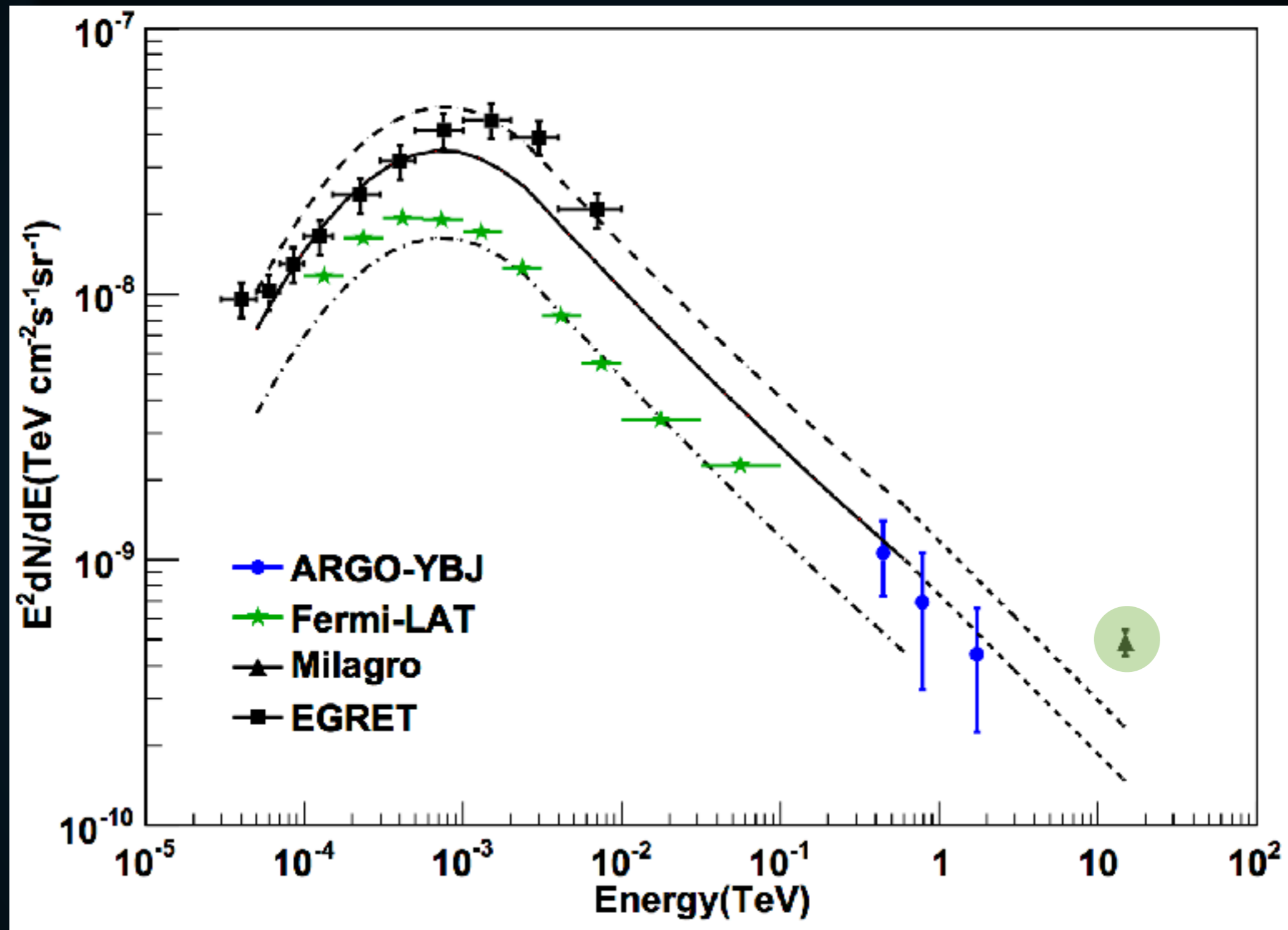
$$\frac{\partial \psi}{\partial t} = q(\vec{r}, p) + \vec{\nabla} \cdot (D_{xx} \vec{\nabla} \psi - \vec{V} \psi) + \frac{\partial}{\partial p} p^2 D_{pp} \frac{\partial}{\partial p} \frac{1}{p^2} \psi - \frac{\partial}{\partial p} \left[p \psi - \frac{p}{3} (\vec{\nabla} \cdot \vec{V}) \psi \right] - \frac{1}{\tau_f} \psi - \frac{1}{\tau_r} \psi$$

Solved Numerically:
e.g. Galprop

Gas/ISRF



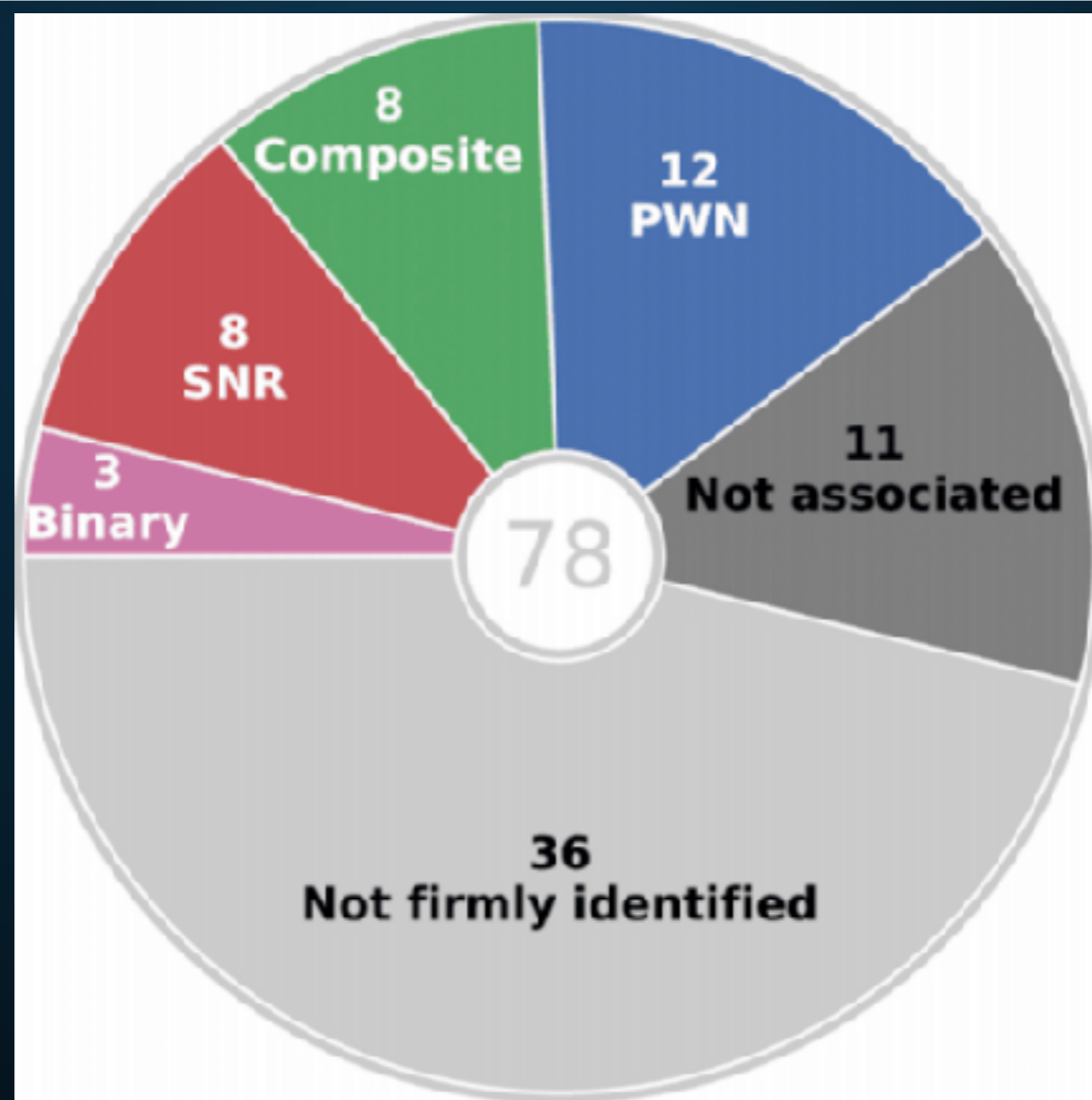
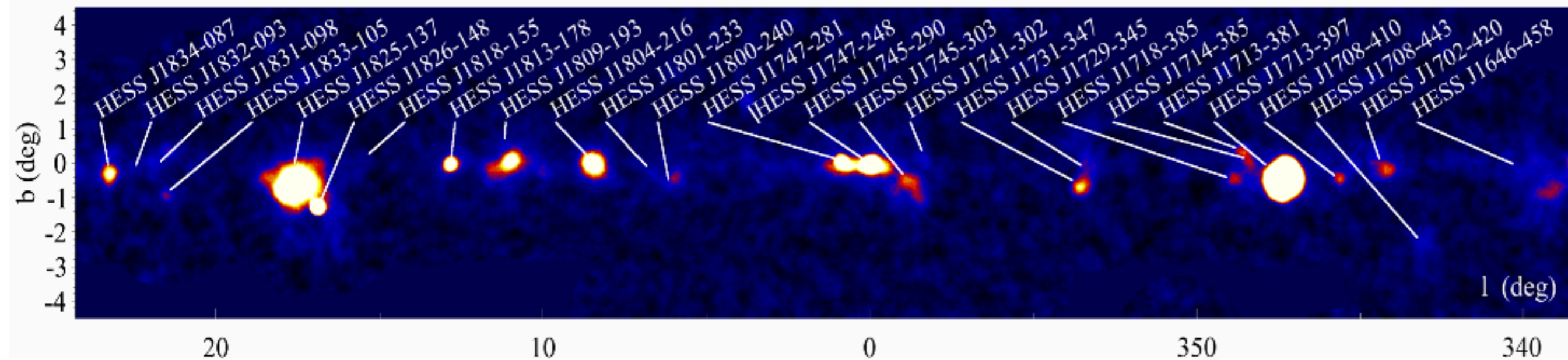
Cracks in the story...

CRACKS IN THE STORY

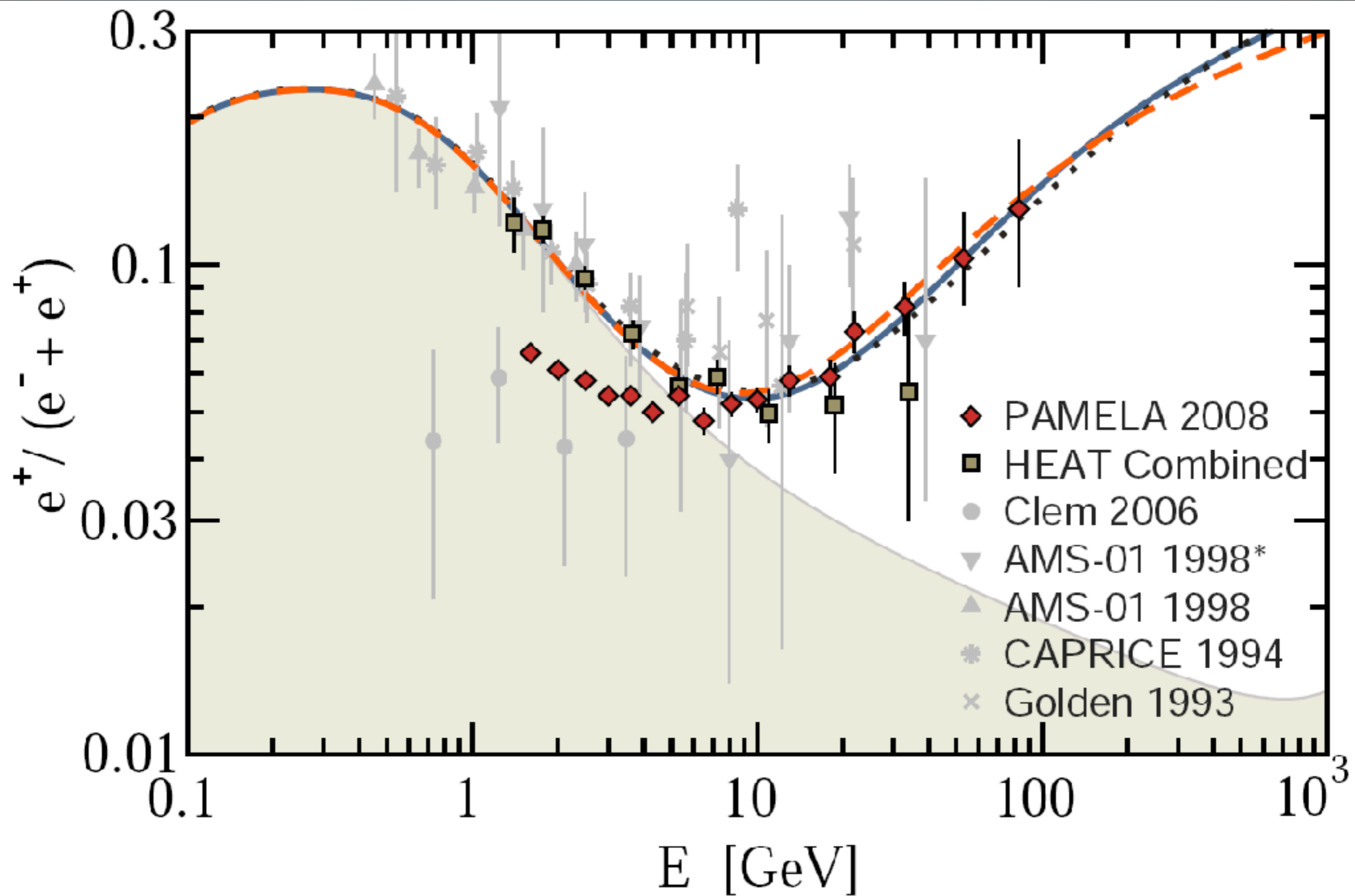
- **Milagro observations found an excess in TeV gamma-ray emission along the Galactic plane.**

CRACKS IN THE STORY

HESS Collaboration 2018



CRACKS IN THE STORY

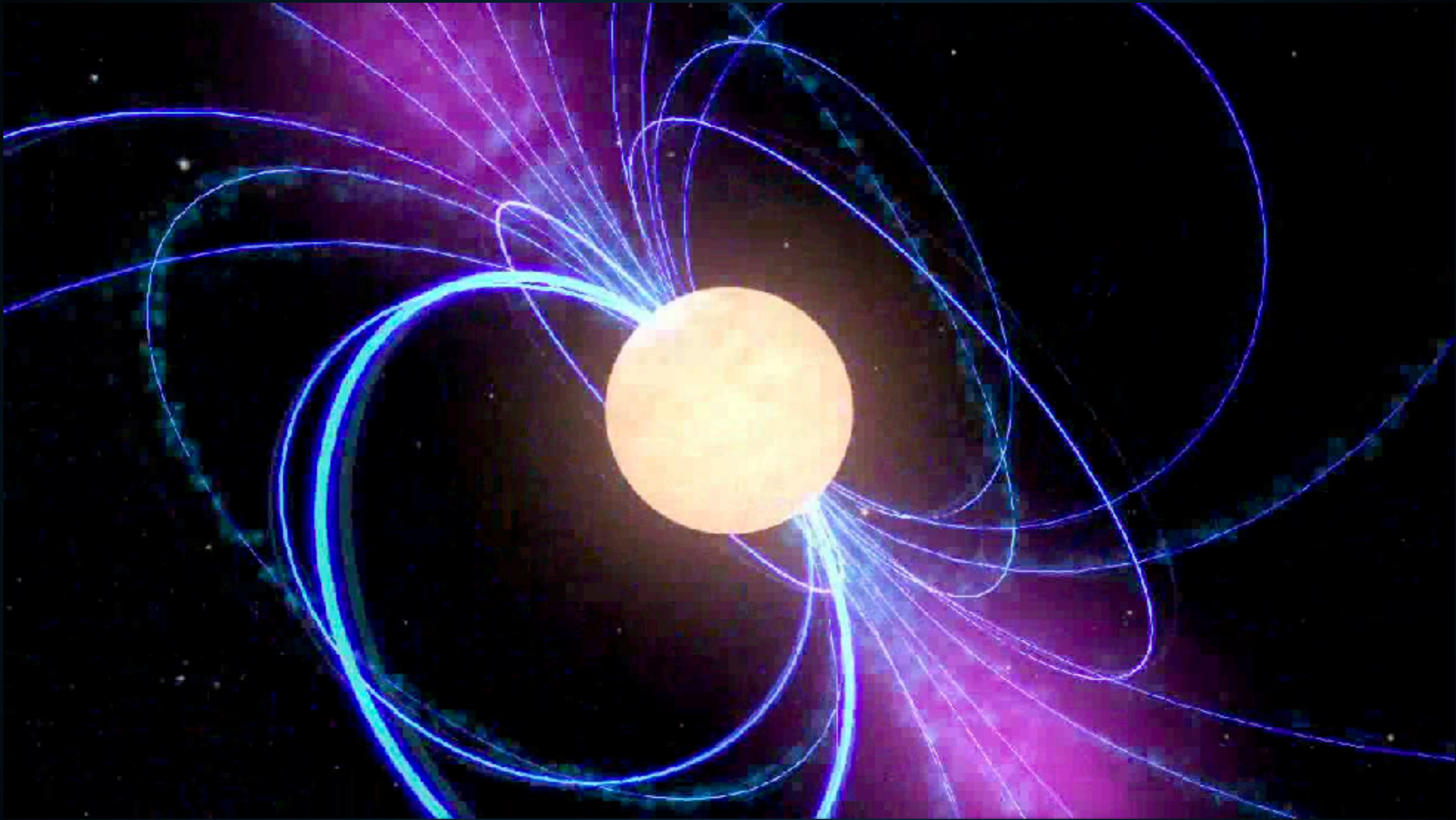


A NEW PICTURE

- **In this talk, I will argue that electrons and positrons dominate the Milky Way's energetics at TeV energies:**
 - **1.) Pulsars dominate the diffuse TeV gamma-ray emission.**
 - **2.) Pulsars produce the majority of the bright TeV sources.**
 - **3.) Pulsars are responsible for the rising positron fraction.**

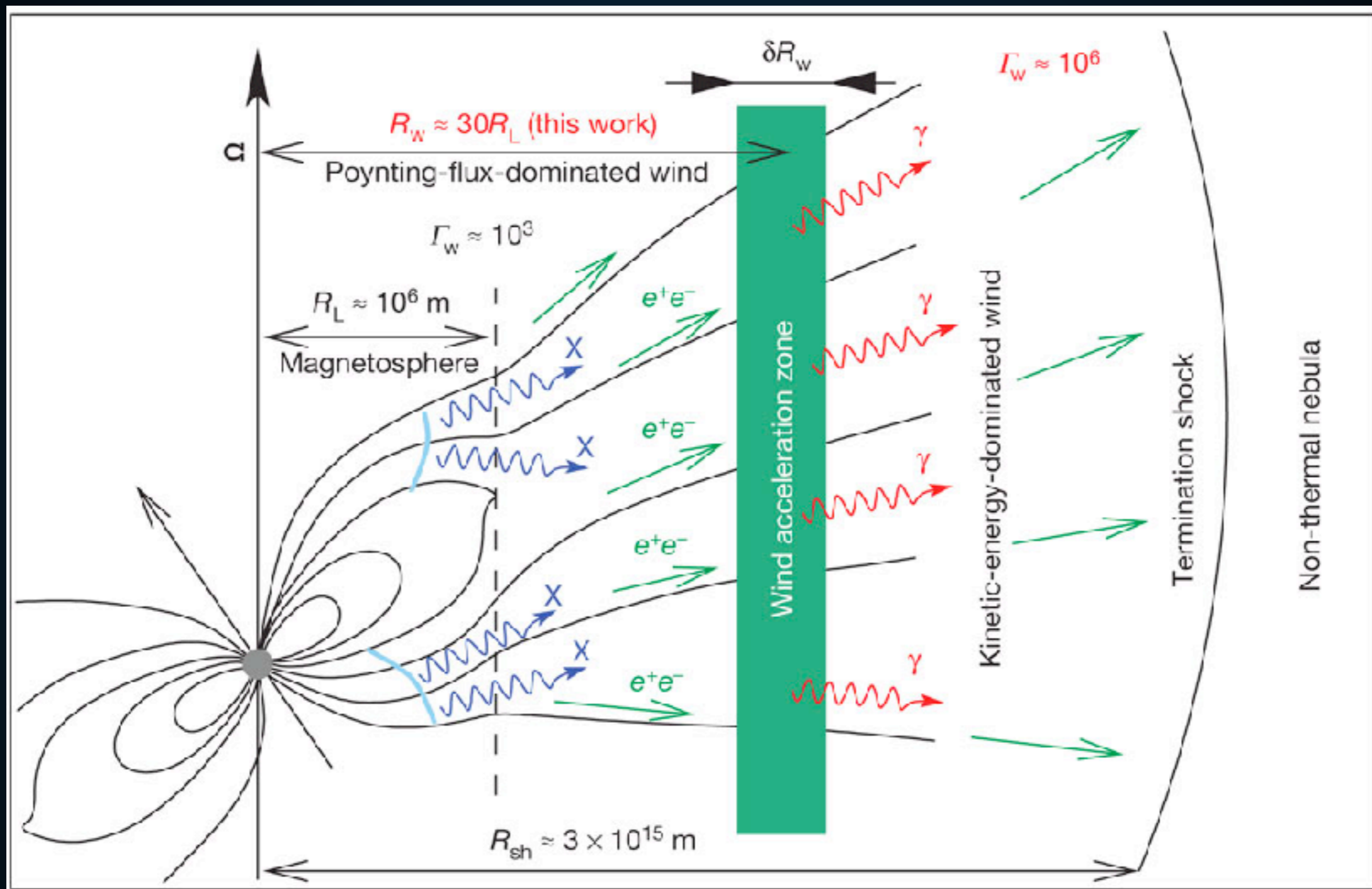
What do we know about pulsars?

PULSARS AS ASTROPHYSICAL ACCELERATORS



- **Rotational Kinetic Energy of the neutron star is the ultimate power source of all emission in this problem.**

PRODUCTION OF ELECTRON AND POSITRON PAIRS



- **Electrons boiled off of the pulsar surface produce e^+e^- pairs.**
- **Final e^+e^- Spectrum is model dependent.**

REACCELERATION IN THE PULSAR WIND NEBULA



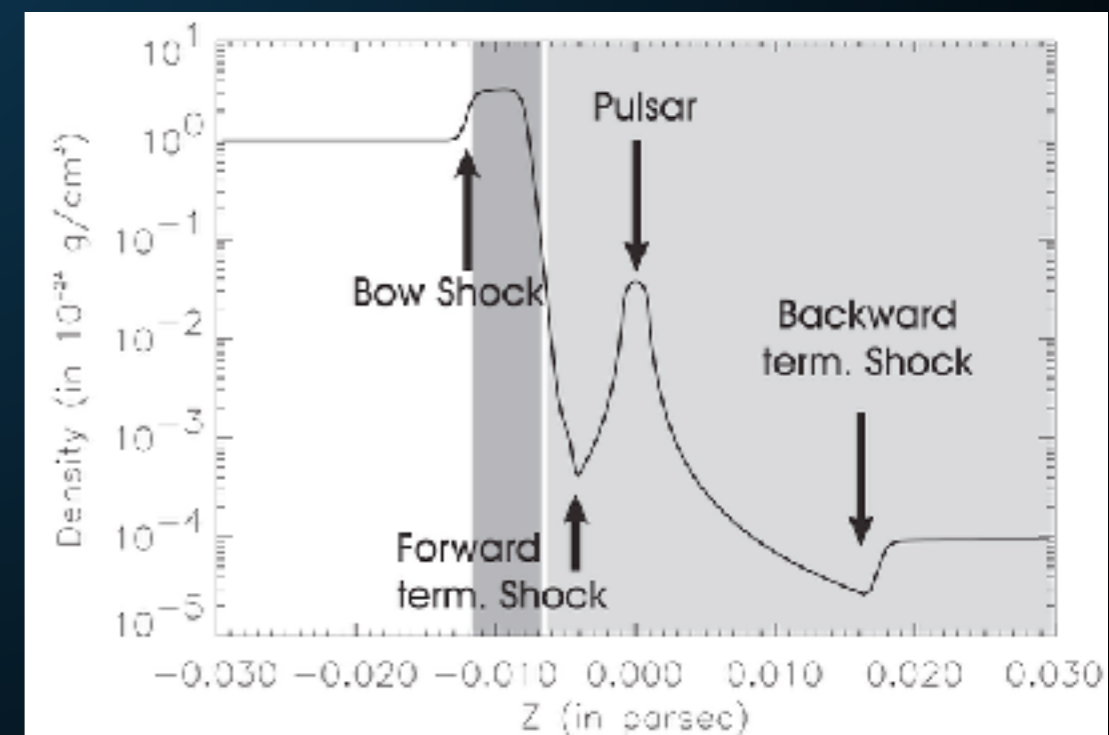
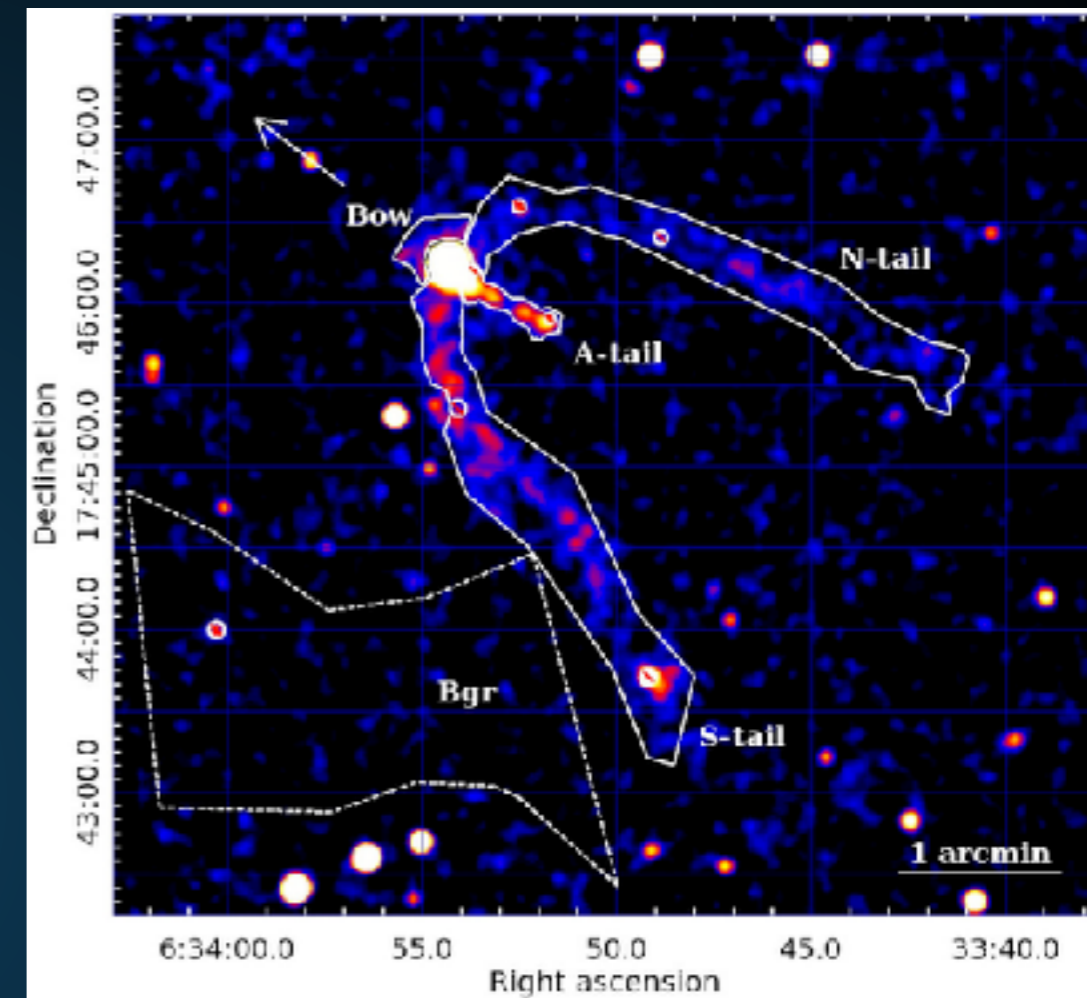
Blandford & Ostriker (1978)
Hoshino et al. (1992)
Coroniti (1990)
Sironi & Spitkovsky (2011)

- **PWN termination shock:**
 - **Voltage Drop > 30 PV**
 - **e^+e^- energy > 1 PeV**
(known from synchrotron)
- **Resets e^+e^- spectrum.**
- **Many Possible Models:**
 - **1st Order Fermi-Acceleration**
 - **Magnetic Reconnection**
 - **Shock-Driven Reconnection**

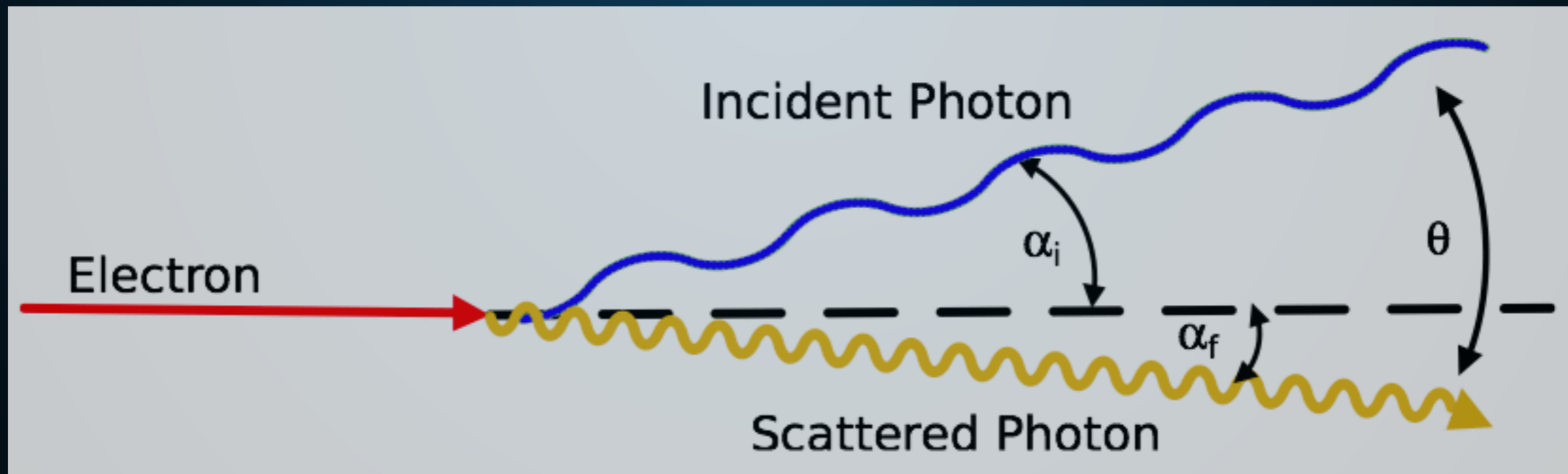
- **Extent of radio and X-Ray PWN is approximately 1 pc.**
- **Termination shock produced when ISM energy density stops the relativistic pulsar wind.**

$$R_{\text{PWN}} \simeq 1.5 \left(\frac{\dot{E}}{10^{35} \text{ erg/s}} \right)^{1/2} \times \left(\frac{n_{\text{gas}}}{1 \text{ cm}^{-3}} \right)^{-1/2} \left(\frac{v}{100 \text{ km/s}} \right)^{-3/2} \text{ pc}$$

- **NOTE: The radial extent of PWN is explained by a known physical mechanism.**



High energy electrons should also make gamma-rays.



New Observations!



HAWC OBSERVATIONS OF GEMINGA AND MONOGEM



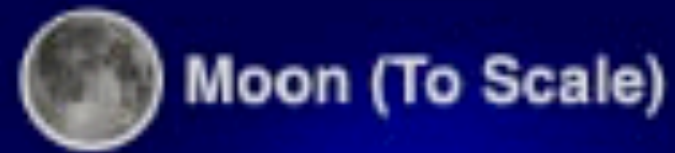
- Angular Resolution

Geminga

PSR B0656+14

- Geminga
 - $4.9 \times 10^{-14} \text{ TeV}^{-1} \text{ cm}^{-2} \text{ s}^{-1}$ (7 TeV)
 - $1.4 \times 10^{31} \text{ TeV s}^{-1}$ (7 TeV)
 - 25 pc extension
 - 300 kyr

HAWC OBSERVATIONS OF GEMINGA AND MONOGEM



- Angular Resolution

Geminga

PSR B0656+14

- Monogem
 - $2.3 \times 10^{-14} \text{ TeV}^{-1} \text{ cm}^{-2} \text{ s}^{-1}$ (7 TeV)
 - $1.1 \times 10^{31} \text{ TeV s}^{-1}$ (7 TeV)
 - 25 pc extension
 - 110 kyr

HAWC OBSERVATIONS OF GEMINGA AND MONOGEM



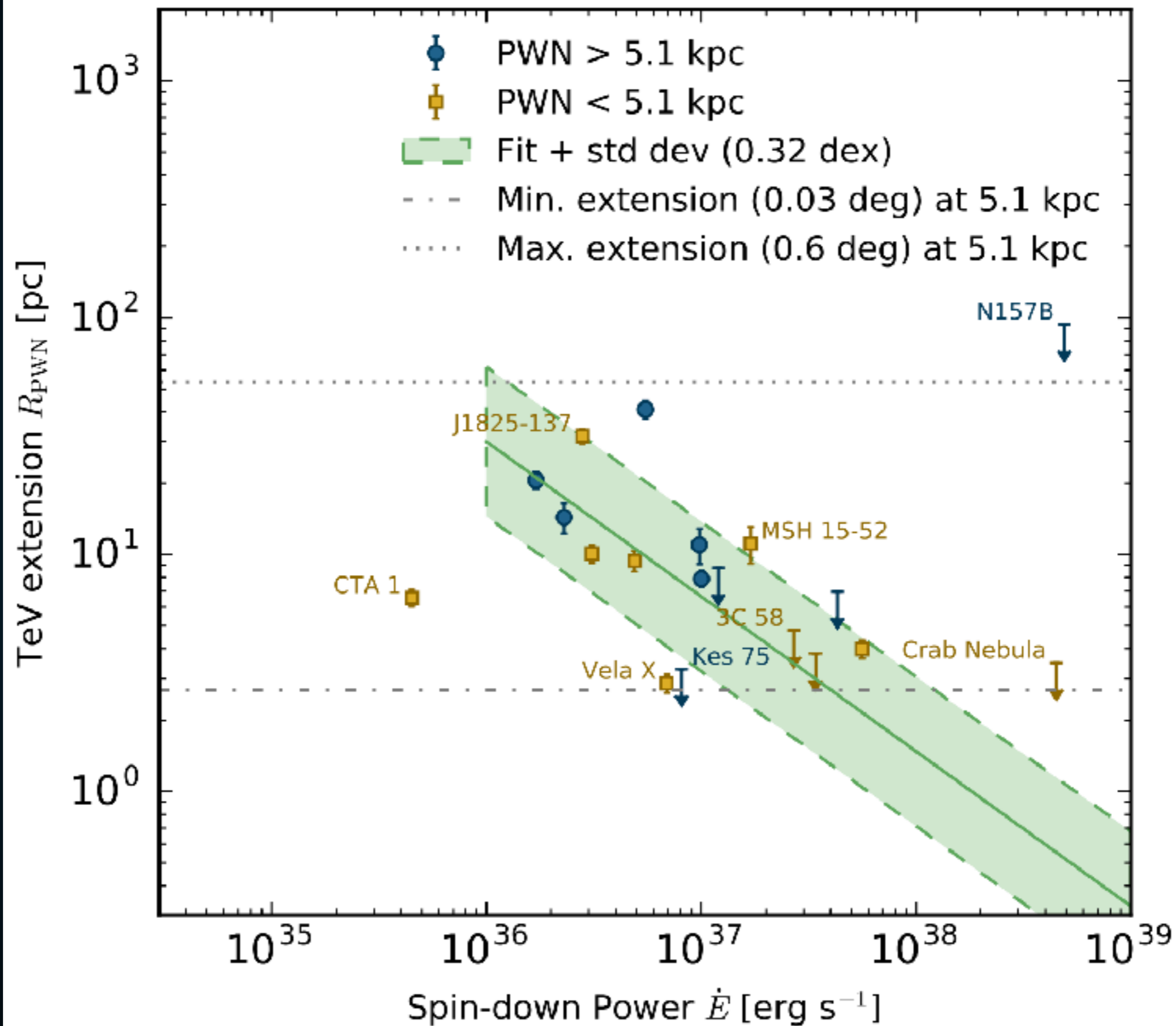
- Angular Resolution

Geminga

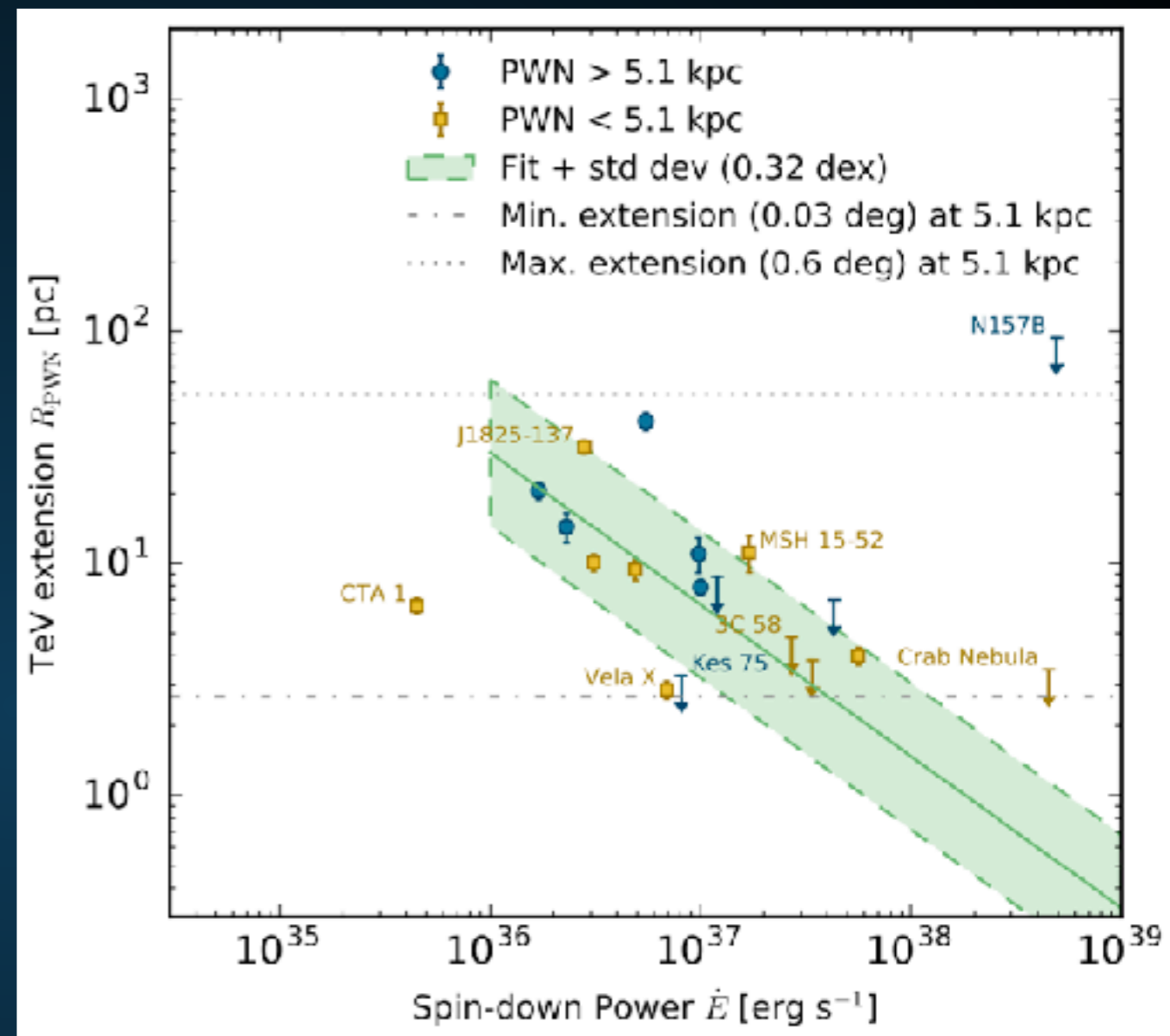
PSR B0656+14

- Emission is:
 - Very hard spectrum
 - Does not trace gas
 - **Almost certainly leptonic.**





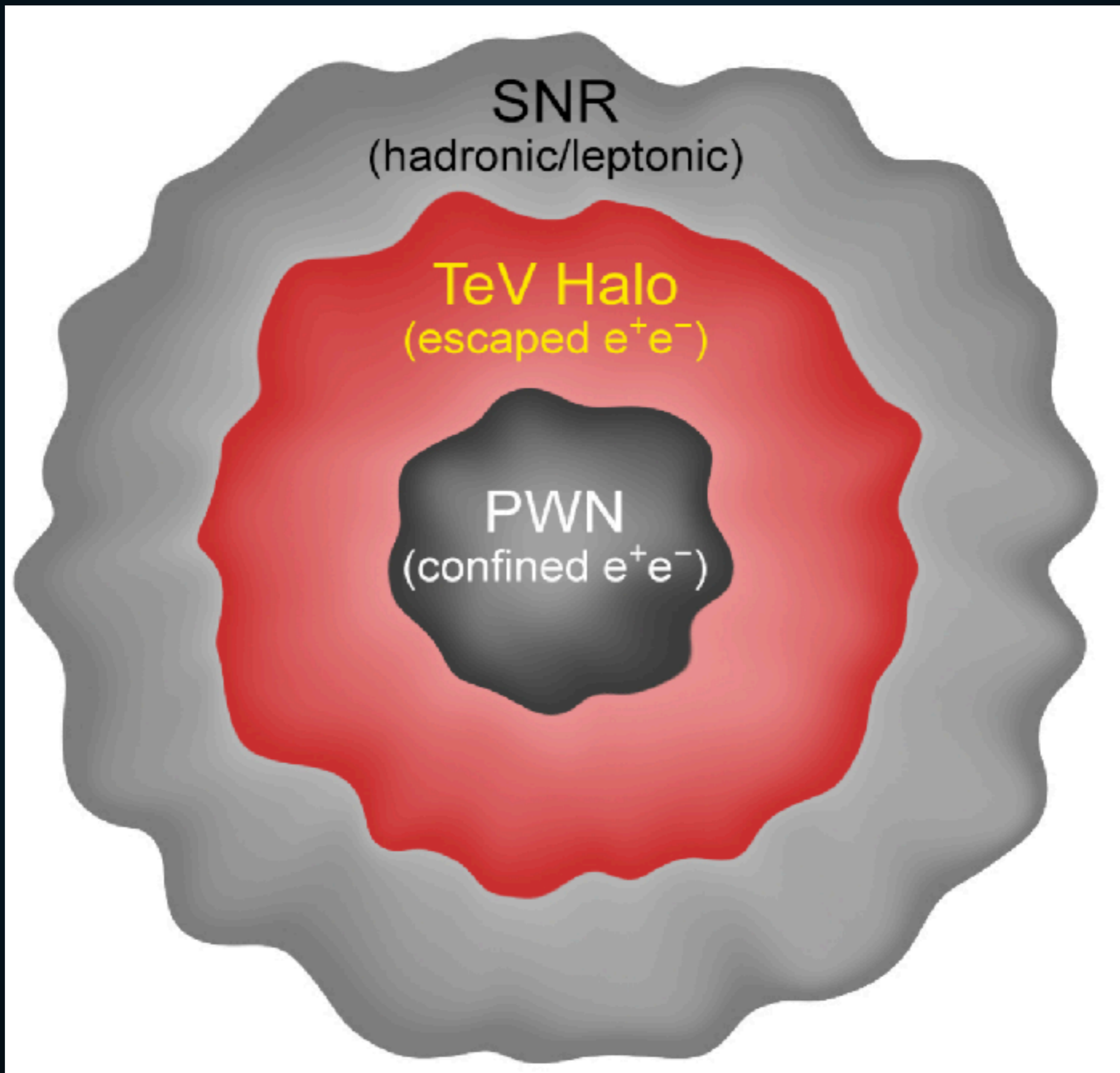
- They are much larger than the PWN.
- Especially at low-energies.



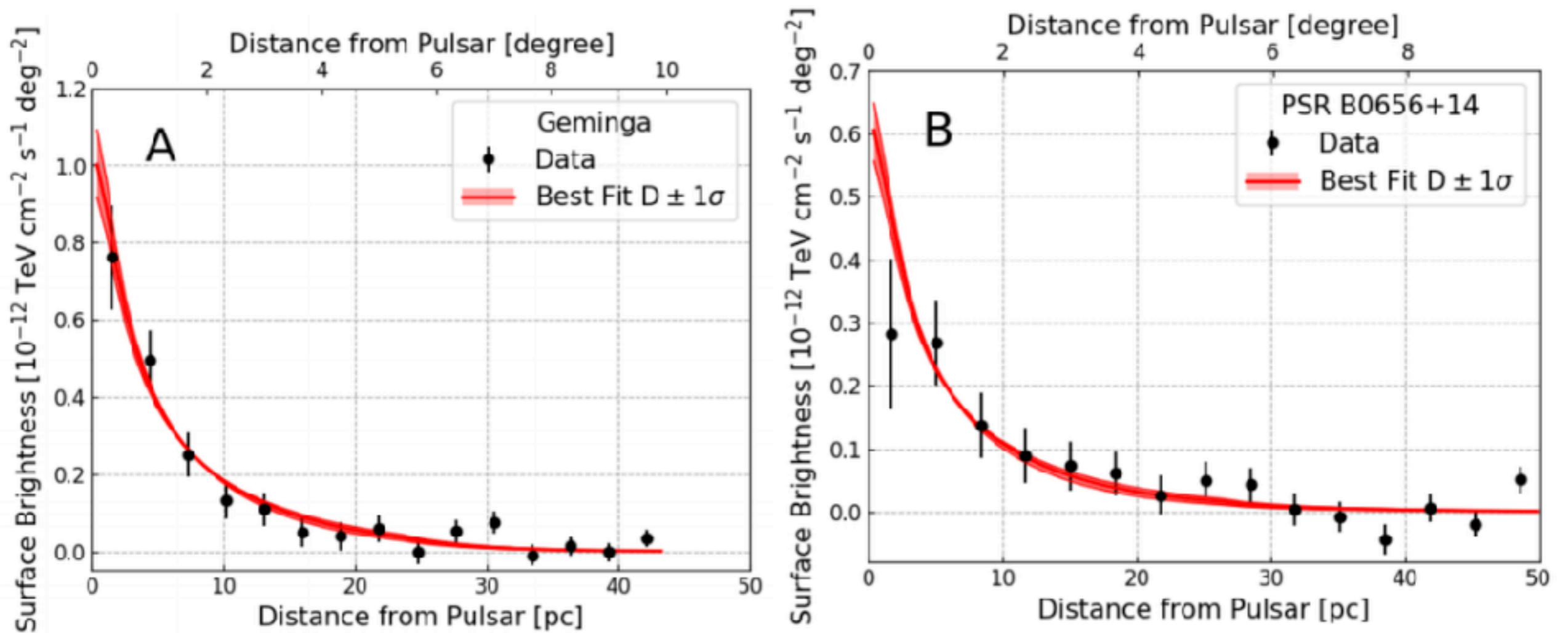
NOTE: This has the opposite energy dependence as the X-Ray PWN.

$$R_{\text{PWN}} \simeq 1.5 \left(\frac{\dot{E}}{10^{35} \text{ erg/s}} \right)^{1/2} \times \left(\frac{n_{\text{gas}}}{1 \text{ cm}^{-3}} \right)^{-1/2} \left(\frac{v}{100 \text{ km/s}} \right)^{-3/2} \text{ pc}$$

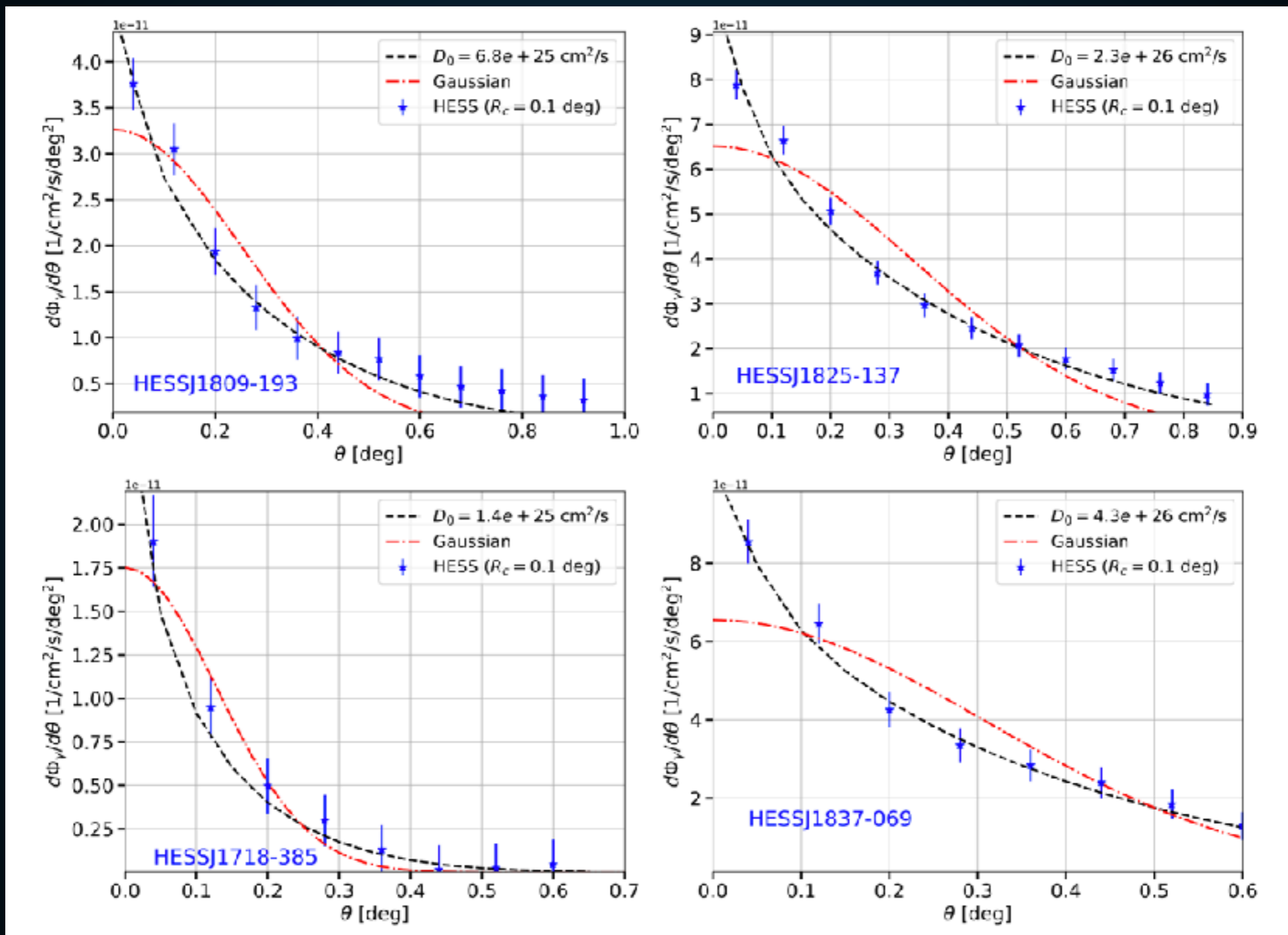
TEV HALOS



THE ELECTRONS PROPAGATE DIFFUSIVELY



- Morphology of Geminga and Monogem are fit by diffusion.
- Diffusion coefficient near the pulsar is quite small.

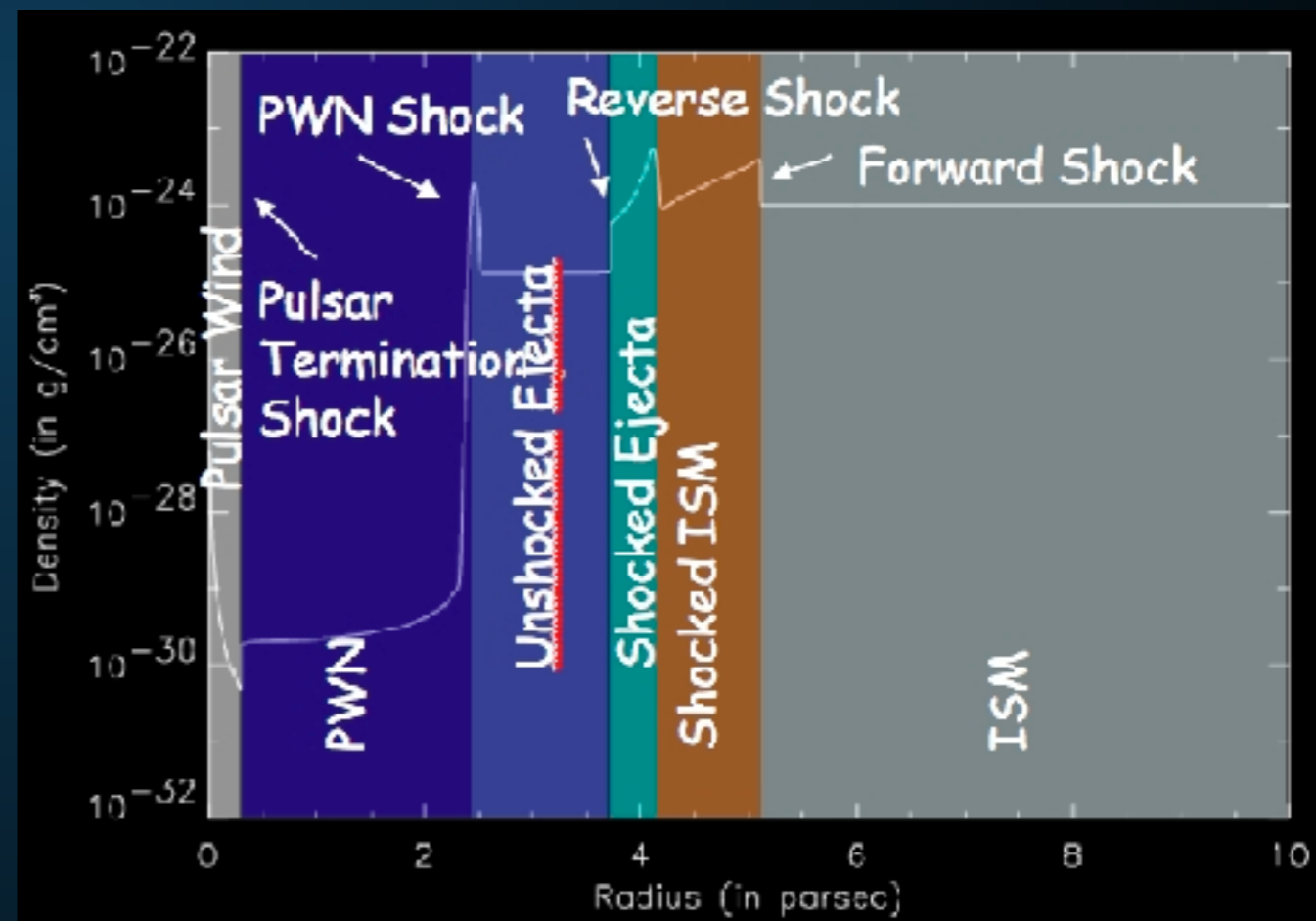


- And similar morphologies are seen in HESS sources.

TeV HALOS

- **TeV halos are a new feature**
 - **3 orders of magnitude larger than PWN in volume**
 - **Opposite energy dependence**

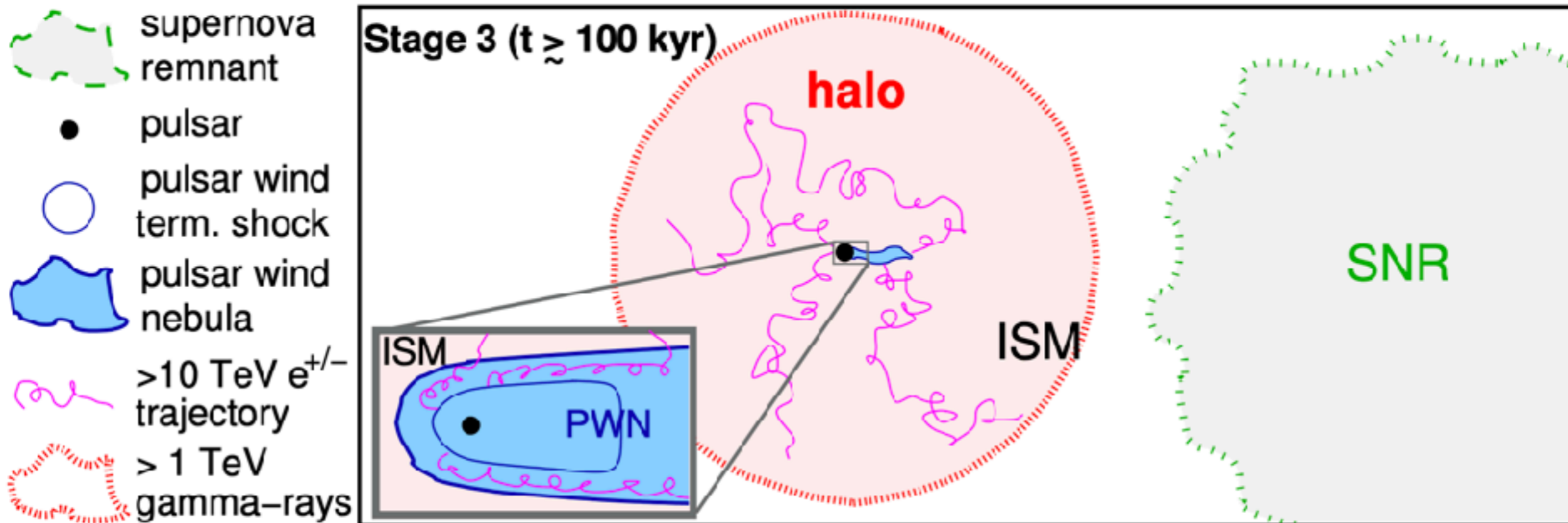
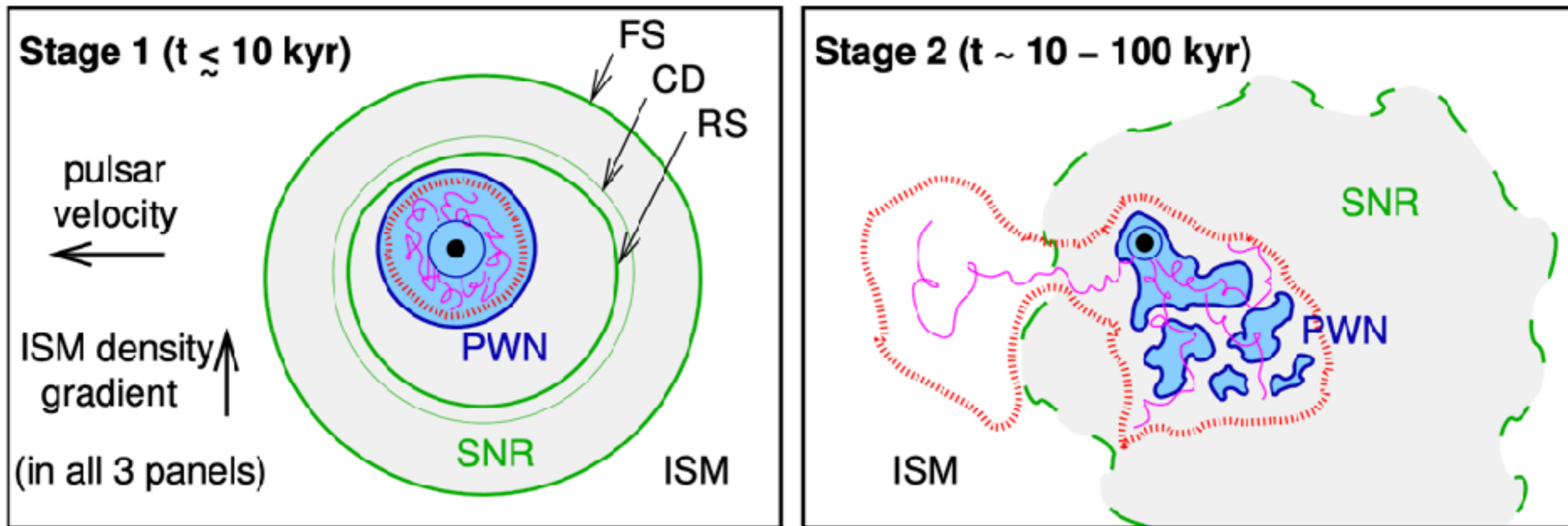
- **PWN are morphologically connected to the physics of the termination shock**
- **TeV halos need a similar morphological description.**



SOME COMPLEXITY IN TERMINOLOGY

- **An alternative definition of a “TeV halo” has been used by Giacinti et al. 2019 (1907.12121)**
- **Linden et al. (2017) - A TeV halo is a leptonic gamma-ray source surrounding a pulsar, where the electrons are diffusing through the medium (rather than being driven by convective pulsar winds).**
- **Giacinti et al. (2019) - A TeV halo is a leptonic gamma-ray source surrounding a pulsar, where the emission stems from a region where the electron density falls below the ambient ISM electron density.**

SOME COMPLEXITY IN TERMINOLOGY



We'll go back to the model later...

What do TeV observations tell us about pulsars?

TEV HALOS - AN EMPIRICAL MODEL

- **Assume that every pulsar converts an equivalent fraction of its spin down power into gamma-rays, with the same spectrum as Geminga.**
- **This statement is well supported:**
 - **Observed because they are the two closest sources.**
 - **Many similar HESS Sources**

TEV HALOS - AN EMPIRICAL MODEL

- Assume that every pulsar converts an equivalent fraction of its spin down power into gamma-rays, with the same spectrum as Geminga.

| ATNF Name | Dec. (°) | Distance (kpc) | Age (kyr) | Spindown Lum. (erg s^{-1}) | Spindown Flux ($\text{erg s}^{-1} \text{kpc}^{-2}$) | 2HWC |
|------------|----------|----------------|-----------|---------------------------------------|---|----------------|
| J0633+1746 | 17.77 | 0.25 | 342 | $3.2\text{e}34$ | $4.1\text{e}34$ | 2HWC J0631+169 |
| B0656+14 | 14.23 | 0.29 | 111 | $3.8\text{e}34$ | $3.6\text{e}34$ | 2HWC J0700+143 |
| B1951+32 | 32.87 | 3.00 | 107 | $3.7\text{e}36$ | $3.3\text{e}34$ | — |
| J1740+1000 | 10.00 | 1.23 | 114 | $2.3\text{e}35$ | $1.2\text{e}34$ | — |
| J1913+1011 | 10.18 | 4.61 | 169 | $2.9\text{e}36$ | $1.1\text{e}34$ | 2HWC J1912+099 |
| J1831-0952 | -9.86 | 3.68 | 128 | $1.1\text{e}36$ | $6.4\text{e}33$ | 2HWC J1831-098 |
| J2032+4127 | 41.45 | 1.70 | 181 | $1.7\text{e}35$ | $4.7\text{e}33$ | 2HWC J2031+415 |
| B1822-09 | -9.58 | 0.30 | 232 | $4.6\text{e}33$ | $4.1\text{e}33$ | — |
| B1830-08 | -8.45 | 4.50 | 147 | $5.8\text{e}35$ | $2.3\text{e}33$ | — |
| J1913+0904 | 9.07 | 3.00 | 147 | $1.6\text{e}35$ | $1.4\text{e}33$ | — |
| B0540+23 | 23.48 | 1.56 | 253 | $4.1\text{e}34$ | $1.4\text{e}33$ | — |

ASSUMPTION: PULSAR POPULATION MODELS

- Use a generic model for pulsar luminosities
- $B_0 = 10^{12.5} \text{ G}$ ($\pm 10^{0.3} \text{ G}$)
- $P_0 = 0.3 \text{ s}$ ($\pm 0.15 \text{ s}$)
- Spindown Timescale of $\sim 10^4 \text{ yr}$ (depends on B_0)
- Galprop model for supernova distances

PsrPopPy: An open-source package for pulsar population simulations

D. Bates^{1,2}, D. R. Lorimer^{1,3}, A. Rane¹ and J. Swiggum¹

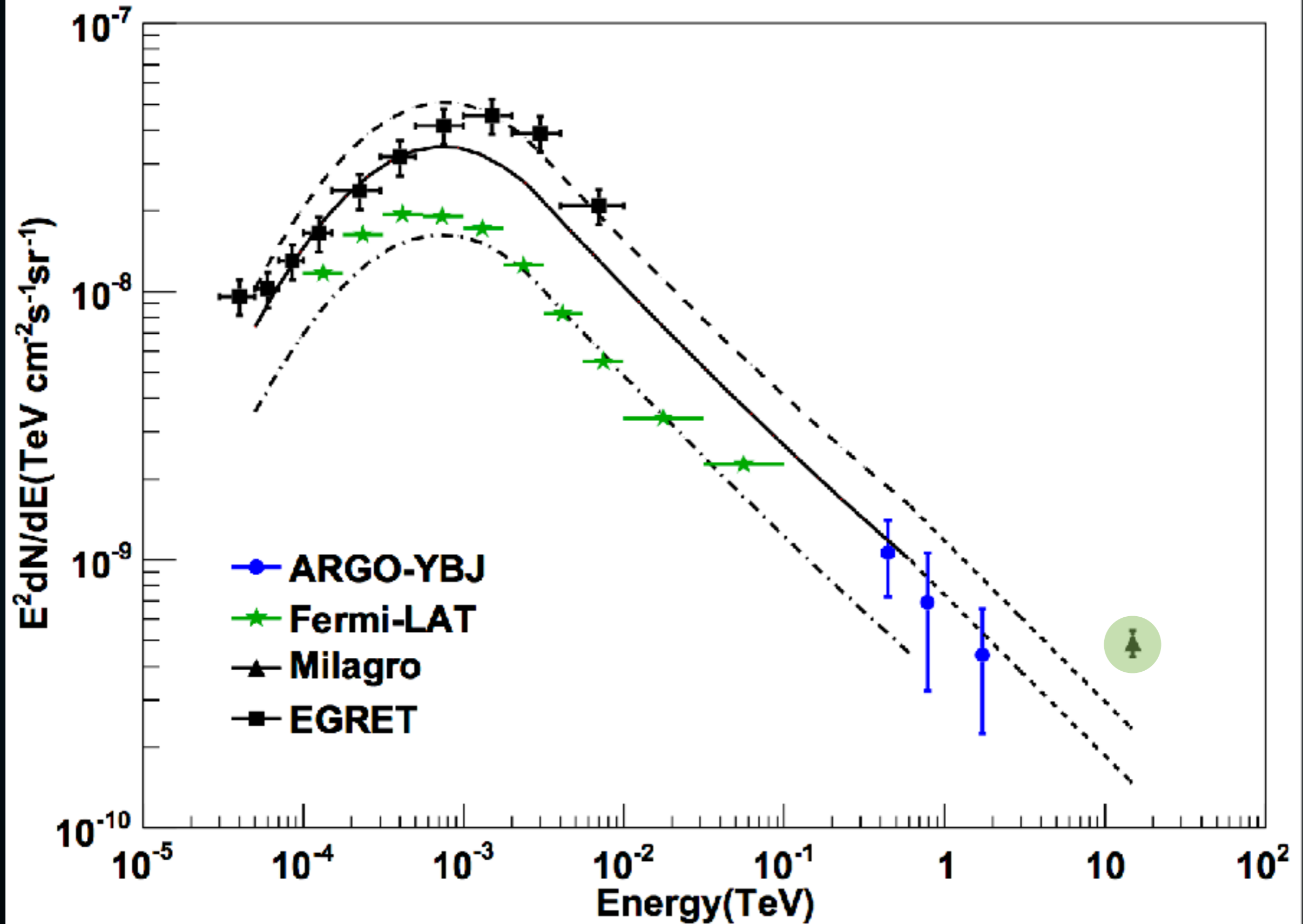
¹Department of Physics and Astronomy, West Virginia University, Morgantown, WV, 26506 USA
²Centre for Astrophysics, School of Physics and Astronomy, The University of Manchester, Manchester M13 9PL, UK
³Astronomy Observatory, PO Box 2, Green Bank, WV 24944, USA

software package for the simulation of pulsar populations. The codebase is written in Python, which remain in their original language, and improving the simulation support.

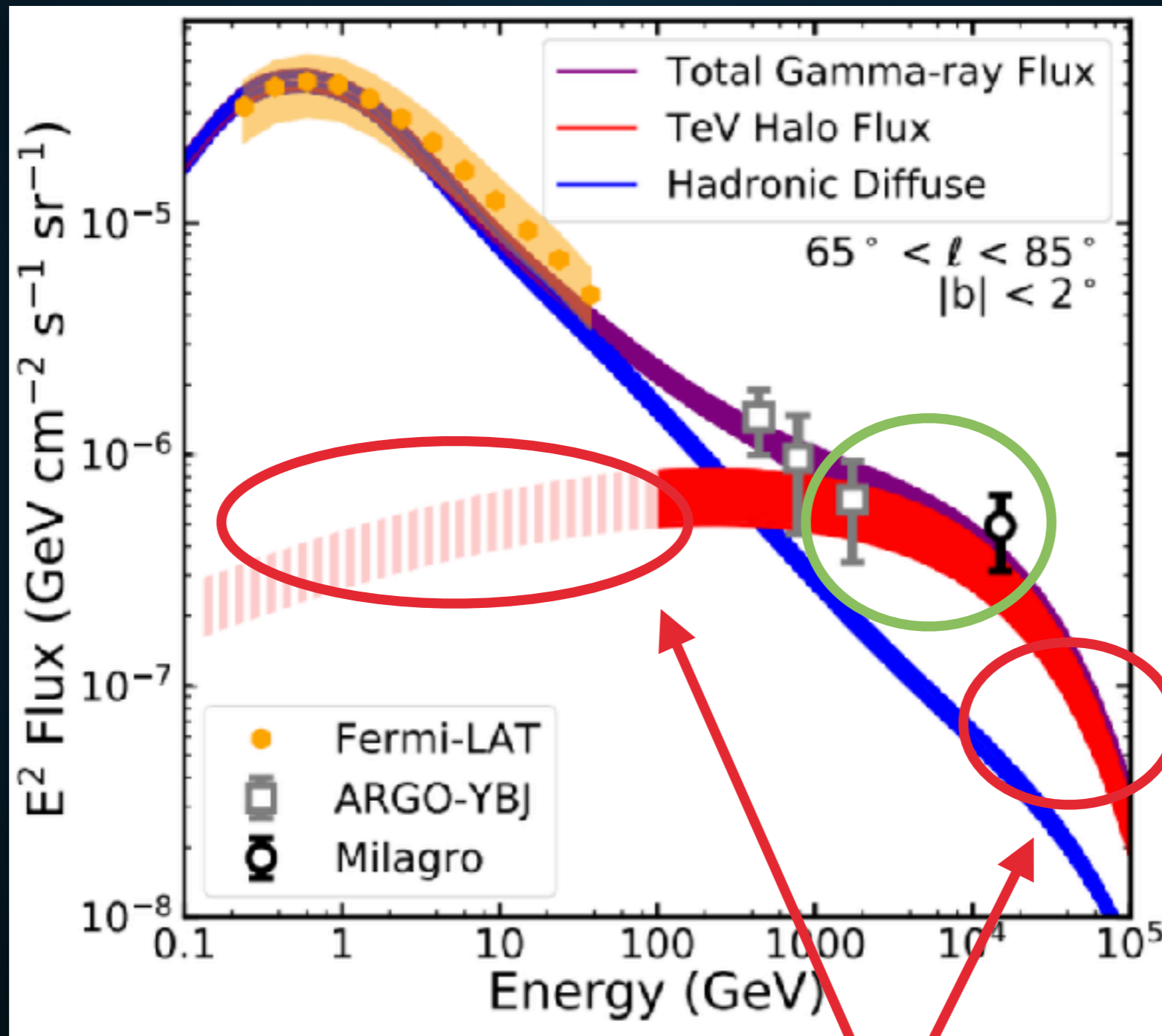
Implication I:

Most TeV emission is produced by TeV halos

IMPLICATION I: THE TEV EXCESS



- TeV halos naturally explain the TeV excess!



spectral assumption!

Implication II:

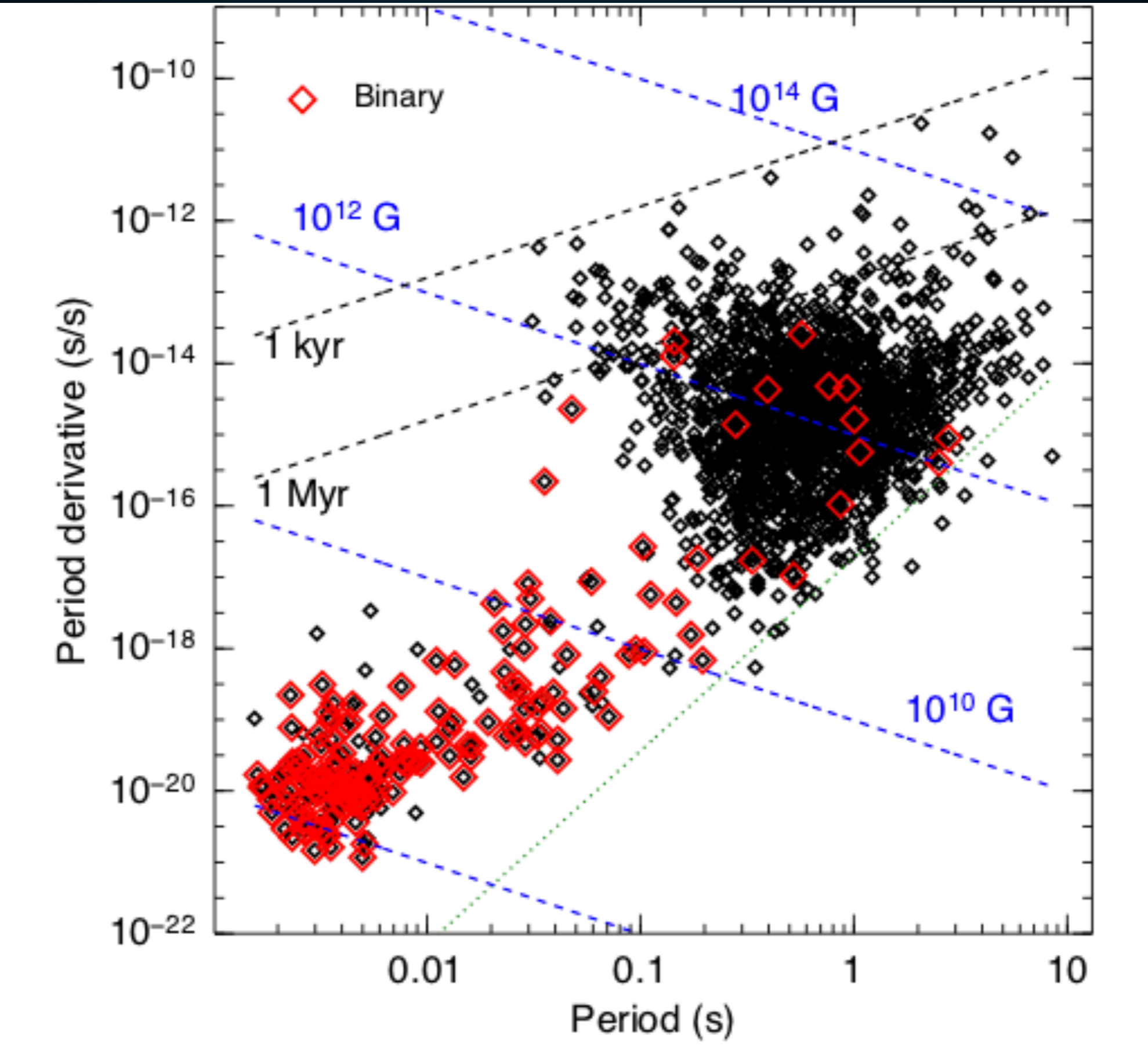
Most TeV gamma-ray sources are TeV halos.

TEV HALO NUMEROLOGY

- **HAWC has observed 39 sources.**
- **5 are coincident with old (>100 kyr) pulsars**

- **12 others coincident with young (<100 kyr) pulsars**
 - **TeV emission may be contaminated by SNR**

WHY DO WE CARE?

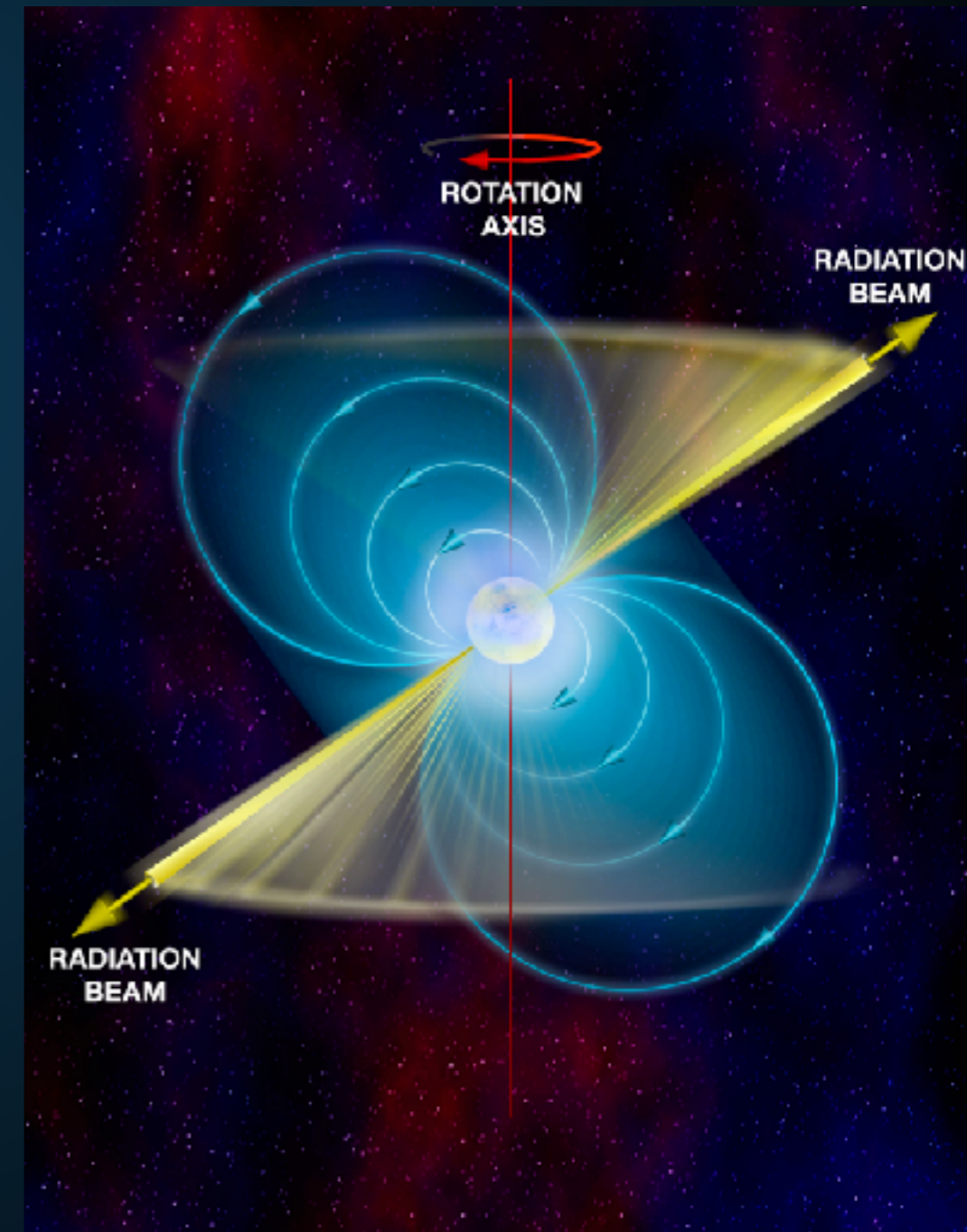


- **Radio pulsars are beamed!**

- **Beaming fraction is small**

$$f = \left[1.1 \left(\log_{10} \left(\frac{\tau}{100 \text{ Myr}} \right) \right)^2 + 15 \right] \%$$

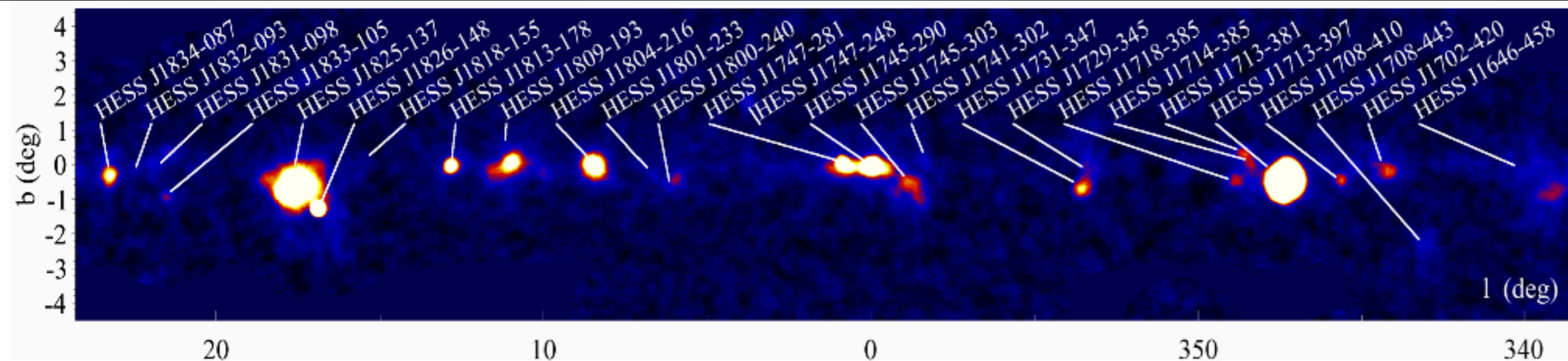
- **This varies between 15-30%.**
- **Most pulsars are unseen in radio!**



| 2HWC Name | ATNF Name | Distance (kpc) | Angular Separation | Projected Separation | Expected Flux ($\times 10^{-15}$) | Actual Flux ($\times 10^{-15}$) | Flux Ratio | Expected Extension | Actual Extension | Age (kyr) | Chance Overlap |
|-----------|------------|----------------|--------------------|----------------------|-------------------------------------|-----------------------------------|------------|--------------------|------------------|-----------|----------------|
| J0700+143 | B0656+14 | 0.29 | 0.18° | 0.91 pc | 43.0 | 23.0 | 1.87 | 2.0° | 1.73° | 111 | 0.0 |
| J0631+169 | J0633+1746 | 0.25 | 0.89° | 3.88 pc | 48.7 | 48.7 | 1.0 | 2.0° | 2.0° | 342 | 0.0 |
| J1912+099 | J1913+1011 | 4.61 | 0.34° | 27.36 pc | 13.0 | 36.6 | 0.36 | 0.11° | 0.7° | 169 | 0.30 |
| J2031+415 | J2032+4127 | 1.70 | 0.11° | 3.26 pc | 5.59 | 61.6 | 0.091 | 0.29° | 0.7° | 181 | 0.002 |
| J1831-098 | J1831-0952 | 3.68 | 0.04° | 2.57 pc | 7.70 | 95.8 | 0.080 | 0.14° | 0.9° | 128 | 0.006 |

| 2HWC Name | ATNF Name | Distance (kpc) | Angular Separation | Projected Separation | Expected Flux ($\times 10^{-15}$) | Actual Flux ($\times 10^{-15}$) | Flux Ratio | Expected Extension | Actual Extension | Age (kyr) | Chance Overlap |
|-----------|------------|----------------|--------------------|----------------------|-------------------------------------|-----------------------------------|------------|--------------------|------------------|-----------|----------------|
| J1930+188 | J1930+1852 | 7.0 | 0.03° | 3.67 pc | 23.2 | 9.8 | 2.37 | 0.07° | 0.0° | 2.89 | 0.002 |
| J1814-173 | J1813-1749 | 4.7 | 0.54° | 44.30 pc | 243 | 152 | 1.60 | 0.11° | 1.0° | 5.6 | 0.61 |
| J2019+367 | J2021+3651 | 1.8 | 0.27° | 8.48 pc | 99.8 | 58.2 | 1.71 | 0.28° | 0.7° | 17.2 | 0.04 |
| J1928+177 | J1928+1746 | 4.34 | 0.03° | 2.27 pc | 8.08 | 10.0 | 0.81 | 0.11° | 0.0° | 82.6 | 0.002 |
| J1908+063 | J1907+0602 | 2.58 | 0.36° | 16.21 pc | 40.0 | 85.0 | 0.47 | 0.2° | 0.8° | 19.5 | 0.26 |
| J2020+403 | J2021+4026 | 2.15 | 0.18° | 6.75 pc | 2.48 | 18.5 | 0.134 | 0.23° | 0.0° | 77 | 0.01 |
| J1857+027 | J1856+0245 | 6.32 | 0.12° | 13.24 pc | 11.0 | 97.0 | 0.11 | 0.08° | 0.9° | 20.6 | 0.06 |
| J1825-134 | J1826-1334 | 3.61 | 0.20° | 12.66 pc | 20.5 | 249 | 0.082 | 0.14° | 0.9° | 21.4 | 0.14 |
| J1837-065 | J1838-0655 | 6.60 | 0.38° | 43.77 pc | 12.0 | 341 | 0.035 | 0.08° | 2.0° | 22.7 | 0.48 |
| J1837-065 | J1837-0604 | 4.78 | 0.50° | 41.71 pc | 8.3 | 341 | 0.024 | 0.10° | 2.0° | 33.8 | 0.68 |
| J2006+341 | J2004+3429 | 10.8 | 0.42° | 80.07 pc | 0.48 | 24.5 | 0.019 | 0.04° | 0.9° | 18.5 | 0.08 |

- Correcting for the beaming fraction implies that 56_{-11}^{+15} TeV halos are currently observed by HAWC.
- However, only 39 total HAWC sources.



The H.E.S.S. Galactic plane survey

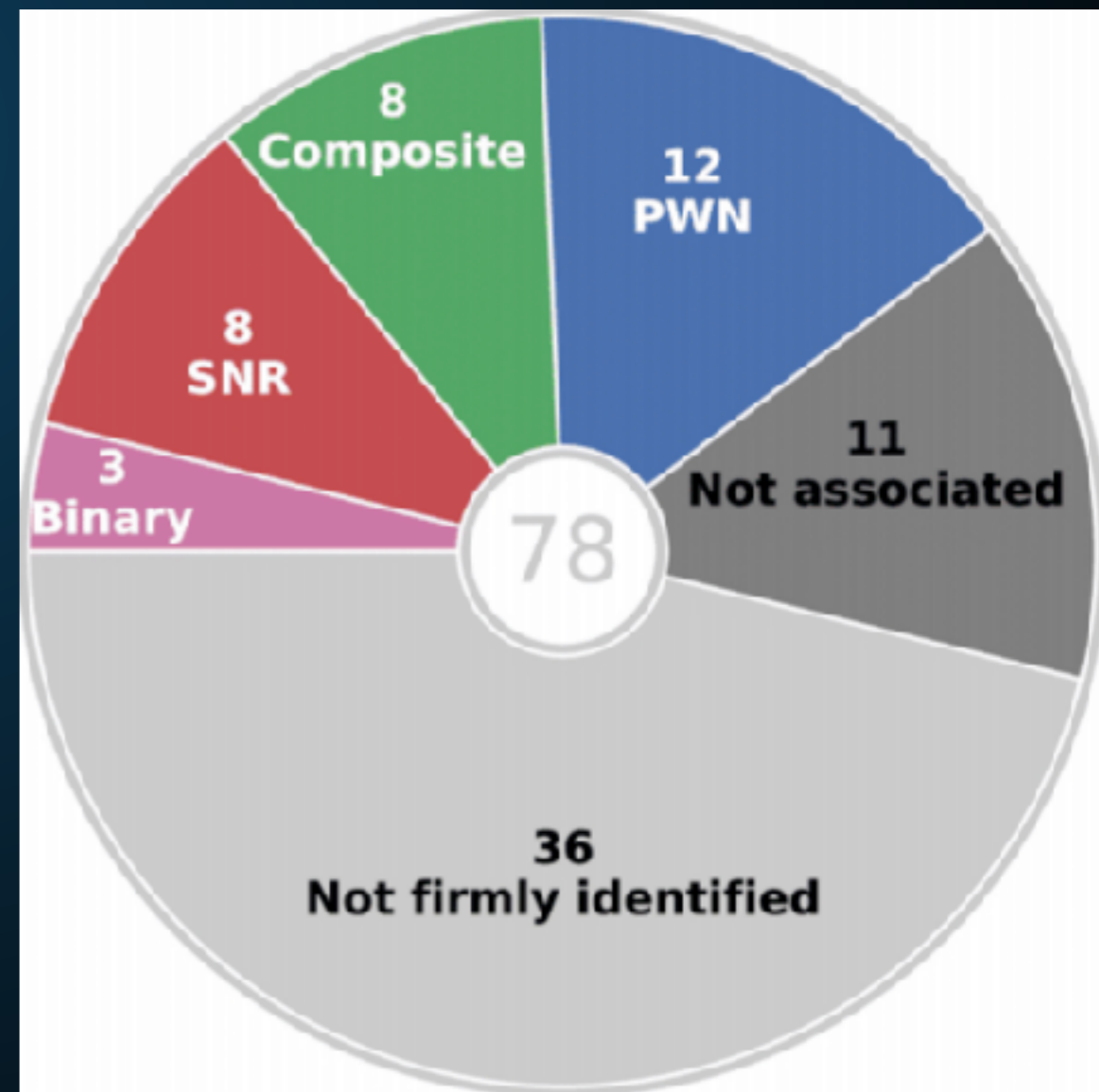
H.E.S.S. Collaboration, H. Abdalla¹, A. Abramowski², F. Aharonian^{3,4,5}, F. Ali Bakhtiari⁶, F.D. Amgüneş⁷, M. Arakawa⁸, M. Arrieta⁹, P. Aubert²⁴, M. Backes⁵, A. Balzer⁵, M. Barnard¹, Y. Becherini¹⁰, J. Becker Tjus¹¹, D. Berg¹², S. Bernhard¹³, K. Bernlöhr⁵, R. Blackwell¹⁴, M. Böttcher¹⁵, C. Boisson¹⁵, J. Bolmont¹⁶, S. Bourneuf¹⁷, P. Bouvier¹⁸, J. Brugéon¹⁷, F. Brun²⁰, P. Brun¹⁸, M. Bryan¹⁹, M. Büchele²⁰, T. Bulik¹⁹, M. Capasso²⁰, S. Carrigan^{5,46}, S. Caroff²¹, A. Cassi²², S. Casanova^{21,2}, M. Cerutti²⁰, N. Chakraborty², R.C.O. Chaves^{13,22}, A. Chen²³, I. Chiodini²⁴, S. Colantoni²⁵, B. Condon²⁶, J. Conrad^{27,28}, I.D. Davids³, I. Decker¹⁵, C. Deil³, J. Devin¹⁷, F. deWit¹⁴, L. Dixon², A. Djannati-Ati²¹, W. Dominik³, A. Donati²², L.O'C. Drury⁵, K. Duison²², I. Dyks²⁴, T. Edwards³, K. Egberts²⁵, P. Egger³, G. Emery¹⁶, I.-P. Emmerwin²⁹, S. Eschbach³⁰, C. Fabian^{27,31}, S. Fegan³⁰, M.V. Fernandes², A. Fiasson³², O. Fontaine³³, A. Fofana³, S. Funk³⁰, M. Funkhouser³², S. Gabici³¹, Y.A. Gallani¹¹, T. Garrigoux¹¹, H. Gasi^{5,49}, F. Gast³⁴, G. Giacinti³⁵, B. Giebels³⁰, D. Glawion²⁵, J.F. Glicenstein³², D. Goebel³⁶, M.-H. Grondin³⁰, J. Hahn³⁷, M. Haupt³⁸, J. Hawkes³⁹, G. Heinzelmann⁴⁰, G. Henri³⁵, G. Hermann³, J.A. Hinton³, W. Hofmann³, C. Högelschum³⁵, T.L. Holch⁷, M. Holler³⁷, D. Huns², A. Ivascenko¹, H. Iwasaki⁴¹, A. Jacholkowska¹⁶, M. Janzky³⁸, D. Jankowsky³⁶, F. Jankowsky³⁶, M. Jng²², L. Jouvin³², I. Jung-Richardt³⁵, M.A. Kastendieck³, K. Kataryjnski³⁰, M. Katarugawa⁴¹, U. Katz³⁰, D. Kerszberg¹⁶, D. Khangulyan¹², B. Khelifi³¹, J. King³, S. Klepser²⁷, D. Klochkov³², W. Kluzniak³¹, Nu. Komin²², K. Korack³, S. Krauss¹¹, M. Krauss¹⁶, P.P. Krüger¹, H. Laifka³⁰, G. Lamastra²⁴, J. Lan¹⁴, J.-F. Laes², J. Lefaucher³⁵, A. Lémère³¹, M. Lemoine-Goumard³⁹, J.-P. Lenain¹³, E. Leser²⁷, T. Lohse²⁷, M. Lorenz¹⁶, R. Liu⁷, R. López-Coto⁷, I. Lyova²⁷, V. Marandon²⁷, D. Malyshe²⁰, A. Marcowith³⁷, C. Mariotti²⁰, R. Marx², G. Mauria²¹, N. Maxted^{14,45}, M. Mayer⁷, P.J. McIntyre¹², M. Meyer²⁷, A.M.W. Mitchell³, R. Moderski³⁴, M. Mohamed²⁵, L. Mohrmann²⁴, K. Mori²⁷, E. Moulin¹³, T. Murach²⁷, S. Nakashima⁴⁴, M. de Narrois²⁰, H. Ndiyavala¹, F. Niederwanger¹², J. Niemiec²¹, L. Oakes³³, P. O'Brien³³, H. Odaka⁴⁴, S. Ohm²⁷, M. Ostrowski²⁸, I. Oya³⁷, M. Padovani³⁷, M. Pater³, R.D. Parsons², M. Paz Arribas³, N.W. Pekeur¹, G. Pelletier²⁰, C. Perennes¹⁶, R.-O. Perreot³², B. Prynay¹⁶, Q. Piel²⁴, S. Pita³¹, V. Poireau²⁴, H. Poon³, D. Prokhorov³⁶, H. Prokoph¹², G. Pühlhofer²⁹, M. Pusch^{31,10}, A. Quirrenbach²⁵, S. Raab³⁵, R. Raab¹³, A. Reimer³, O. Reimer¹², M. Renaud¹⁷, R. de los Reyes³, F. Rieger^{2,41}, L. Rinchiuso¹⁸, C. Romoli⁵, G. Rowell¹⁴, B. Rudas³⁴, C.B. Rulten¹⁵, S. Saif-Harj⁵⁰, V. Sahakian^{6,5}, S. Saito⁵¹, D.A. Sanchez²⁴, A. Santangelo²⁹, M. Sasaki³⁵, M. Sazdovitch³⁵, R. Schlickeiser¹¹, F. Schüssler³⁸, A. Schulz²⁷, U. Schwaneke⁷, S. Schwemmer²⁵, M. Seglar-Arroyo¹⁸, M. Settimo¹⁶, A.S. Seyffert¹, N. Shah²², I. Shkoni³⁶, K. Shrivastava⁸, R. Simons⁵, H. Sol¹⁵, F. Spanier³, M. Spar-Jacob³, L. Stawarz³⁰, R. Steenkamp⁵, C. Stegmann^{35,37}, C. Steppa³⁵, I. Sushch¹, T. Takahashi⁴⁴, J.-P. Tavernet¹⁶, T. Tavner²¹, A.M. Taylor³⁷, R. Terrier³⁸, L. Tibaldo³, D. Tiziani³⁶, M. Tlaczyszcak², C. Theureau²⁰, M. Tsuru¹⁷, N. Tsuji⁴⁰, R. Tufts², Y. Uchiyama⁴², D.J. van der Walt¹, C. van Reensburg¹, B. van Soelen⁴⁰, G. Vasileiadis¹⁷, J. Vely³⁰, C. Venter¹, A. Viana^{3,46}, P. Vincent¹⁵, J. Vink⁵, F. Voisin³⁴, H.J. Volk², I. Vourvachis², Z. Wadiasingh¹, S.J. Wagner²⁵, P. Wagner³⁰, R. White³, A. Wierzcholska²¹, P. Willmann³⁰, A. Wornlein³⁰, D. Wevers³, R. Yung³, D. Zhebrakov³⁰, M. Zacharias¹, R. Zanin², A.A. Zdziarski³⁴, A. Zech¹⁵, F. Zeh³⁰, A. Ziegler²⁶, J. Zorn², and N. Zywucka¹⁸

(Affiliations can be found after the references)

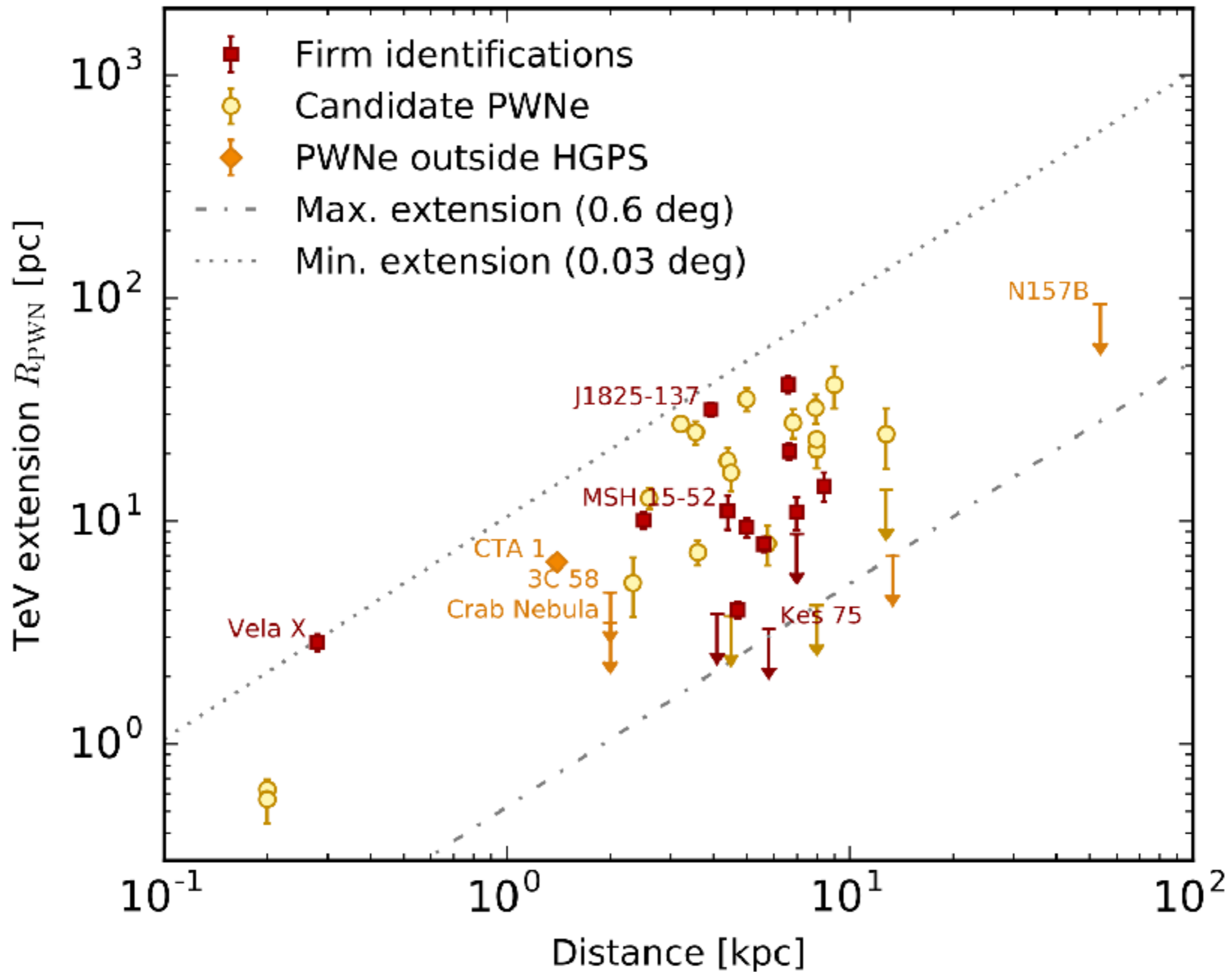
April 10, 2018

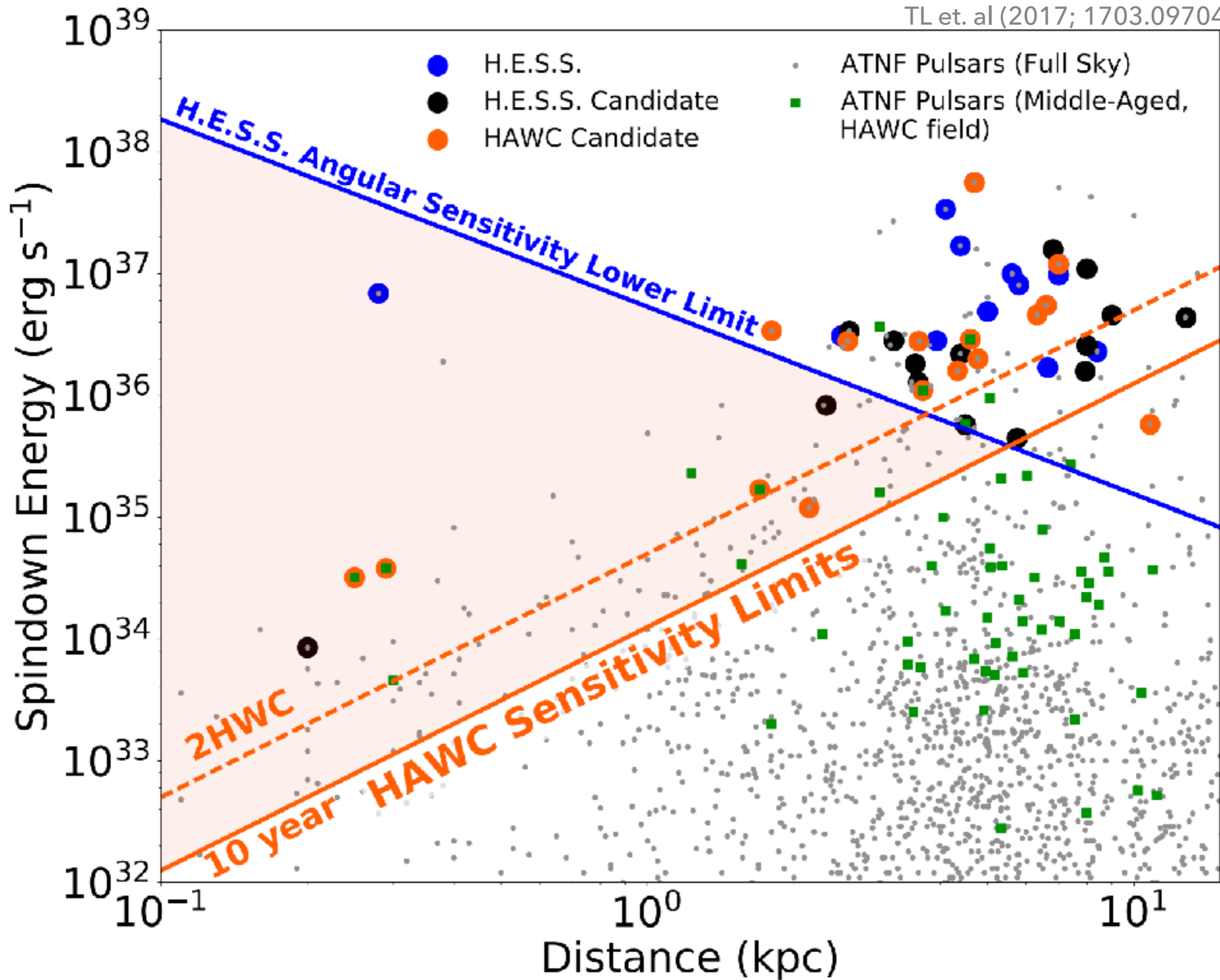
ABSTRACT

We present the results of the most comprehensive survey of the Galactic plane in very high energy (VHE) γ -rays, including a public release of Galactic sky maps, a catalog of VHE sources, and the discovery of 16 new sources of VHE γ -rays. The High Energy Spectroscopic System (H.E.S.S.) Galactic plane survey (HGPS) was a decade-long observation program carried out by the H.E.S.S. I array of Cherenkov telescopes in Namibia from 2004 to 2013. The observations amount to nearly 2700 h of quality-selected data, covering the Galactic plane at longitudes from $l = 250^\circ$ to 65° and latitudes $|b| \leq 3^\circ$. In addition to the unprecedented spatial coverage, the HGPS also features a relatively high angular resolution ($0.08^\circ \approx 5$ arcmin mean point spread function 68% containment radius), sensitivity ($\leq 1.5\%$ Crab flux for point-like sources), and energy range (0.2 to 100 TeV). We constructed a catalog of VHE γ -ray sources from the HGPS data set with a systematic procedure for both source detection and characterization of morphology and spectrum. We present this likelihood-based method in detail, including the introduction of a model component to account for unresolved, large-scale emission along the Galactic plane. In total, the resulting HGPS catalog contains 78 VHE sources, of which 14 are not re-analyzed here, for example, due to their complex morphology, namely shell-like sources and the Galactic center region. Where possible, we provide a firm identification of the VHE source or plausible associations with sources in other astronomical catalogs. We also studied



WHY IS HAWC IMPORTANT





FIRST DETECTIONS!

[[Previous](#) | [Next](#) | [ADS](#)]

HAWC detection of TeV emission near PSR B0540+23

ATel #10941; *Colas Riviere (University of Maryland), Henrike Fleischhack (Michigan Technological University), Andres Sandoval (Universidad Nacional Autonoma de Mexico) on behalf of the HAWC collaboration*

on 9 Nov 2017; 23:11 UT

Credential Certification: Colas Riviere (riviere@umd.edu)

Subjects: Gamma Ray, TeV, VHE, Pulsar

[Tweet](#) [Recommend 5](#)

The High Altitude Water Cherenkov (HAWC) collaboration reports the discovery of a new TeV gamma-ray source HAWC J0543+233. It was discovered in a search for extended sources of radius 0.5° in a dataset of 911 days (ranging from November 2014 to August 2017) with a test statistic value of 36 (6σ pre-trials), following the method presented in [Abeysekara et al. 2017, ApJ, 843, 40](#). The measured J2000.0 equatorial position is RA= 85.78° , Dec= 23.40° with a statistical uncertainty of 0.2° . HAWC J0543+233 was close to passing the selection criteria of the 2HWC catalog ([Abeysekara et al. 2017, ApJ, 843, 40](#), see [HAWC J0543+233 in 2HWC map](#)), which it now fulfills with the additional data.

HAWC J0543+233 is positionally coincident with the pulsar PSR B0540+23 ($\dot{E} = 4.1e+34$ erg s $^{-1}$, dist = 1.56 kpc, age = 253 kyr). It is the third low \dot{E} dot, middle-aged pulsar announced to be detected with a TeV halo, along with Geminga and B0656+14. It was predicted to be one of the next such detection by HAWC by [Linden et al., 2017, arXiv:1703.09704](#).

Using a simple source model consisting of a disk of radius 0.5° , the measured spectral index is -2.3 ± 0.2 and the differential flux at 7 TeV is $(7.9 \pm 2.3) \times 10^{-15}$ TeV $^{-1}$ cm $^{-2}$ s $^{-1}$. The errors are statistical only. Further morphological and spectral analysis as well as studies of the systematic uncertainty are ongoing.

[[Previous](#) | [Next](#) | [ADS](#)]

HAWC detection of TeV source HAWC J0635+070

ATel #12013; *Chad Brisbois (Michigan Technological University), Colas Riviere (University of Maryland), Henrike Fleischhack (Michigan Technological University), Andrew Smith (University of Maryland) on behalf of the HAWC collaboration*

on 6 Sep 2018; 14:47 UT

Credential Certification: Colas Riviere (riviere@umd.edu)

Subjects: Gamma Ray, TeV, VHE, Pulsar

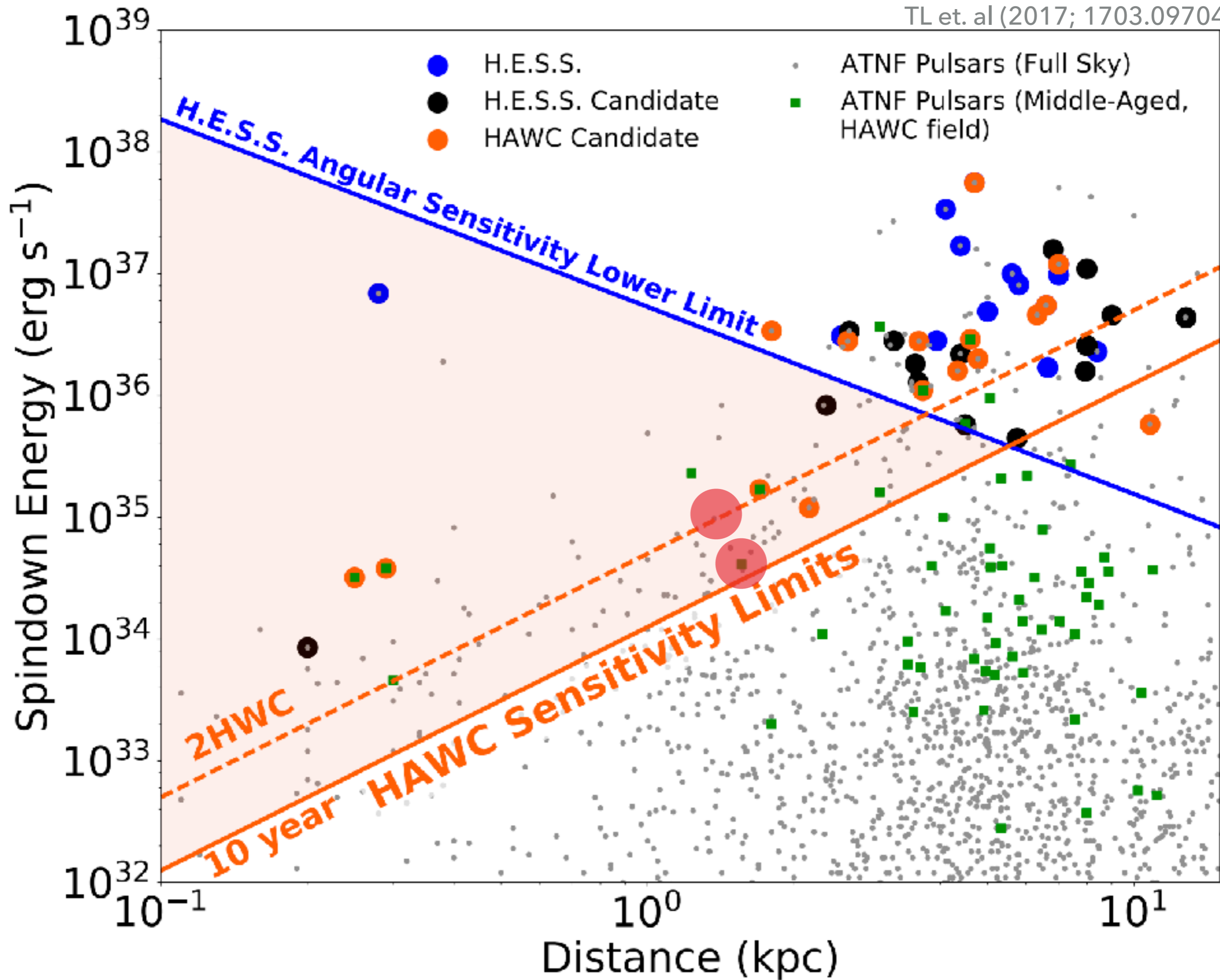
[Tweet](#) [Recommend 2](#)

The High Altitude Water Cherenkov (HAWC) collaboration reports the discovery of a new TeV gamma-ray source HAWC J0635+070. It was discovered in a search for extended sources covering 1128 days of HAWC observations with a test statistic value of 27 ($>5\sigma$ pre-trials), following the method presented in [\[Abeysekara et al. 2017, ApJ, 843, 40\]](#). Its significance in the 2HWC data set excluded it from being included in the catalog ($\sim 3.5\sigma$ pre-trials), but with the addition of ~ 600 more days of data it now satisfies that criterion. The best-fit J2000.0 equatorial position is RA= $98.71 \pm 0.20^\circ$, Dec= $7.00 \pm 0.22^\circ$, with a Gaussian 1-sigma extent of $0.65^\circ \pm 0.18^\circ$.

The spectral energy distribution is well-fit by a power law with spectral index -2.15 ± 0.17 . The differential flux at 10 TeV is $(8.6 \pm 3.2) \times 10^{-15}$ TeV $^{-1}$ cm $^{-2}$ s $^{-1}$. All errors are statistical only; further morphological and spectral analysis as well as studies of the systematic uncertainty are ongoing.

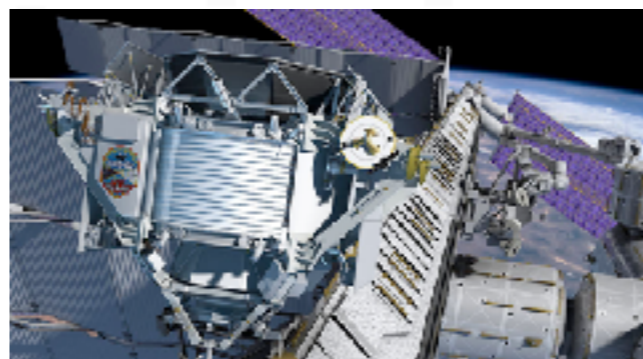
Given its spectrum and morphology, we believe HAWC J0635+070 may be the TeV halo of the pulsar PSR J0633+0632 ($\dot{E} = 1.2e+35$ erg s $^{-1}$, dist = 1.35 kpc, age = 59 kyr, unknown proper motion [[Manchester et al., 2005, AJ, 129](#)]). The gamma-ray spectrum and morphology is compatible with a "Geminga-like" TeV Halo [[Abeysekara et al. 2017, Science, 358, 911](#); [Linden et al., 2017, PRD, 96, 103016](#)]. We encourage follow-up observations at other wavelengths.

- HAWC has detected two additional TeV halos
- Total Count:
 - Middle-Aged: 6
 - Younger: 13



**Implication III: The positron excess is
due to pulsar activity**

Positron fraction



10^{-1}

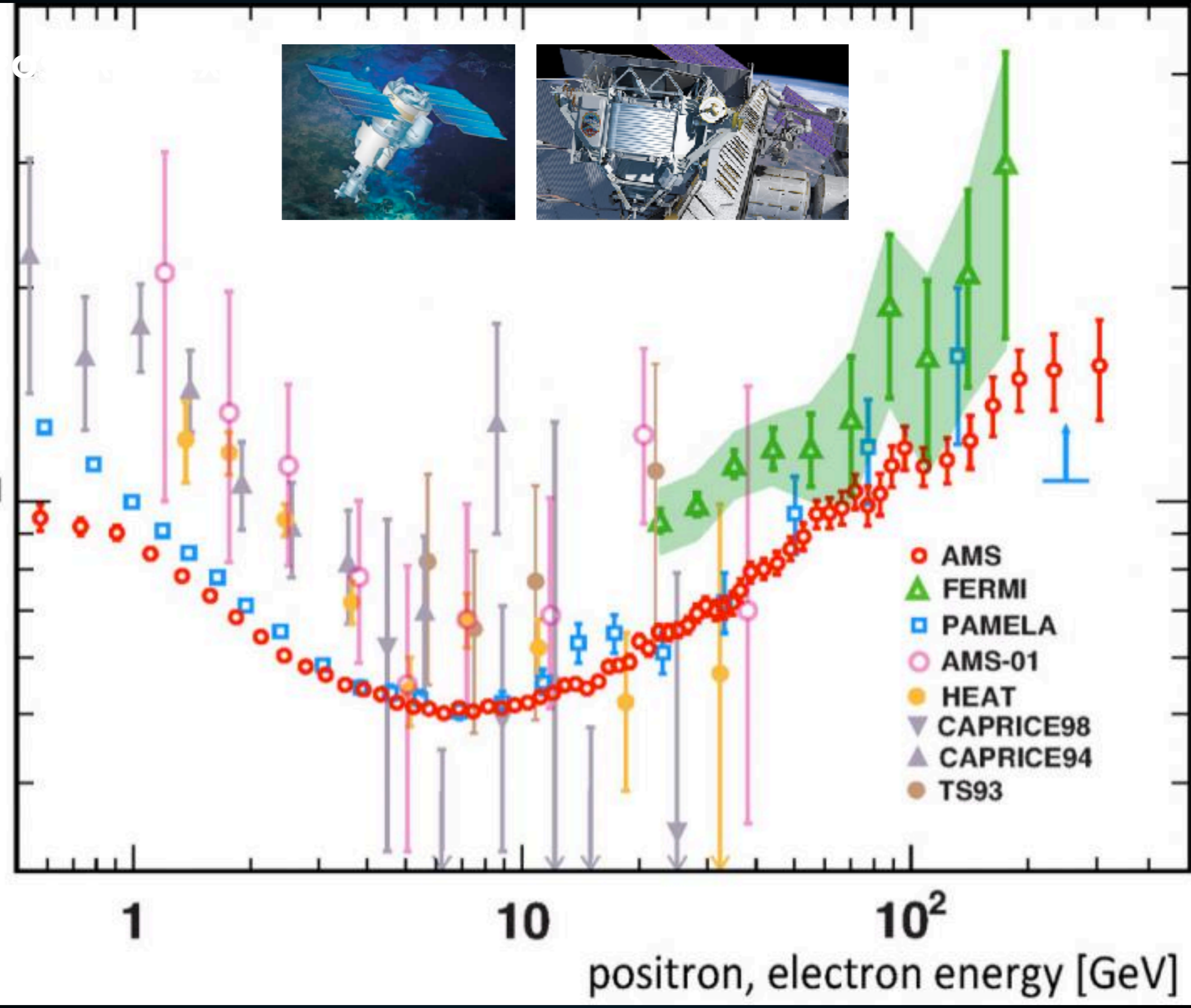
1

10

10^2

positron, electron energy [GeV]

- AMS
- △ FERMI
- PAMELA
- AMS-01
- HEAT
- ▽ CAPRICE98
- ▲ CAPRICE94
- TS93



PULSARS PRODUCE THE POSITRON EXCESS

- **What were the uncertainties in pulsar models?**

- **I: The e^+e^- production efficiency?**

Profumo (0812.4457); Malyshev et al. (0903.1310)

%.

A quantitative discussion of plausible values for f_{e^\pm} was recently given in Ref. [38]. We shall not review their discussion here, but Ref. [38] argues (see in particular their very informative App. B and C) that in the context of a standard model for the pulsar wind nebulae, a reasonable range for f_{e^\pm} falls between 1% and 30%.

- **II: The e^+e^- spectrum.**

- **III: The propagation of e^+e^- to Earth.**

PULSARS PRODUCE THE POSITRON EXCESS

- **What were the uncertainties in pulsar models?**

- **I: The e^+e^- production efficiency?**

- **II: The e^+e^- spectrum.**

Hooper et al. (0810.1527)

part of their energy adiabatically because of the expansion of the wind. The energy spectrum injected by a single pulsar depends on the environmental parameters of the pulsar, but some attempts to calculate the average spectrum injected by a population of mature pulsars suggest that the spectrum may be relatively hard, having a slope of $\sim 1.5-1.6$ [18]. This spectrum, however, results from a complex interplay of individual pulsar spectra, of the spatial and age distributions of pulsars in the Galaxy, and on the assumption that the chief channel for pulsar spin down is magnetic dipole radiation. Due to the related uncertainties, variations from this injection spectra cannot be ruled out. Typically, one concentrates the attention on pulsars of age $\sim 10^5$ years because younger pulsars are likely to still

- **III: The propagation of e^+e^- to Earth.**

TEV HALOS ANSWER THE KEY QUESTIONS!

| Name | Tested radius [$^{\circ}$] | Index | $F_{\gamma} \times 10^{15}$ [$\text{TeV}^{-1} \text{cm}^{-2} \text{s}^{-1}$] | TeVCat |
|----------------|---------------------------------|------------------|---|---------|
| 2HWC J0631+169 | - | -2.57 ± 0.15 | 6.7 ± 1.5 | Geminga |
| " | 2.0 | -2.23 ± 0.08 | 48.7 ± 6.9 | Geminga |
| 2HWC J0635+180 | - | -2.56 ± 0.16 | 6.5 ± 1.5 | Geminga |

- We assume a power-law electron injection spectrum with an exponential cutoff

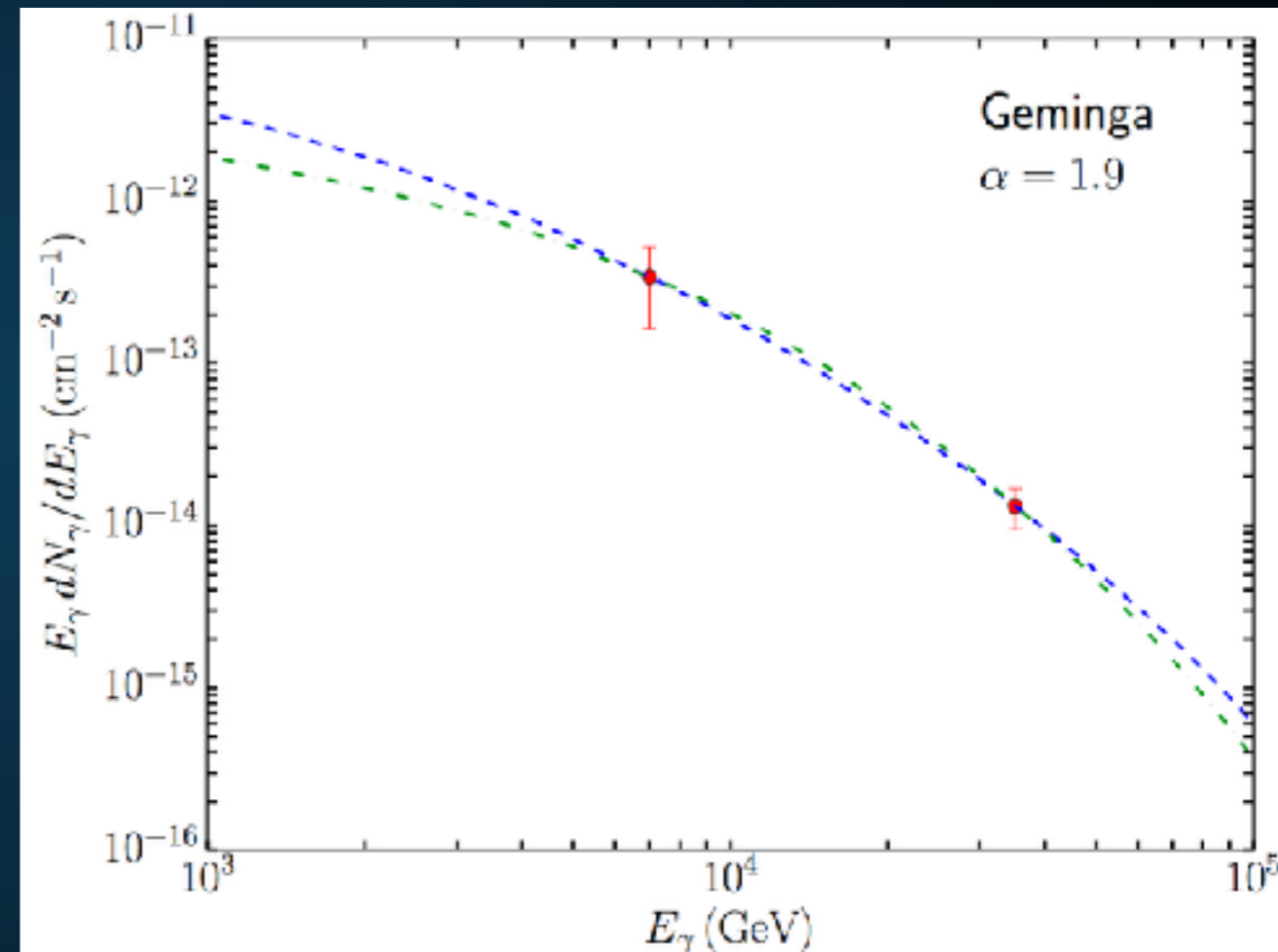
- Best Fit:

$$-1.9 < \alpha < -1.5$$

$$E_{\text{cut}} \cong 50 \text{ TeV}$$

$$\sim 3\text{-}9 \times 10^{33} \text{ erg s}^{-1} !$$

9-27% of the total pulsar spin-down power!



PULSARS PRODUCE THE POSITRON EXCESS

- **What were the uncertainties in pulsar models?**

- **I: The e^+e^- production efficiency?**

- **II: The e^+e^- spectrum.**

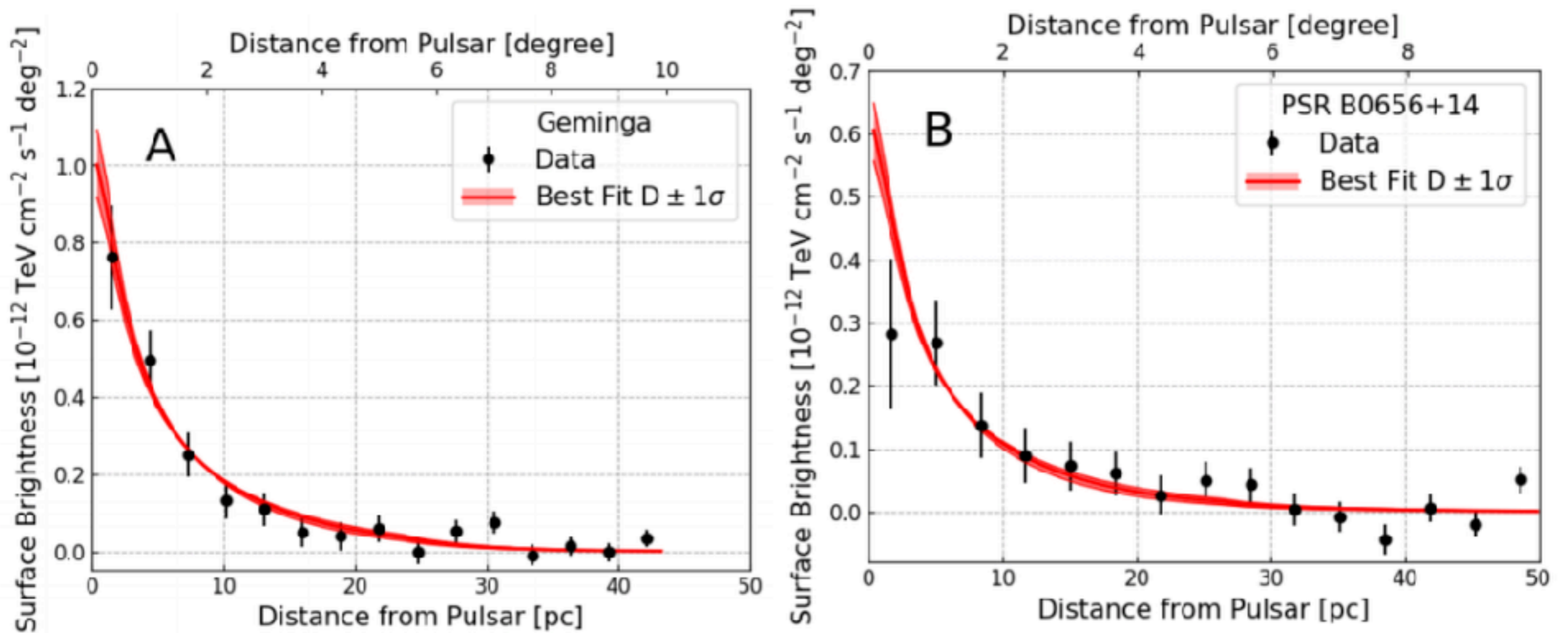
- **III: The propagation of e^+e^- to Earth.**

Malyshev et al. (0903.1310)

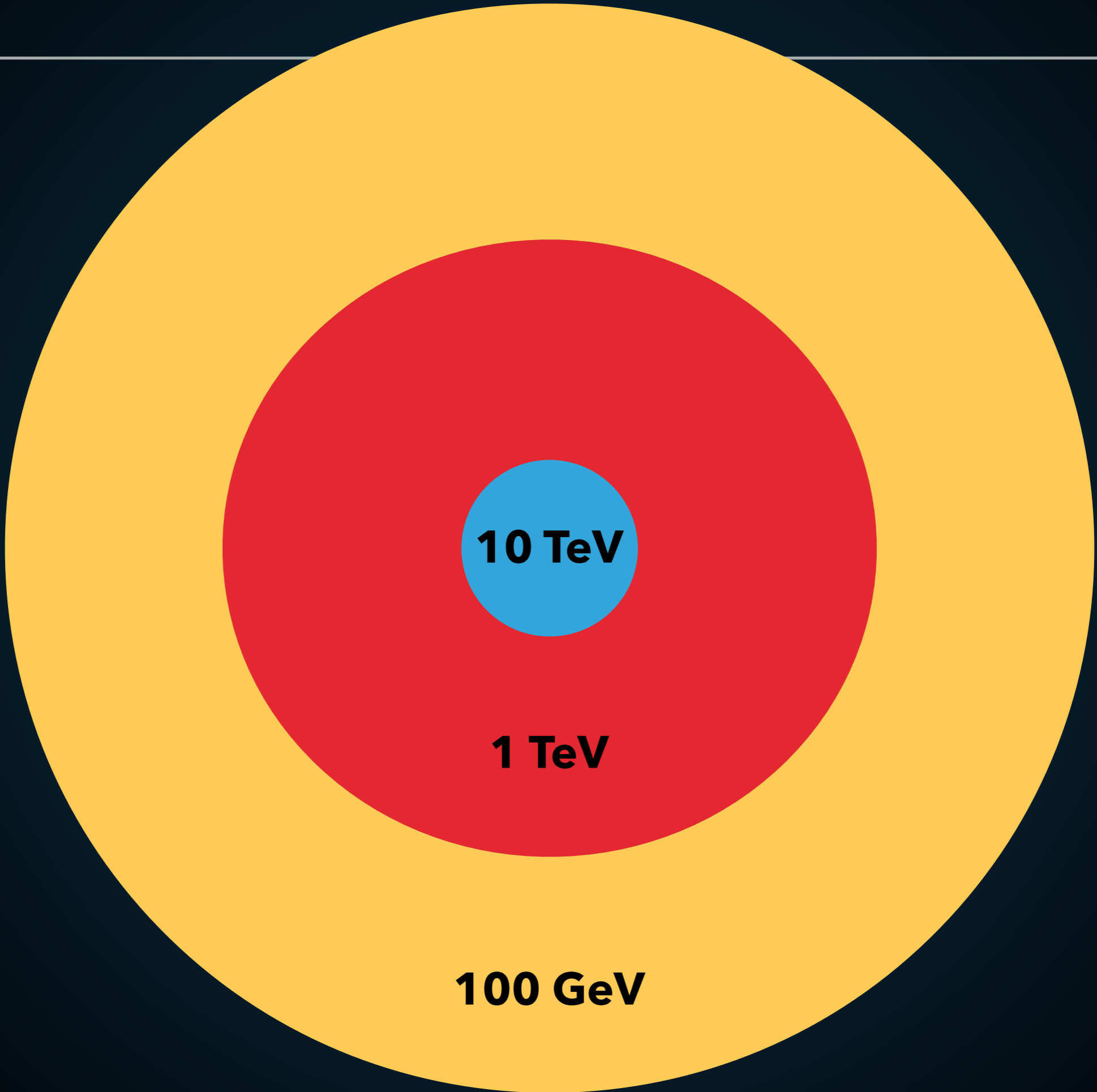
The observed spectrum on Earth of electrons and positrons injected by pulsars is also strongly dependent on propagation effects. In particular, the observed cutoff in the flux of electrons from a pulsar can be much smaller than the injection cutoff due to energy losses (“cooling”) during propagation. We define the cooling break, $E_{br}(t)$, as the maximal energy electrons can have after propagating for time t . Since – as stated above – the typical

Cosmic-ray propagation is the last key.

THE ELECTRONS PROPAGATE DIFFUSIVELY



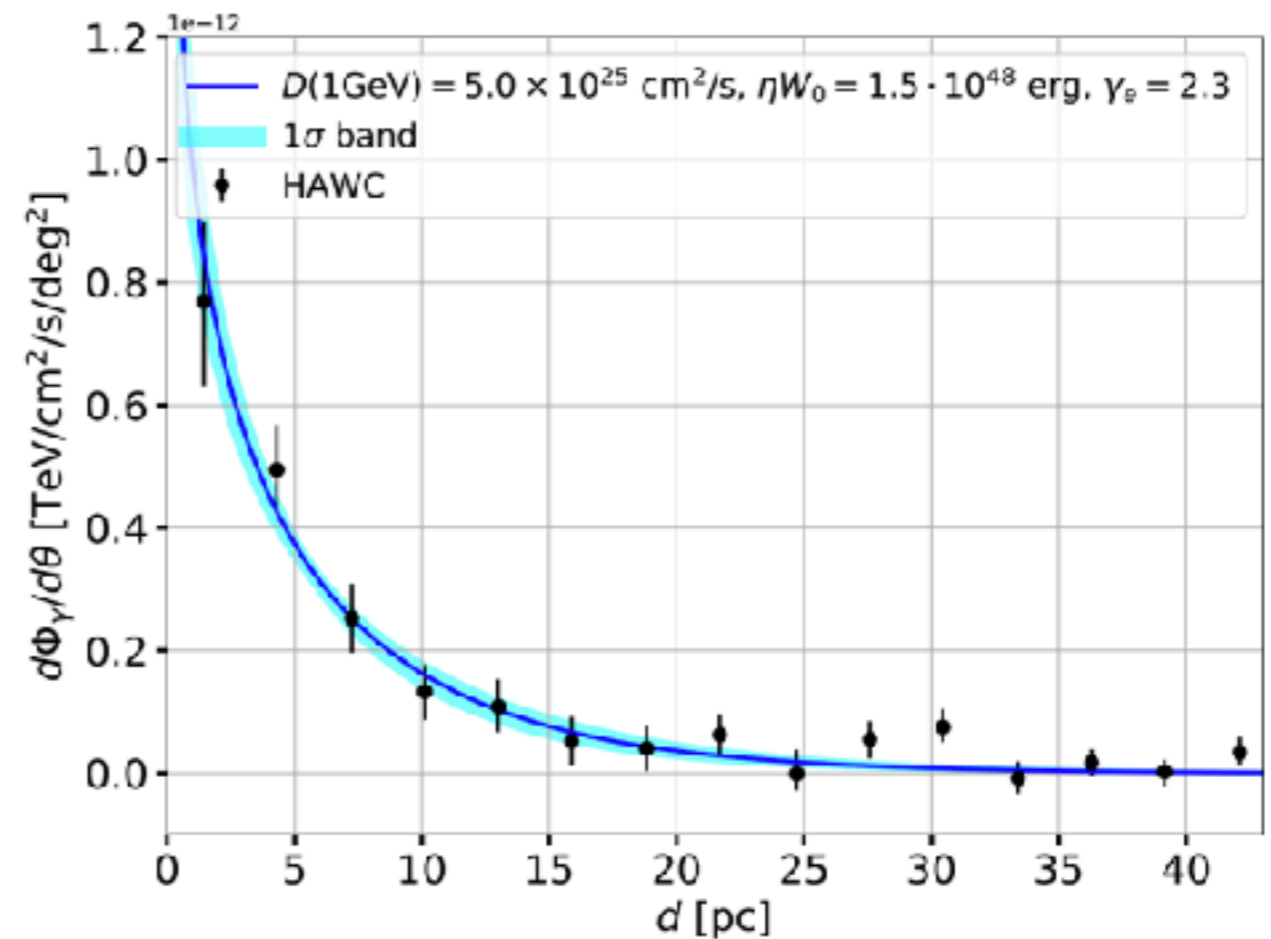
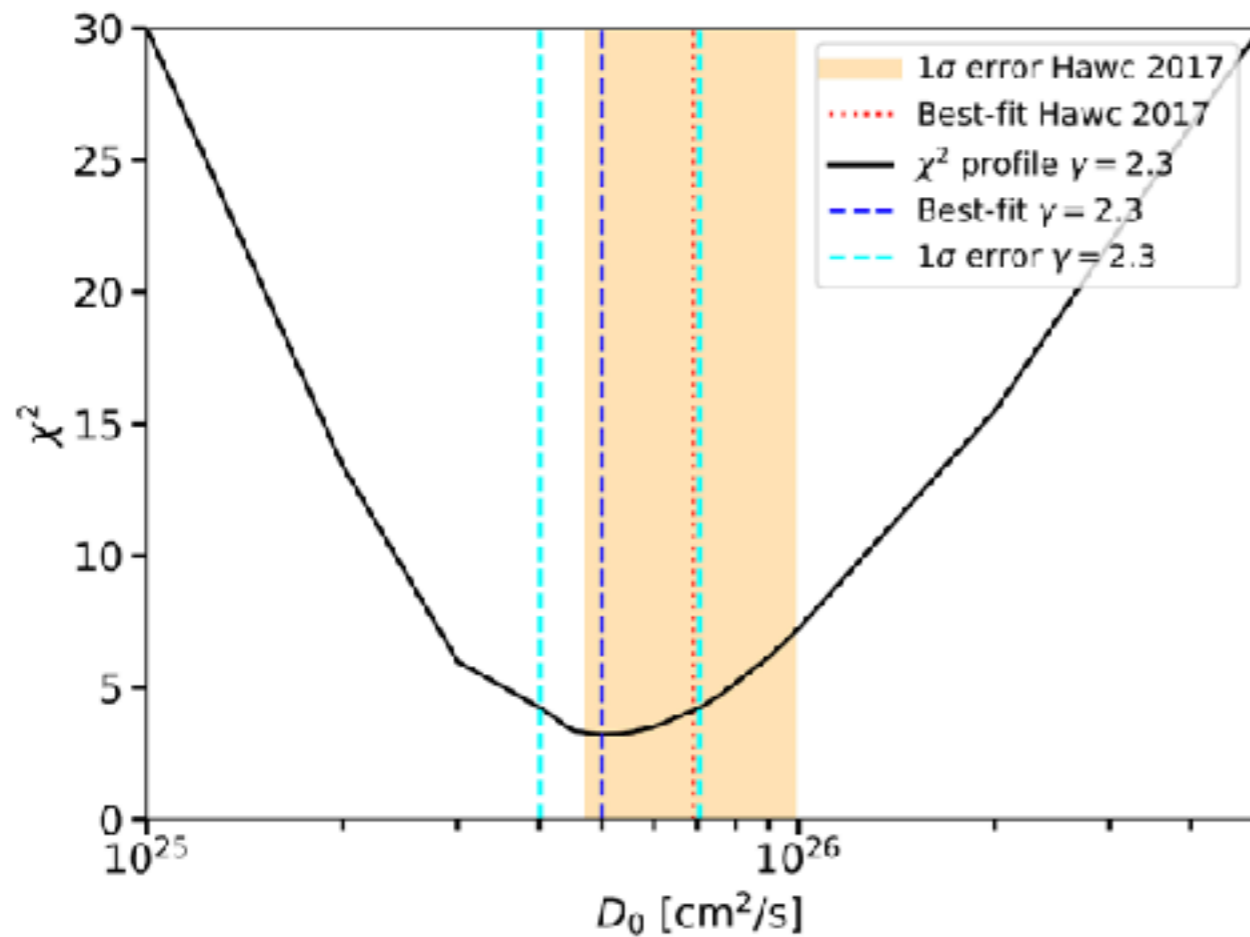
- Morphology of each pulsar fit by diffusion.
- Diffusion coefficient near the pulsar is quite small.



10 TeV

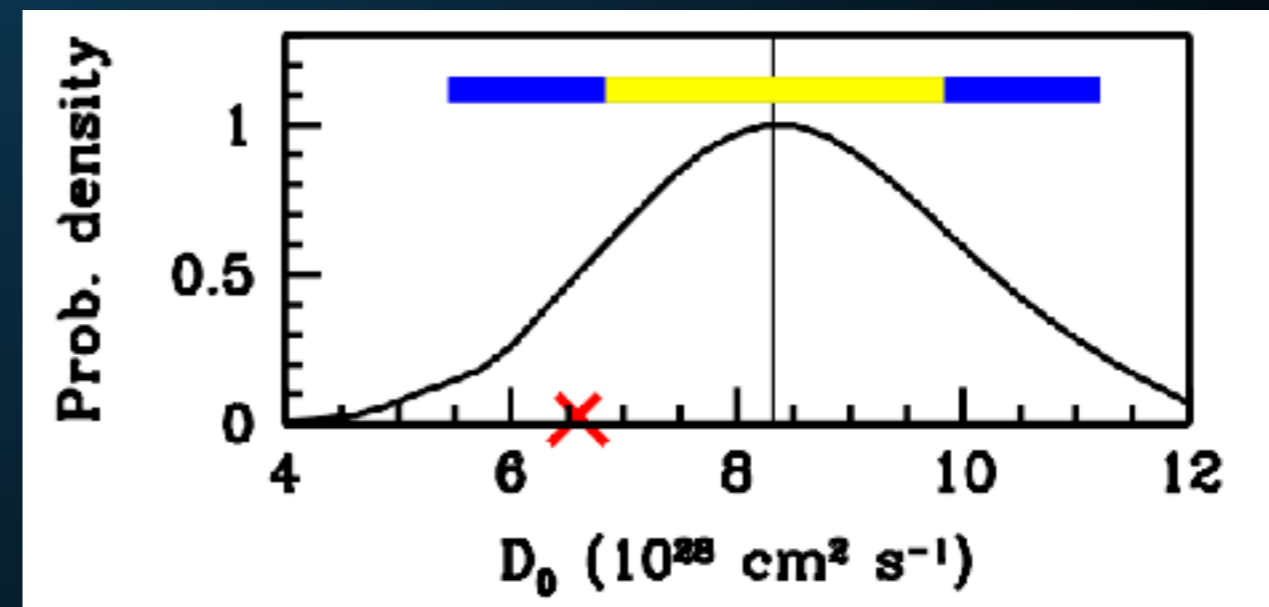
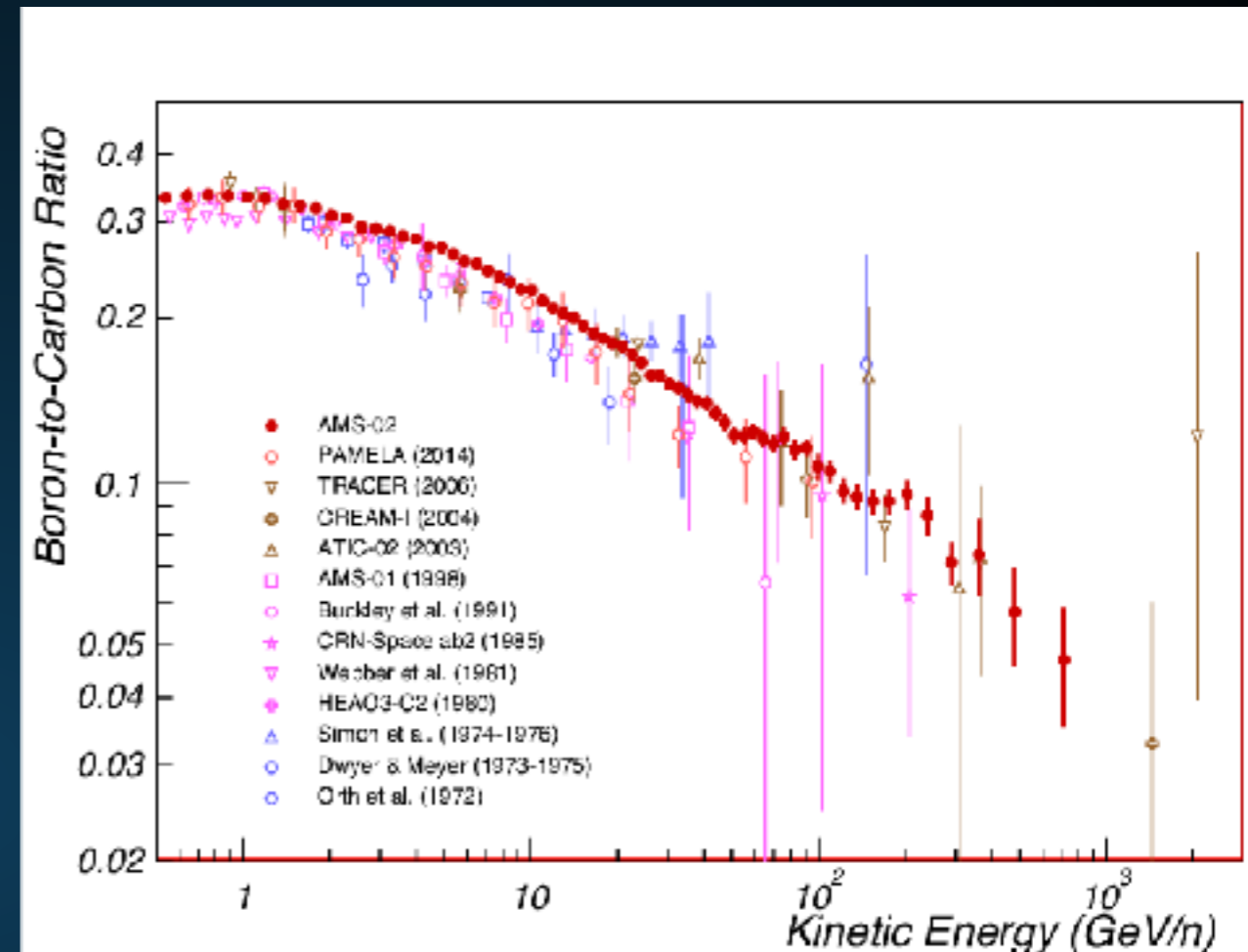
1 TeV

100 GeV

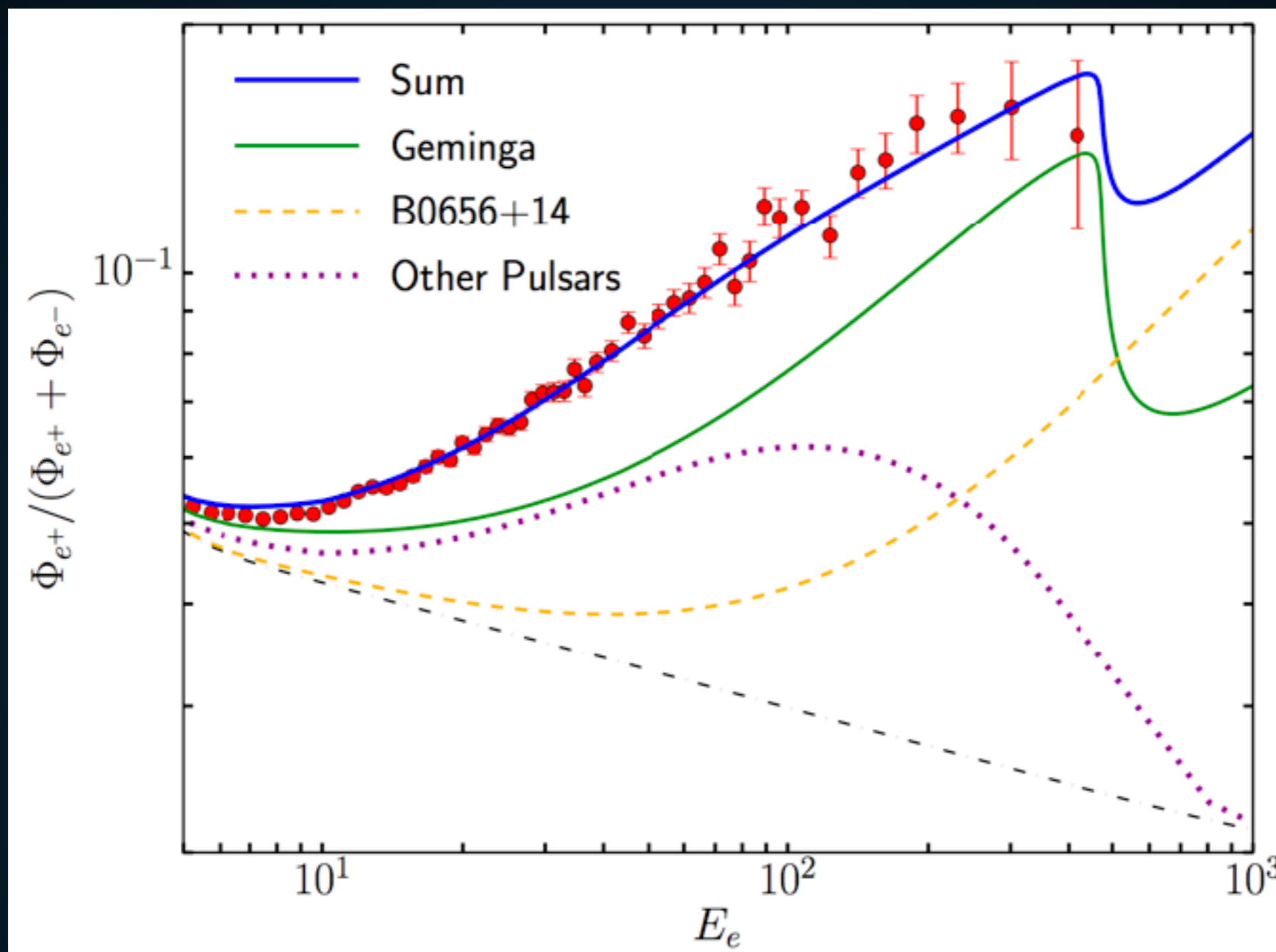


- Observations from the Fermi-LAT telescope have found a similar extension at GeV energies.

- **Cosmic-Ray primary to secondary ratios tell us about:**
 - **The average grammage encountered by cosmic-rays before they escape the galaxy (e.g. B/C)**
 - **The average time cosmic-rays propagate before they escape (eg. $^{10}\text{Be}/^9\text{Be}$).**

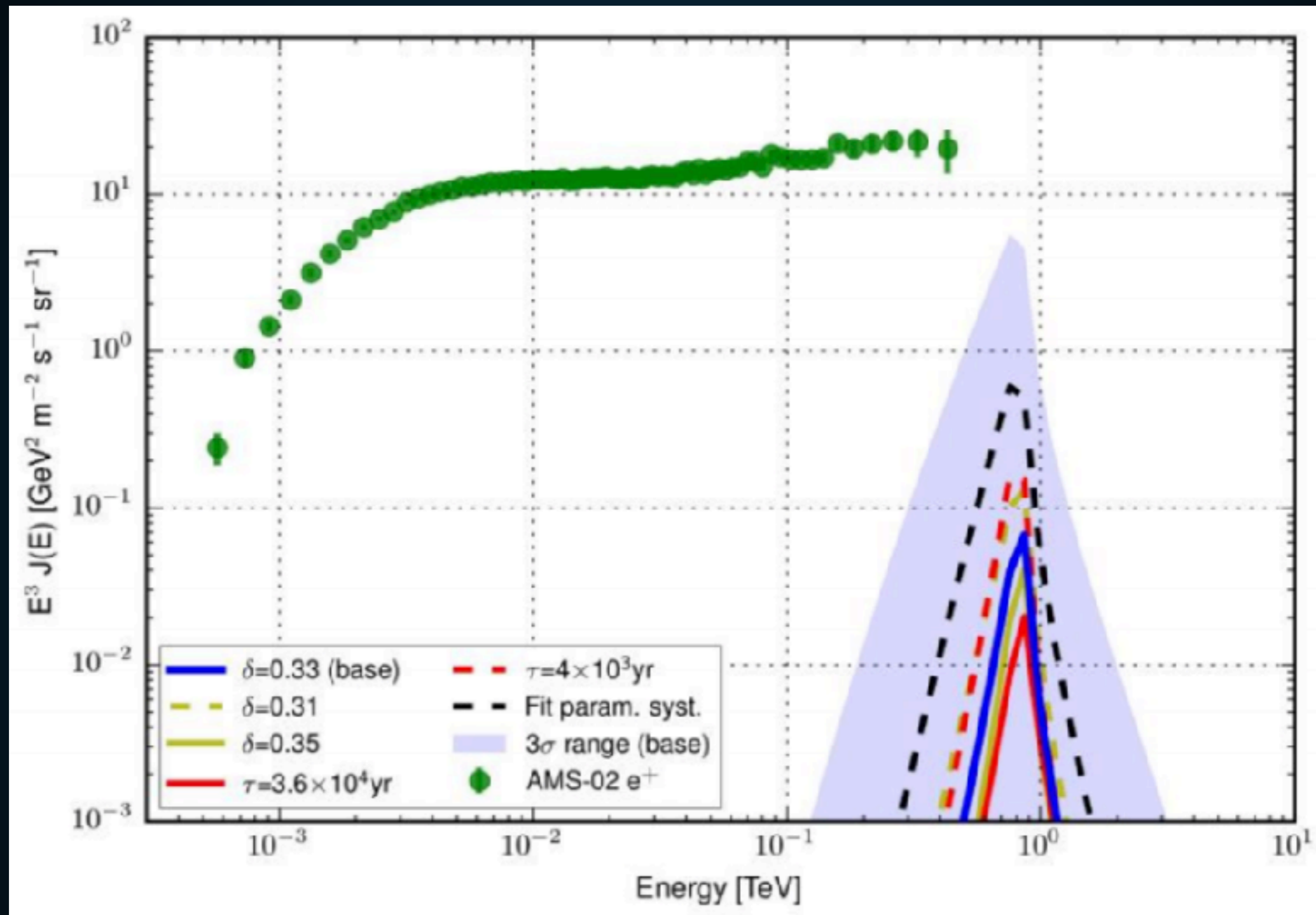


THE POSITRON FRACTION FROM TEV HALOS



- Reasonable models can be exactly fit to the excess.

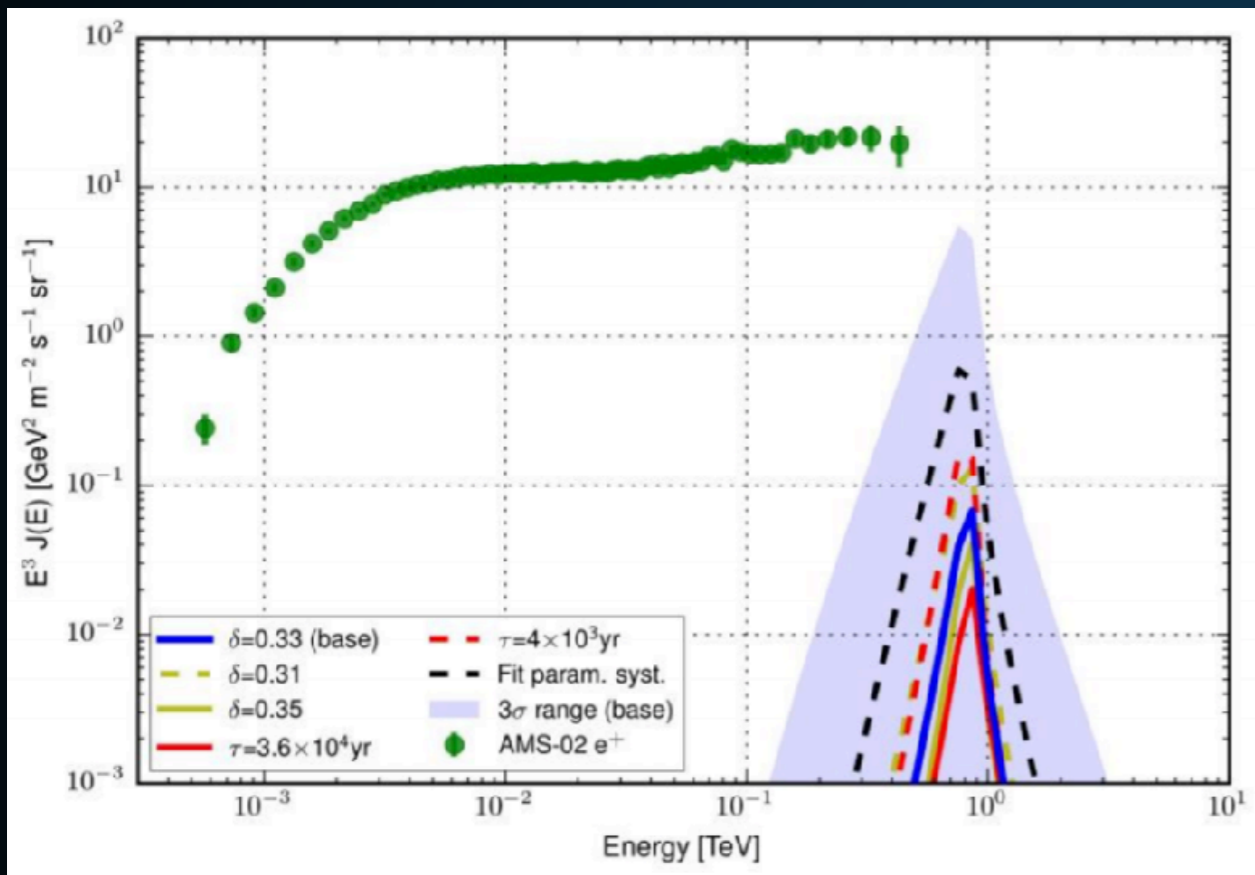
*Braking index slightly changed to fit model to data.



- **HAWC Results show a small contribution from Geminga.**

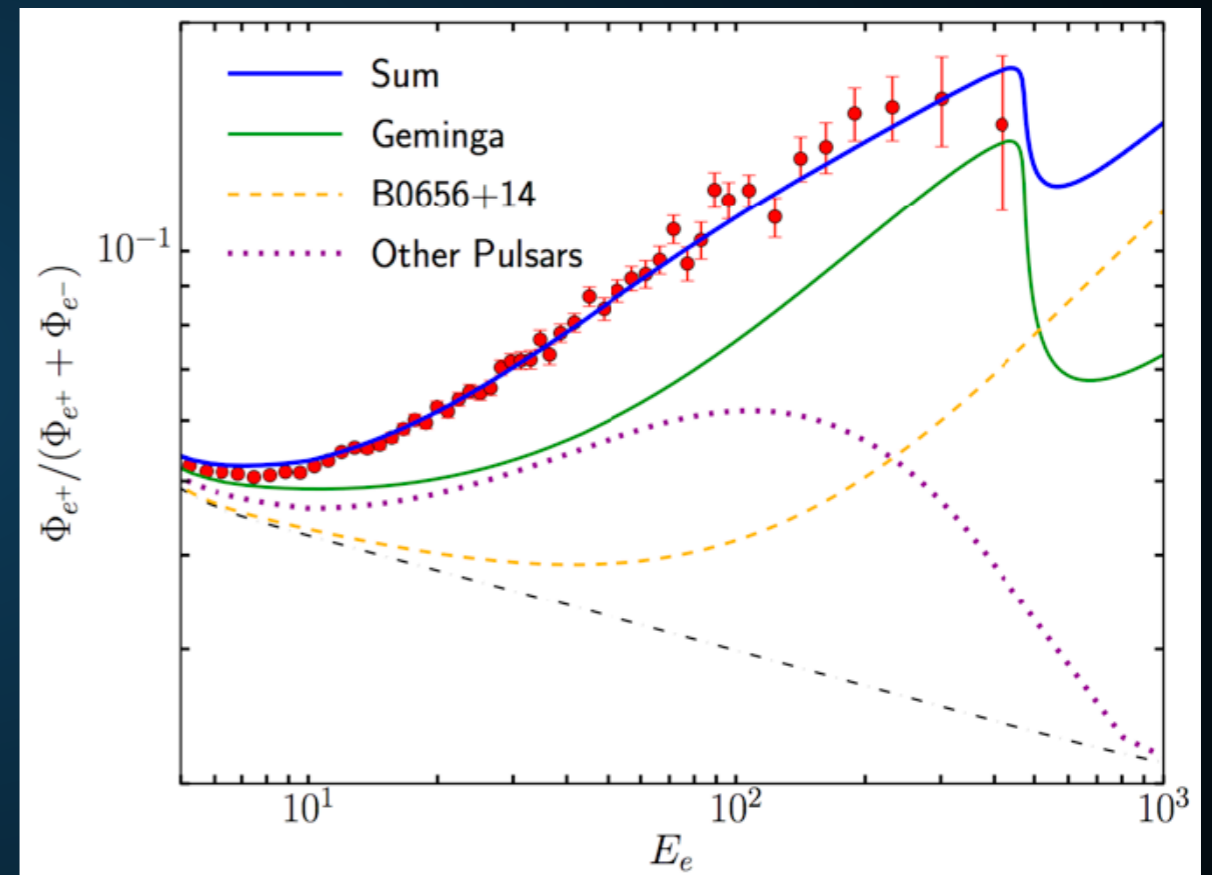
TWO POSSIBLE ASSUMPTIONS

Extrapolate Low-Diffusion Constant
UP to Earth:



100 GeV positrons do not make it to
Earth

Extrapolate the High Diffusion
Constant DOWN to Earth:



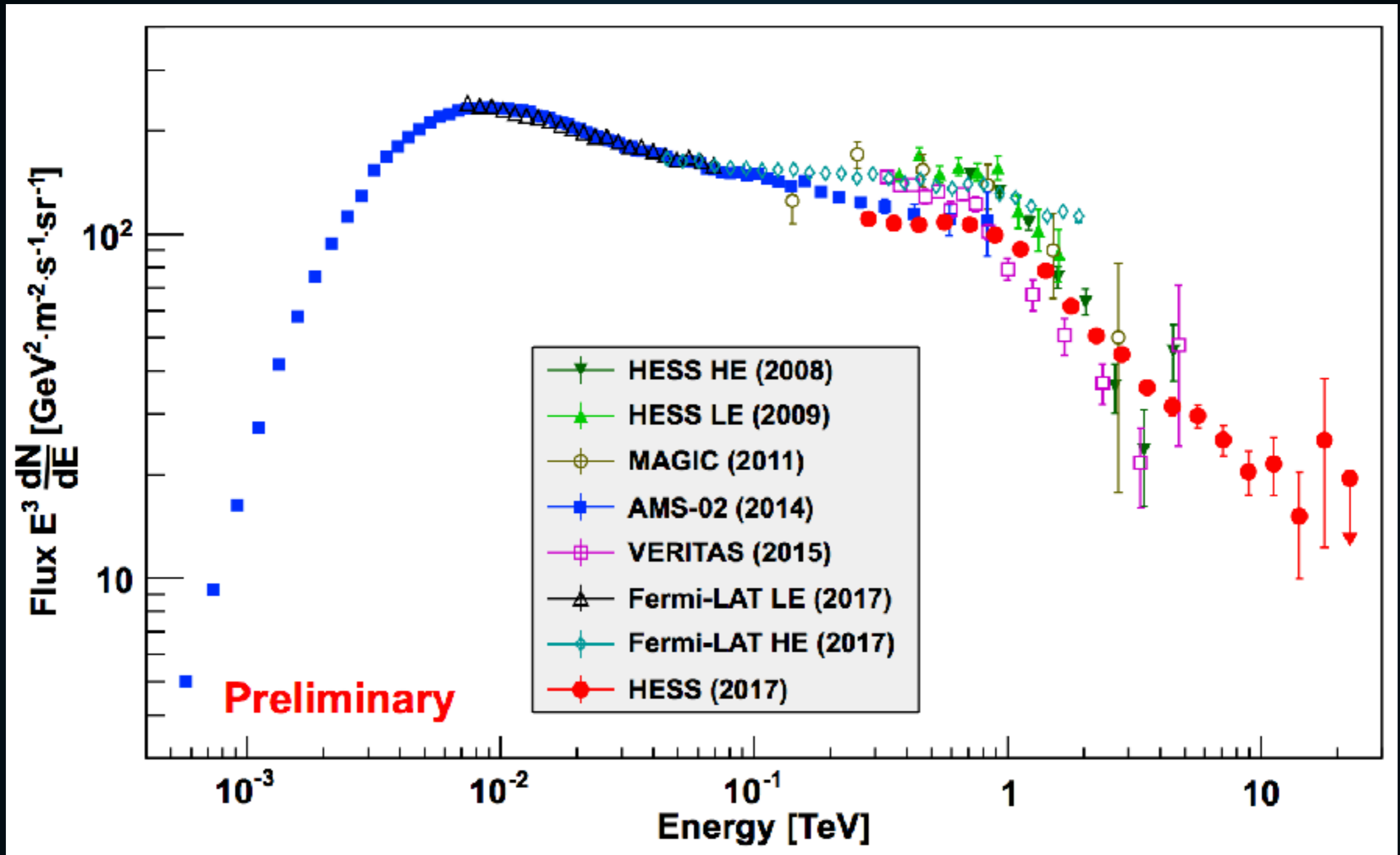
100 GeV positrons do make it to Earth

Hooper et al. (1702.08436)

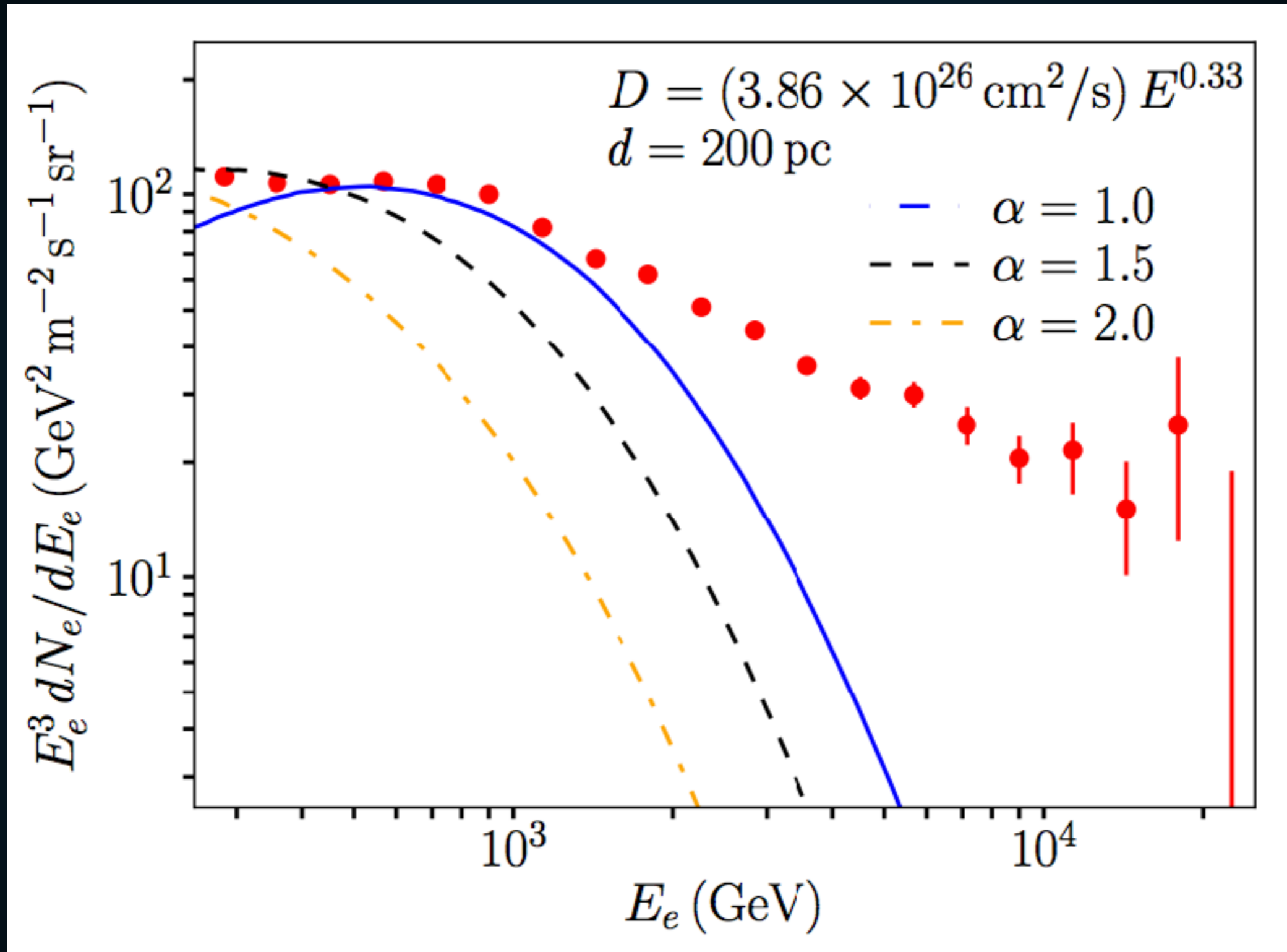
Profumo et al. (1803.09731)

Fang et al. (1803.02640)

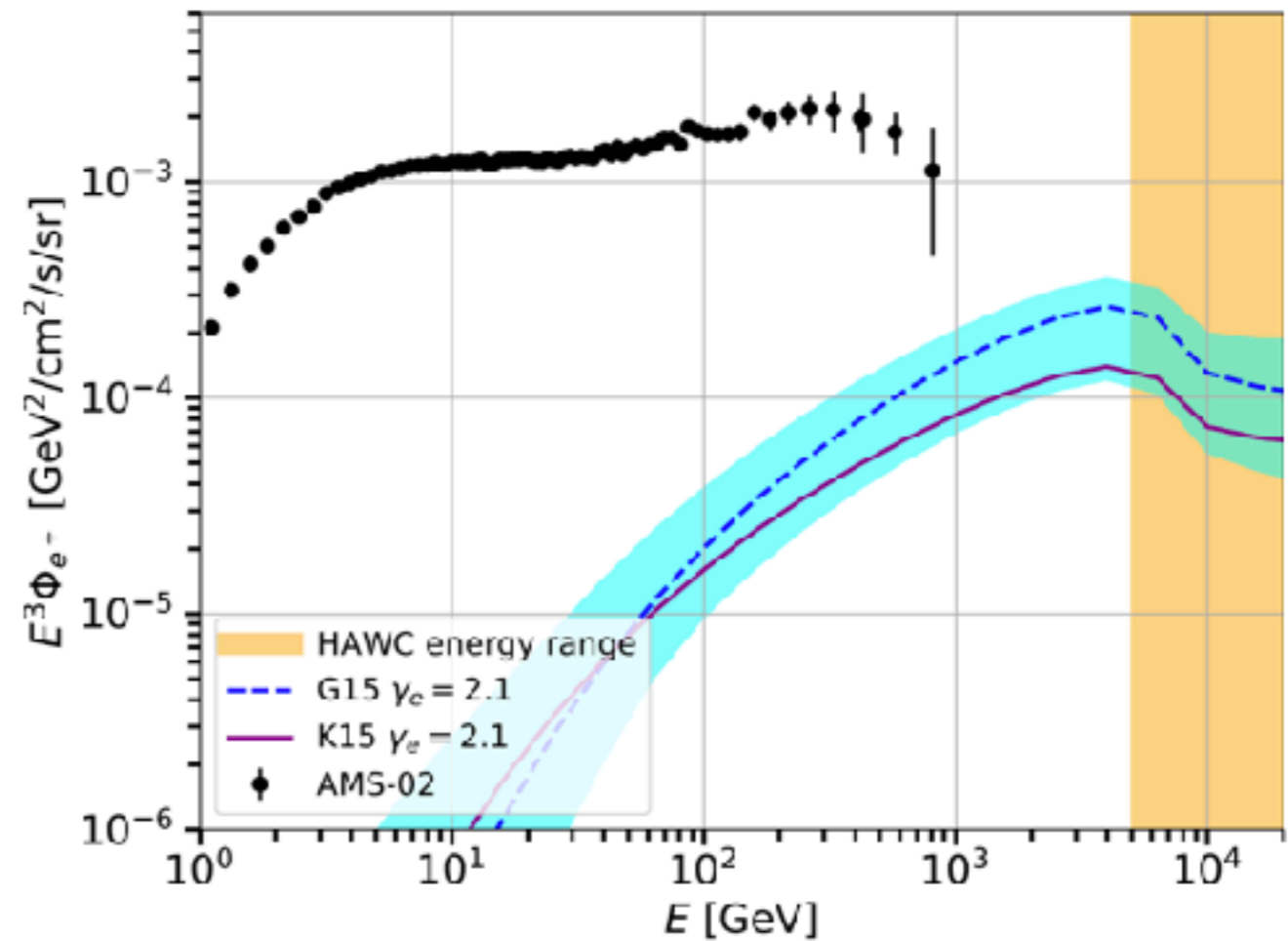
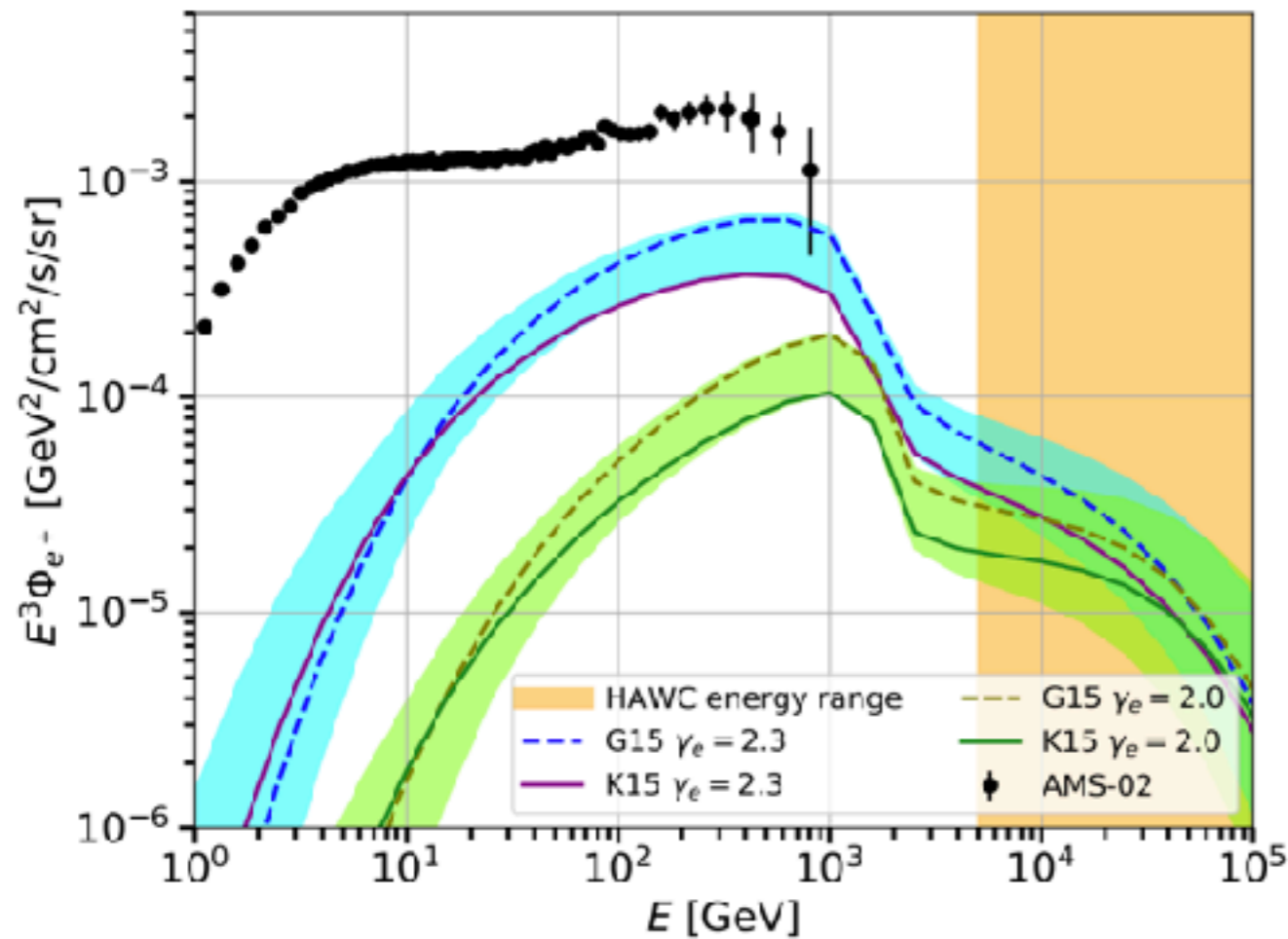
HAWC Collaboration (Science; 1711.06223)



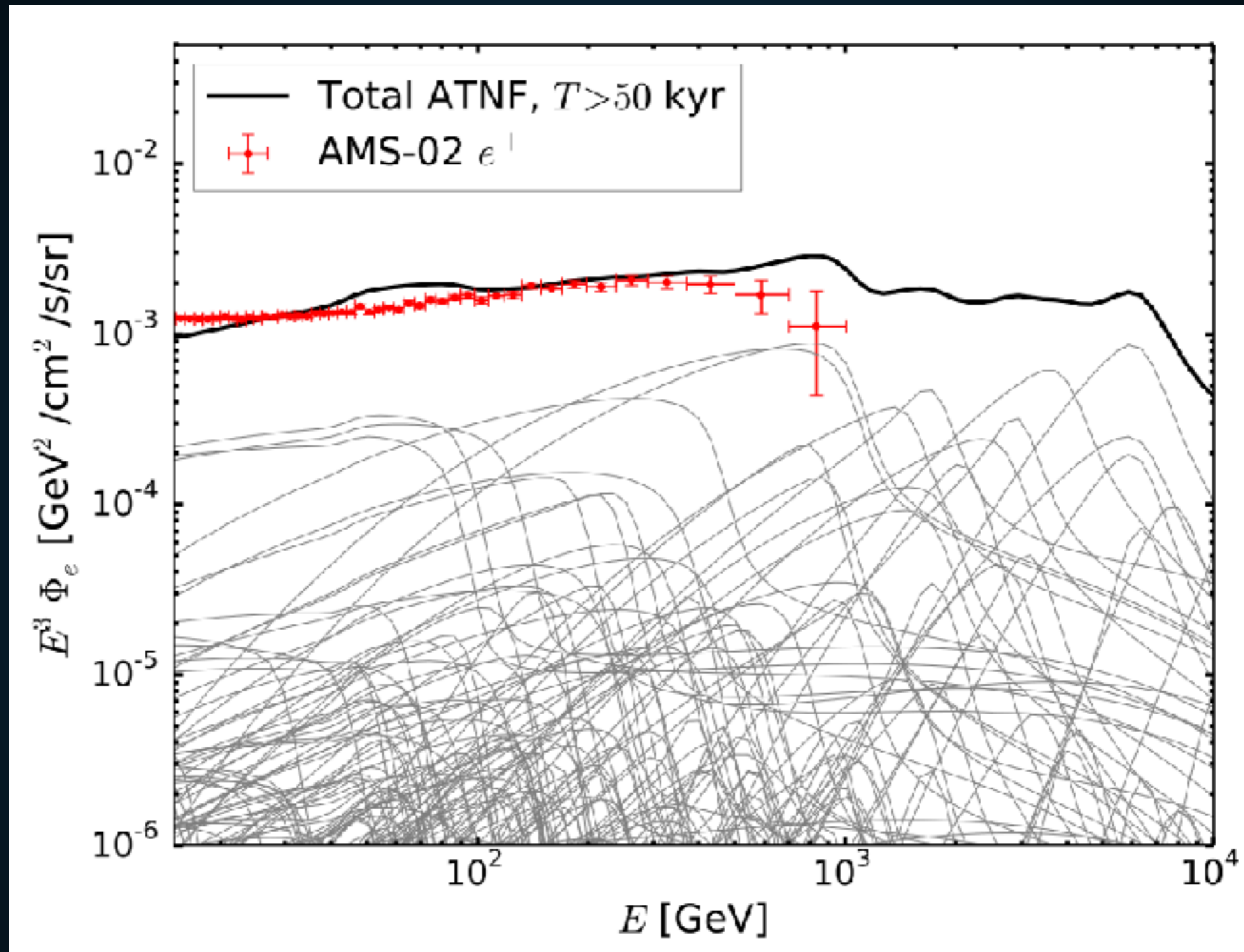
- Recently the HESS telescope detected 20 TeV electrons near Earth.



- If diffusion near Earth is low, then there is no source for these particles.



- **Studies by Di Mauro et al. use the Fermi data and find a much lower cosmic-ray injection efficiency, which is incompatible with HAWC studies.**
- **In these models, the efficiency of Geminga is only 1-2%, allowing Geminga to produce 10-20% of the positron excess.**



- Even using an average efficiency in the 1-2% range, the total contribution from all young pulsars can explain the excess.

ASSUMPTIONS

TeV Gamma-Ray Luminosity Roughly Proportional to Spindown Power

= Pulsars explain the Milagro TeV Excess

+ High Energy
electrons trapped in
TeV halos

= HAWC Sources
are TeV halos

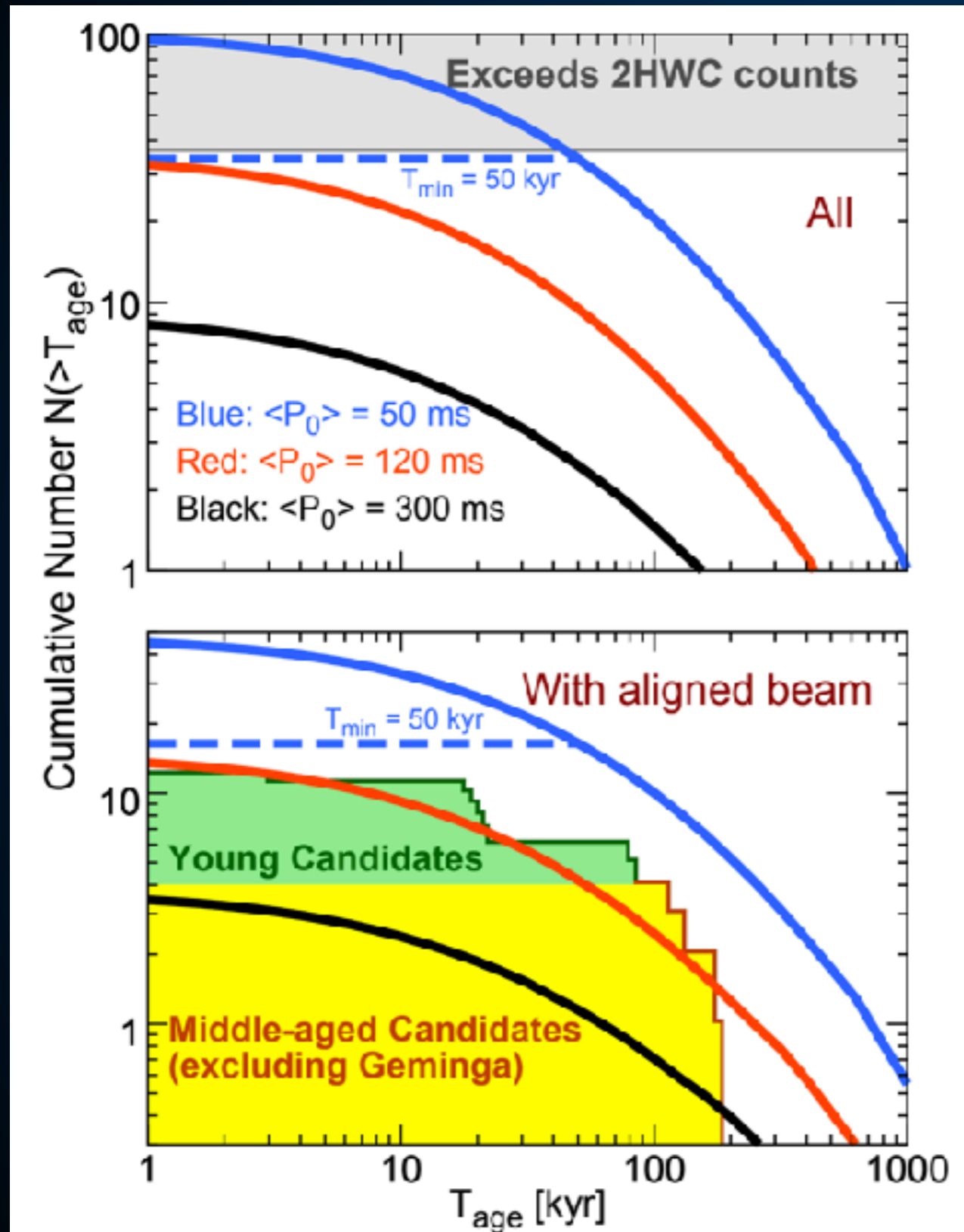
+ Low energy
electrons escape
from TeV halos

= Pulsars explain
the positron excess

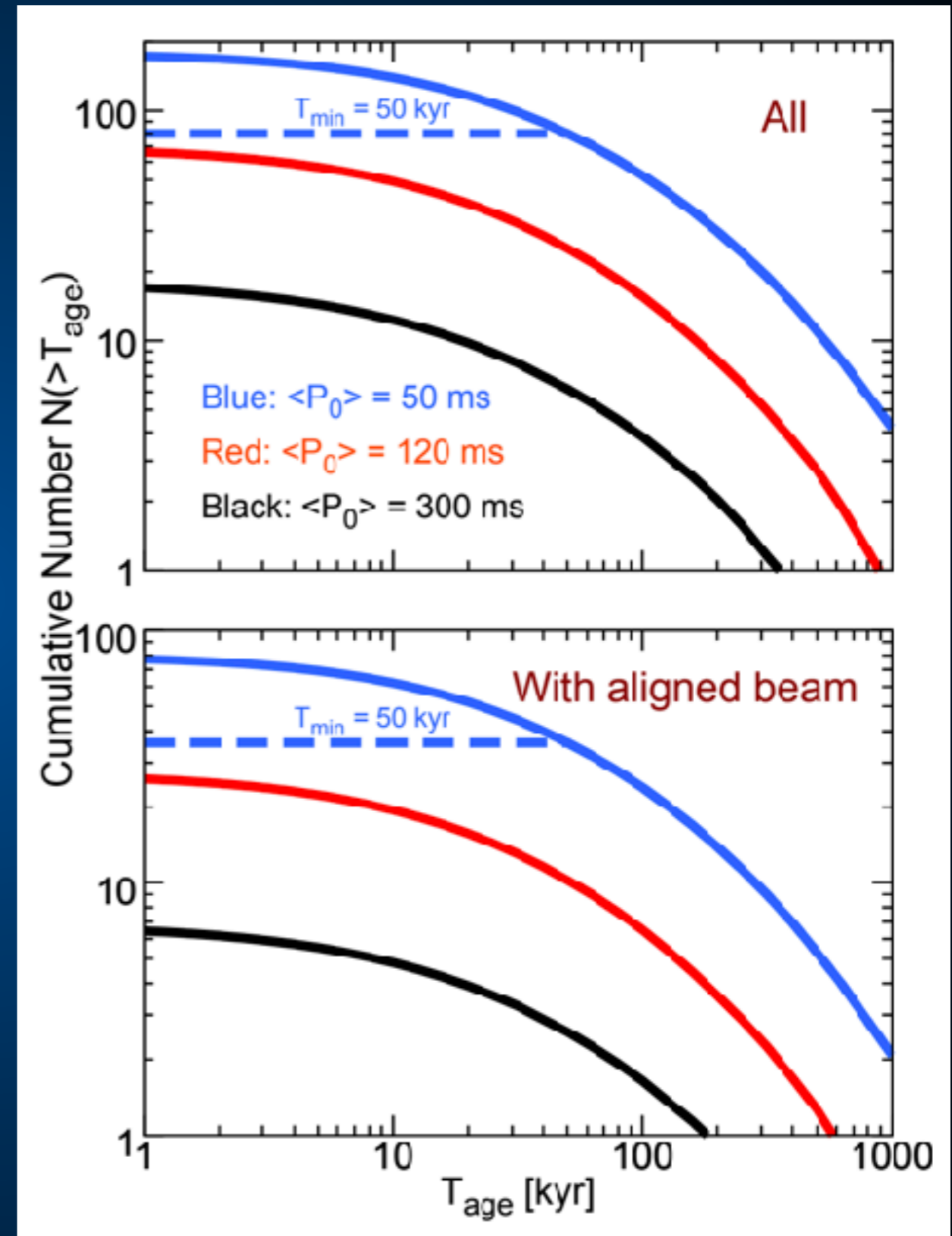


Understanding Pulsars

Sudoh, TL, Beacom (1902.08203)



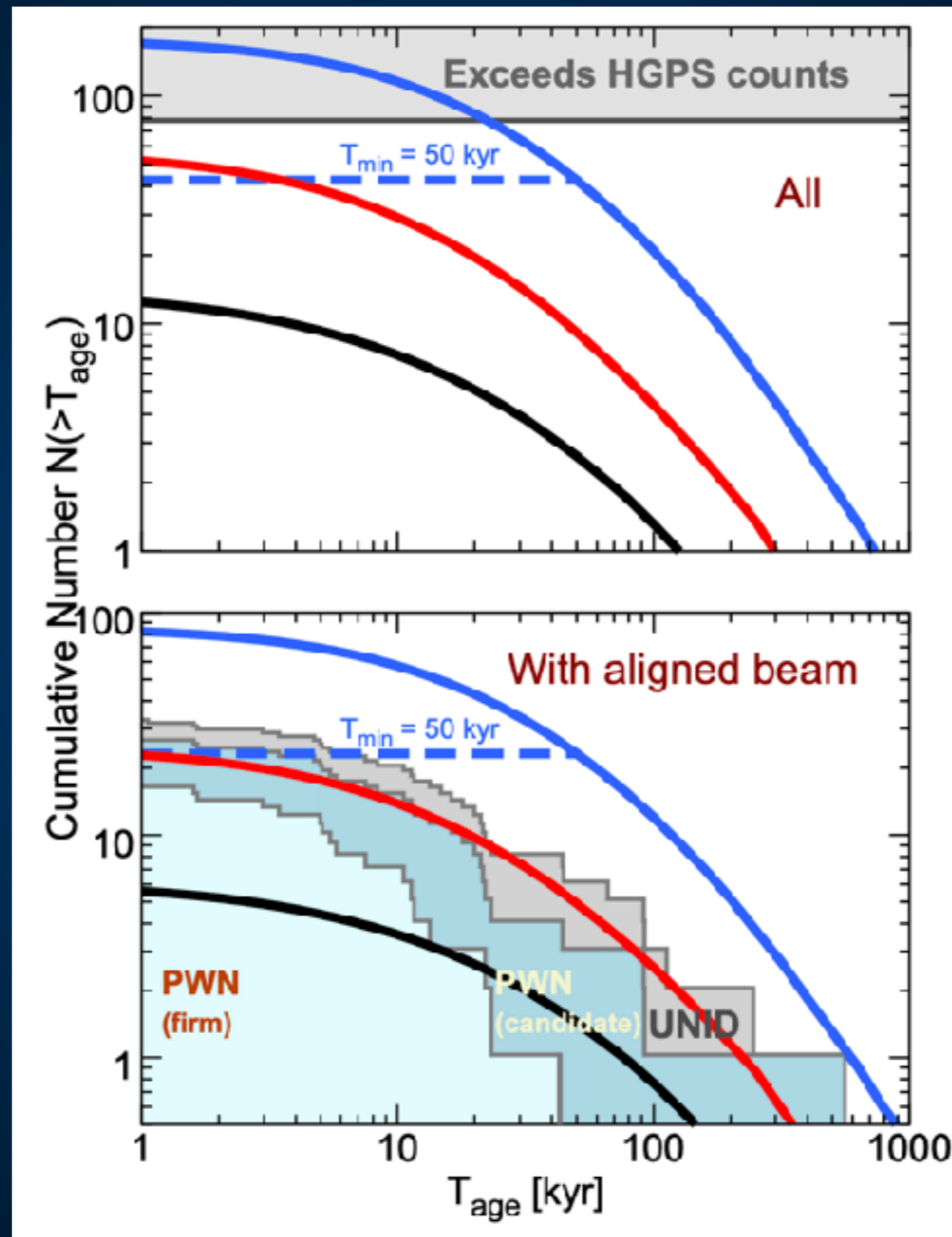
HAWC



HAWC - 10 years

Understanding Pulsars

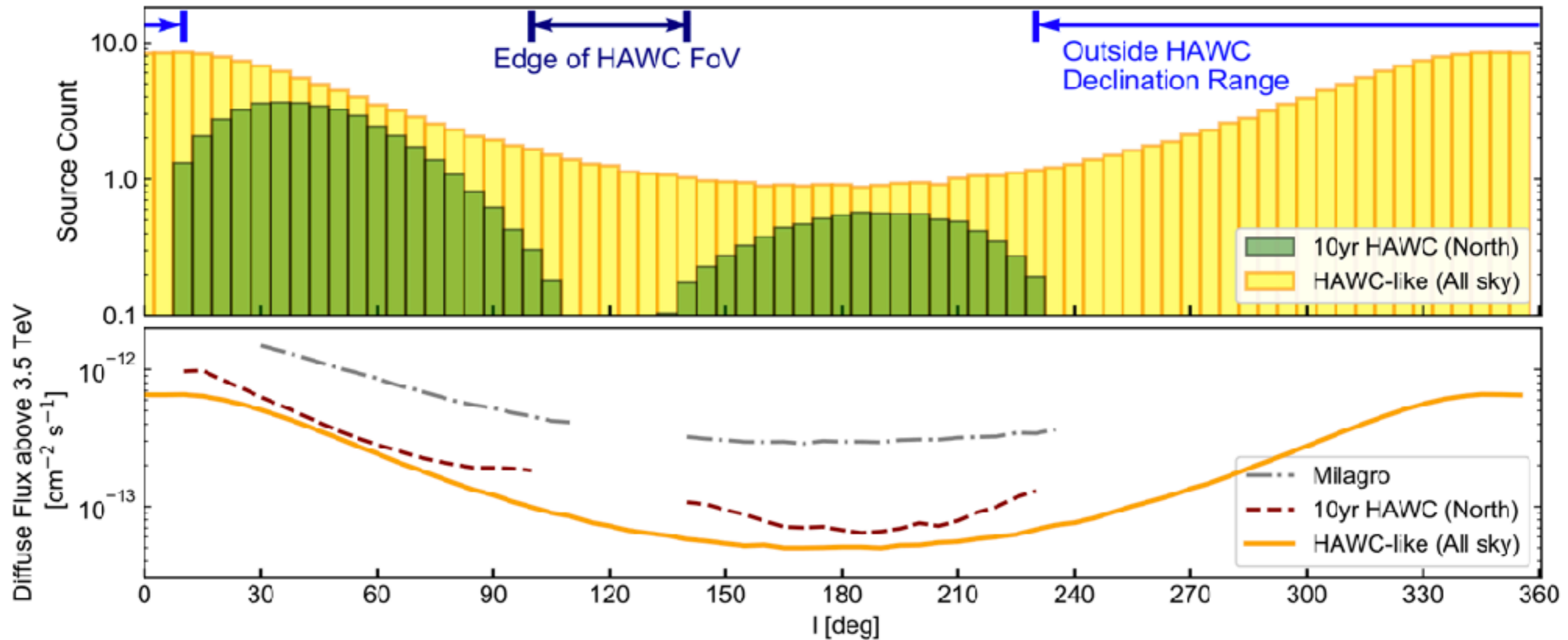
Sudoh, TL, Beacom (1902.08203)



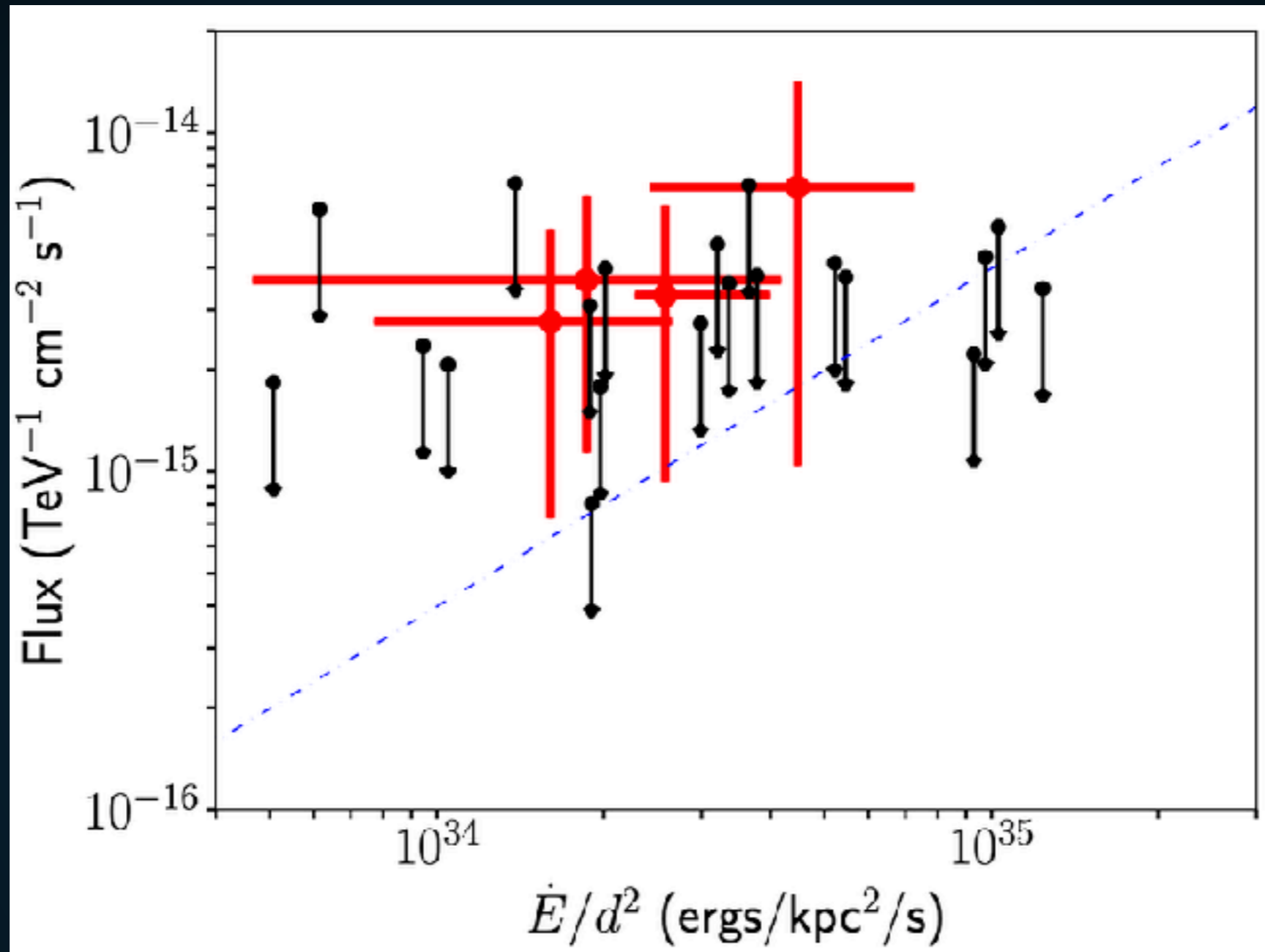
HESS

Detecting New Pulsars

Sudoh, TL, Beacom (1902.08203)

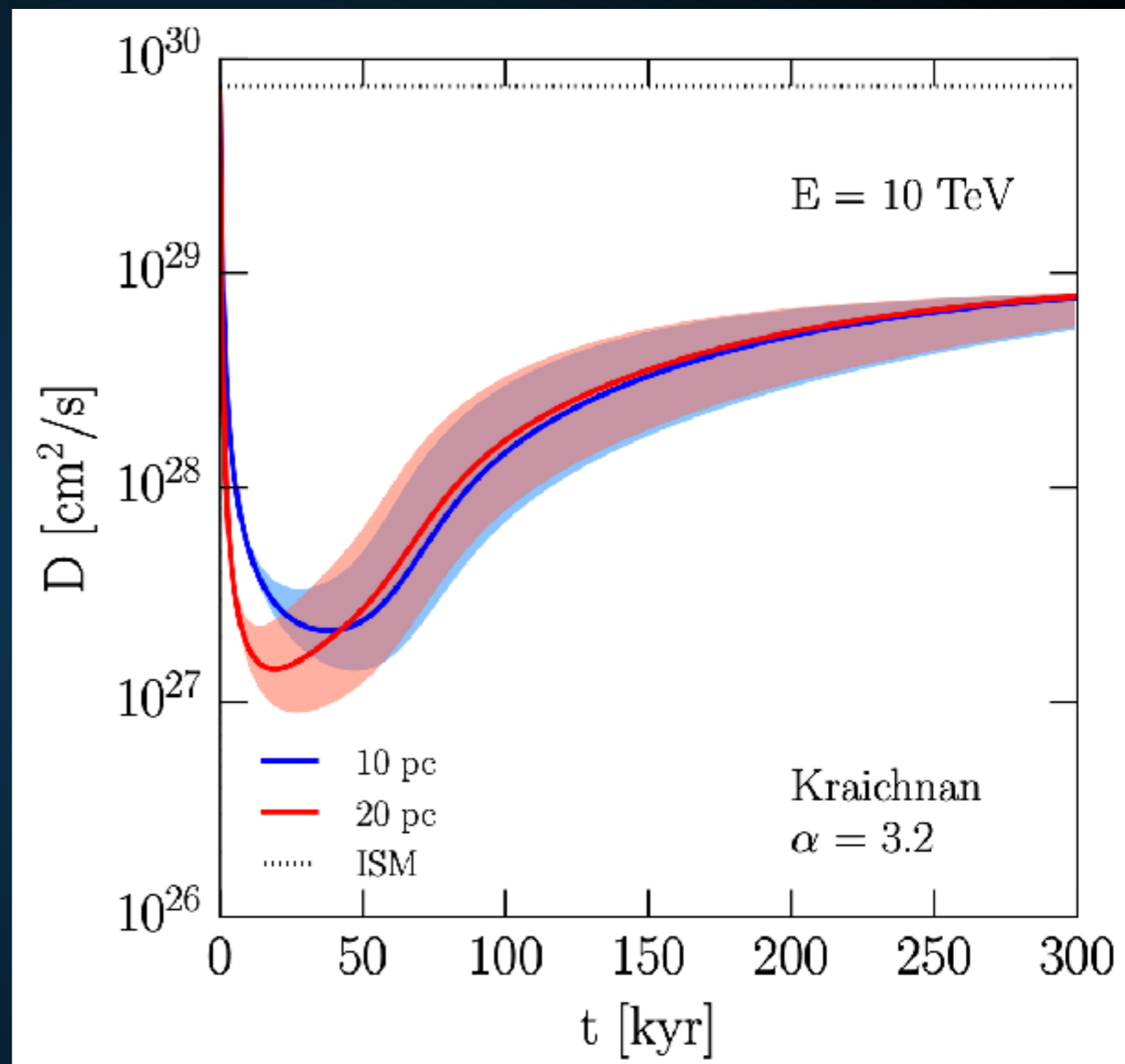


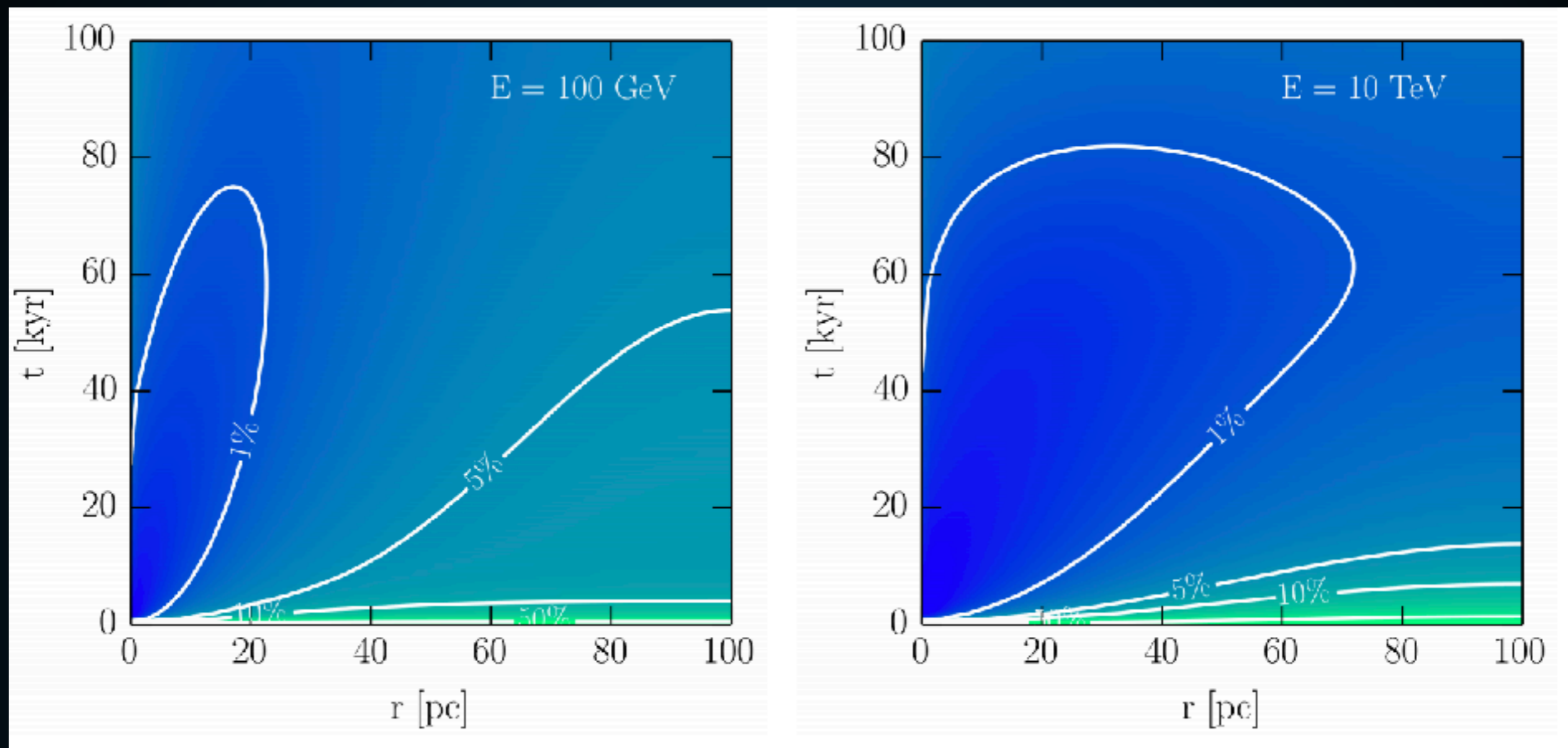
HAWC/LHASSO/SWGO/CTA



- Early evidence that millisecond pulsars also produce TeV halos.
- New opportunities to understand binary evolution.

- **First models that explain low diffusion constant.**
- **New opportunities to understand galactic magnetic fields.**





- Predicts energy-dependent features in cosmic-ray diffusion!

- Should observe coincident synchrotron Halo
- Possible Detection! (G327-1.1)

| | Region | Area (arcsec ²) | Cts (1000) | N _H (10 ²² cm ⁻²) | Photon Index | Amplitude (10 ⁻⁴) | kT (keV) | τ (10 ¹² s cm ⁻³) | Norm. (10 ⁻³) | F ₁ (10 ⁻¹²) | F ₂ | Red. χ ² |
|----|----------------|--------------------------------|---------------|--|--|--|--|---|------------------------------------|--|----------------|------------------------|
| 1 | Compact Source | 84.657 | 6.34 | 1.93 ^{+0.08} _{-0.08} | 1.61 ^{+0.08} _{-0.07} | 1.05 ^{+0.11} _{-0.10} | ... | ... | ... | 0.45 | ... | 0.80 |
| 2 | Cometary PWN | 971.22 | 7.75 | 1.93 | 1.62 ^{+0.08} _{-0.07} | 1.47 ^{+0.16} _{-0.14} | ... | ... | ... | 1.09 | ... | ... |
| 3 | Trail East | 537.42 | 2.13 | 1.93 | 1.84 ^{+0.13} _{-0.12} | 0.44 ^{+0.07} _{-0.06} | ... | ... | ... | 0.27 | ... | ... |
| 4 | Trail West | 766.56 | 3.12 | 1.93 | 1.80 ^{+0.11} _{-0.11} | 0.61 ^{+0.09} _{-0.08} | ... | ... | ... | 0.39 | ... | ... |
| 5 | Trail 1 | 424.45 | 1.98 | 1.93 | 1.76 ^{+0.12} _{-0.12} | 0.39 ^{+0.05} _{-0.05} | ... | ... | ... | 0.26 | ... | ... |
| 6 | Trail 2 | 588.19 | 2.13 | 1.93 | 1.95 ^{+0.11} _{-0.11} | 0.49 ^{+0.07} _{-0.06} | ... | ... | ... | 0.28 | ... | ... |
| 7 | Trail 3 | 994.92 | 2.99 | 1.93 | 2.09 ^{+0.10} _{-0.10} | 0.78 ^{+0.09} _{-0.08} | ... | ... | ... | 0.42 | ... | ... |
| 8 | Trail 4 | 839.48 | 2.38 | 1.93 | 2.28 ^{+0.12} _{-0.12} | 0.74 ^{+0.09} _{-0.09} | ... | ... | ... | 0.37 | ... | ... |
| 9 | Prong East | 828.58 | 1.65 | 1.93 | 1.72 ^{+0.14} _{-0.14} | 0.30 ^{+0.06} _{-0.05} | ... | ... | ... | 0.27 | ... | ... |
| 10 | Prong West | 971.22 | 2.06 | 1.93 | 1.85 ^{+0.14} _{-0.14} | 0.44 ^{+0.08} _{-0.07} | ... | ... | ... | 1.09 | ... | ... |
| 11 | Diffuse PWN* | 20007 | 27.7 | 1.93 | 2.11 ^{+0.04} _{-0.05} | 6.91 ^{+0.37} _{-0.74} | 0.23 ^{+0.14} _{-0.05} | 0.21 ^{+0.88} _{-0.16} | 6.0 ⁺¹⁶ _{-4.0} | 3.68 | 17.7 | 0.82 |
| 12 | Relic PWN* | 26787 | 17.2 | 1.93 | 2.58 ^{+0.07} _{-0.10} | 6.51 ^{+0.53} _{-0.71} | 0.23 | 0.21 | 6.9 ⁺¹⁸ _{-5.5} | 3.14 | 20.3 | ... |

- New opportunities for studying TeV halo morphologies!

- **TeV observations open up a new window into understanding Milky Way pulsars.**
- **Early indications:**
 - **TeV halos produce most of the TeV sources observed by ACTs and HAWC**
 - **TeV halos dominate the diffuse TeV emission in our galaxy.**
 - **Positron Excess is due to pulsar activity**

- **Additional implications:**
 - **Young pulsar braking index**
 - **MSPs?**
 - **Galactic cosmic-ray diffusion**
 - **Source of IceCube neutrinos**
 - **TeV Dark Matter Constraints**